A Study on Burning of Crude Oil in Ice Cavities

A Thesis

Submitted to the Faculty

of the

WORCESTER POLYTECHNIC INSTITUTE

in partial fulfillment of the requirements for the

Degree of Master of Science

in

Fire Protection Engineering

December 2013

Hamed Farmahini Farahani

Approved:

Professor Ali S. Rangwala, Advisor

Professor Albert Simeoni, University of Edinburgh, Committee Member

---

Dr. Xiaochuan Shi, WPI, Committee Member

Professor Kathy A. Notarianni, Department Head

Disclaimer

This document has been reviewed by Bureau of Safety and Environmental Enforcement (BSEE) and approved for publication. Approval does not signify that the contents necessarily reflect the views and policies of the BSEE, nor does mention of the trade names or commercial products constitute endorsement or recommendation for use. This study was funded by the Bureau of Safety and Environmental Enforcement, US Department of the Interior, Washington, D. C., under Contract Number E12PC00056.

Abstract

In situ burning (ISB) is a practical method of oil spill cleanup in icy conditions. This study investigates one example of a likely oil spill scenario; burning oil in an ice cavity. In this situation, unique and unexplored physical processes come into play compared with the classical problem of confined pool fires in vessels. The icy walls of the cavity create a significant heat sink causing notable lateral heat losses especially for small cavity sizes (5-10 cm). Melting of ice because of the heat from the flame causes the geometry of cavity to change. Specifically, the diameter of the pool fire increases as the burning advances. This widening causes the fuel to stretch laterally thereby reducing its thickness at a faster rate. The melted ice water causes the oil layer to rise which causes the ullage height to decrease. The decrease in ullage and increase in diameter counteract the reduction in thickness because of widening or stretching of the fuel layer. There thus exists a strong coupling between the burning rate and the geometry change of the pool and cavity. To explore the problem, experiments were performed in circular ice cavities of varying diameters (5 – 25 cm). The change in shape of the ice cavity and the oil layer thickness are recorded using a combination of visual images, mass loss, and temperature data along the centerline and edge of the cavity. The average burning rate of crude oil in a cavity is greater than the corresponding burning rate in a vessel of equal diameter, yet the burning efficiency (% of fuel consumed during combustion) is lower. For example, the average mass loss rate in a 10 cm ice cavity is 50% higher than a steel vessel of similar size. However, the burning efficiency is lower by 50%. Widening of cavity (170%) contributes to the increase in the average mass burning rate. At the same time heat losses through fuel layer increase because of decrease in fuel thickness by widening of the fuel layer. This coupling is analyzed using a mathematical model which can predict burning rate and efficiency of crude oil in an ice cavity for the range of cavity diameters examined. Extension of the model to larger sizes comparable to realistic situations in the Arctic is discussed.

Acknowledgments

I would like to express my gratitude to my advisor, Prof. Ali Rangwala for his guidance, patience, and providing all the means for doing research. It is a sincere pleasure to thank Prof. Kathy Notarianni who made the whole thing possible for me. I'm grateful that I got to conduct experiments and witness dozens of fire tests during my study. I must also thank Prof. Albert Simeoni who was able to provide me with useful insights for the most part of the project. I should also thank Dr. Lydia Shi lab manager of the Combustion Lab, Sreenivasan Ranganathan, Haoran Li, Minkyu Lee, and Andre DaVitoria who assisted me on every occasion I was in need of help with my experiments. Without question the previous work done by Peter Bellino was the best guidance I could ask.

Finally, I would also like to thank my parents, elder sister, and two elder brothers. They were always supporting me and encouraging me with their best wishes even though they were thousands miles away.

Contents

List of Tables

List of Figures

Nomenclature

C_P	Specific heat of air (1.04 kJ/kg K)
D	Diameter of cavity (m)
g	Acceleration due to gravity (9.8 m/s^2)
L_v	Latent heat of vaporization (kJ/kg)
L	Fuel layer thickness (m)
$\dot{m}$	Mass loss rate (g/s)
$\dot{m}''$	Mass loss rate per unit area (g/s cm^2)
$\dot{Q}$	Total heat (kW)
T	Temperature(K)
V	Volume (ml)

Greek symbols

ρ	Density (kg/m^3)
χ	Fraction of total heat feedback to fuel
λ_l	Conductivity of crude oil (W/m K)

Subscripts

cd	conduction
cv	convection
f	flame
g	gas
i	ice
l	fuel layer
rad	radiation
ref	reflection
rr	re-radiation
w	water

Chapter 1

1.1 General Overview

In-situ burning (referred to ISB) as a response technic to oil spills has been researched and employed in one form or another at a variety of oil spills since 1958, including limited use during the Exxon Valdez accident and more extensive use during the Deepwater Horizon incident. Many researchers and practitioners believe that ISB is especially suitable in ice conditions at Arctic. In Arctic once oil is spilled, it can interact with ice in many different ways (Figure 1.1) and as a consequence many different methods of spill response may be necessary (such as mechanical recovery or use of chemical agents). This has lead researchers to investigate alternative means of spill response that may be more suitable for arctic conditions; one of which includes *in situ* burning [1-7]. This study investigates one example of a likely oil spill scenario for which ISB may be performed- burning oil in a small ice confinement here referred to as ice cavity.

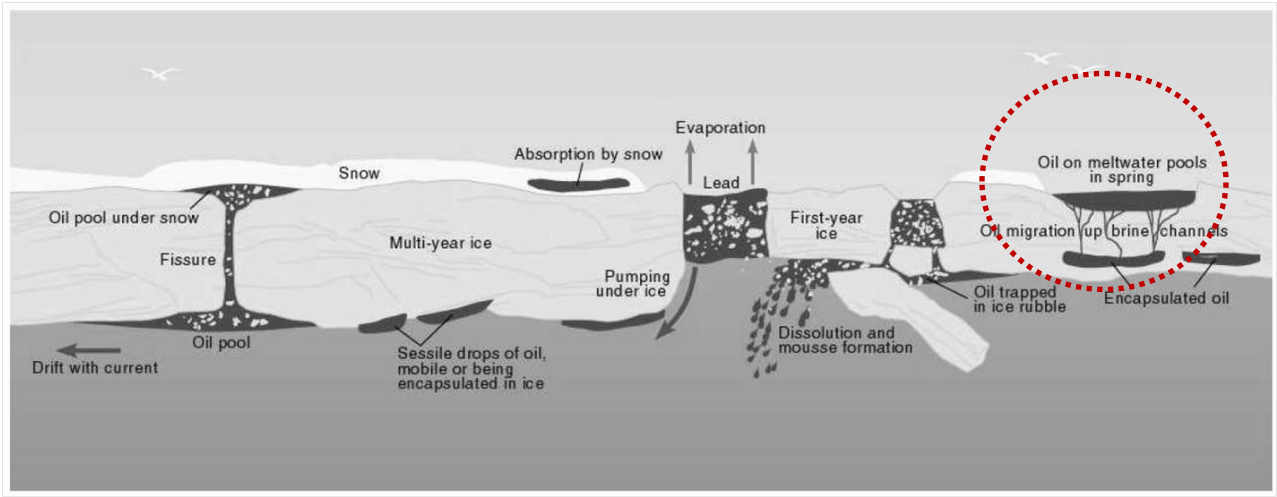

Figure 1.1: A visual description of the oil/ice interaction most applicable to this study[5].

For burning of oil in ice cavities, unique and unexplored physical processes come into play that are not apprehended in the classical problem of confined pool fires in containers. Thus, burning behavior of a possible ISB operation in ice cavities would be different from what is suggested in the literature of pool fires. Since, the success of an ISB is directly depending on the burning

(removal) efficiency, it is essential to investigate the burning behavior (burning rate and efficiency) of fuels in an ice cavity. This forms the general objective of this study. Assuming ISB to be one of the powerful solutions to the problem of oil spills, several fields of study can be determined as shown in Figure 1.2. As mentioned, this study focuses on burning behavior of the fuel when it's burned in an ice cavity. This includes proposing a predictive model for estimating burning rates and burning efficiency.

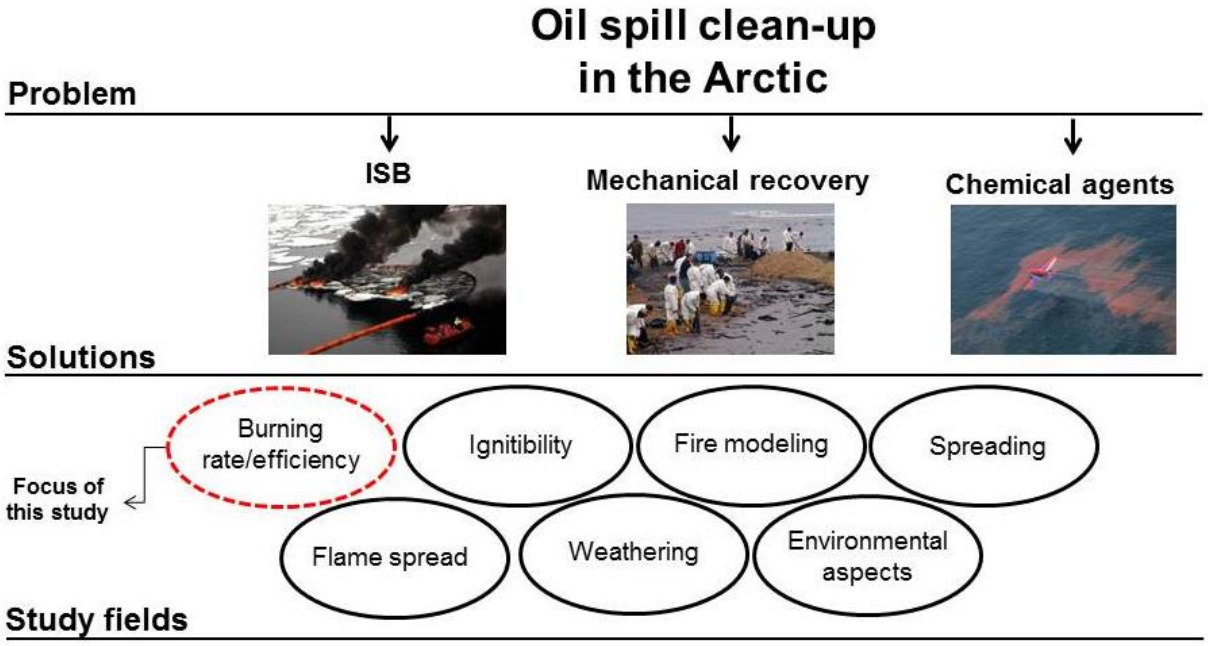

Figure 1.2: A Problem/Solution flow chart.

Because of controversial public perception over air quality and the ability to safely ignite a large oil spill, *in situ* burning was not the preferred method for most oil spills for some periods [8]. However, over the last 30 years, the in situ burning of crude oil spills has become a recognized and accepted method of oil spill cleanup with respect to the more conventional cleanup methods such as boating skimmers [9]. *ISB* is also a proper choice for Arctic operations where remoteness of working sites with ambient temperature commonly below -30 ℃ halts any type of activity. Additionally, in situ burning can have high cleanup efficiency and relatively low post cleanup costs when compared with traditional means under these conditions [10].

As mentioned, the Arctic and sub-Arctic environments add an additional level of complexity by introducing a spill substrate (ice) that is highly unstable at elevated temperatures. Oil released into icy confinement may not be easily cleaned up due to the variable topography of an ice sheet. For this reason, the current chapter is provided to give readers ideas on how different parameters and factors are related to the burning of crude oil in an ice cavity.

This literature review is divided into 4 sections. Current section is aimed to provide a general understanding of ISB. Since any ISB operation deals with burning pools of liquid hydrocarbons, the second section is devoted to a literature review of pool fires. The most relevant research topics in pool fires with respect to ISB are identified to be ignition and flame spread, ullage effect, and pool fire modeling. Reviews of selected publications on each topic are presented in sub-sections. Third section is devoted to the studies related to ISB in different conditions such as open waters and ice-affected waters. The most relevant topics in the third section are identified to be large and small-scale experiments, modeling approaches for ISB, weathering, and environmental aspects of ISB. Again, a review of selected publications on each topic is presented in sub-sections. The final section of this literature review presents a scenario where a liquid fuel burns in an icy environment. More specifically, a scenario where oil is burning inside an ice cavity is reviewed. Only a limited number of researches are conducted for burning of oil confined in ice, thus additional studies related to different aspects of the problem are introduced in the last section of literature review as well.

1.2 Pool Fires

According to Drysdale's book , "An Introduction to Fire Dynamics"[11], the term "pool" is used to describe a liquid with a free surface contained within a confinement. Its depth may be from several meters to a few millimeters. A pool can result due to a liquid fuel release (spill) or can exist as a result of normal storage of fuels in tanks and containers. The nature of a spill fire is highly variable depending on the source of the release, surface features of the substrate (which can be concrete, ground or water) and the point and time of ignition. The depth of the fuel will determine the heat losses to the substrate beneath it and will affect the burning rate. This is demonstrated most clearly by Garo *et al*.[12]. The study by Blinov and Khudiakov published in 1957 still remains the most extensive study performed on pool fire behavior. They studied the rate of burning for pool of different liquid fuels (Gasoline, Tractor kerosene, Diesel

oil, Solar oil) ranging from 3.7×10^{-3} to 22.9 m. The fuel surface was kept at a constant height to remove the effect of ullage height for all the smaller diameters. They found that the regression rate (mm/min) of the fuels was high for small scale laboratory tests (0.01 m and less) and shows a minimum at 0.1 m diameter (Figure 1.3). Further information can be found in various related topic [13, 14].

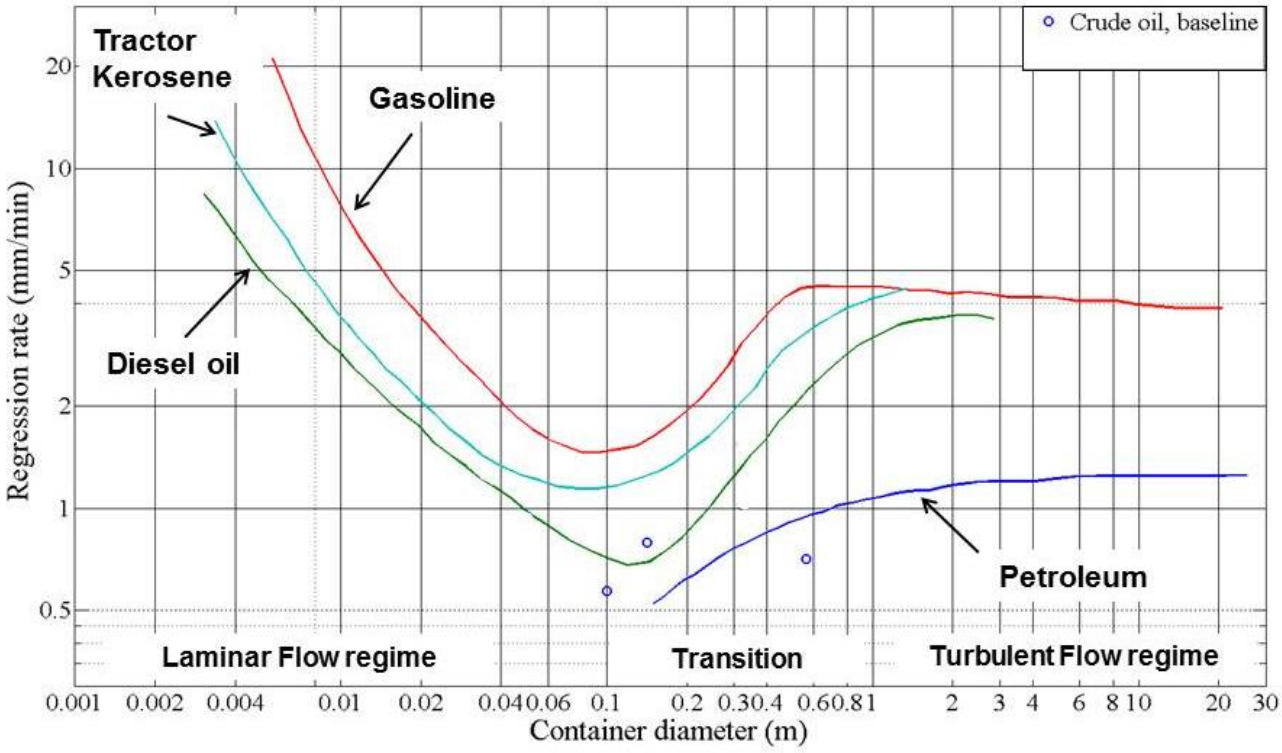

Figure 1. 3: Regression rates for liquid pool fires with diameters in the range of 3.7×10^{-3} to 22.9 m.

1.2.1 Ignition and flame spread

The susceptibility of a pool of liquid fuel to ignition by heat source adjacent to it is a problem of interest both for purely scientific reasons and for its relevance to technical problems such as ISB. Experimentally it has been found that the factors influencing an ignition process depend strongly on whether the fuel temperature is above or below its flash point. For an extreme cold environment the fuel temperature would be below its flash point and the presence of a heat source adjacent to the fuel will not result in fire. Furthermore, other factors such as cross wind speed or the composition of oil itself might play a role. Ignition of an oil slick and flame spreading are strong functions of the temperature of the fuel, its volatility, its degree of

emulsification, and the location of the ignition on the slick relative to the wind. If oil is at a temperature above its flash point, ignition is simple and flame propagation is normally rapid; otherwise ignition and flame spreading can be slow and difficult [8, 15-19]. Specifically, Murad *et al*.[20], investigated two major problems concerning the ignitibility of a pool of liquid fuel. First concern was to define the domain of ignitibility of a pool of fuel at a super flash temperature when it is subjected to a cross wind. The second problem was to identify which parameters control the ignitibility of a liquid pool of fuel at a sub-flash temperature. For the first problem it was found that the presence of a cross wind will decrease the ignitibility domain of a liquid fuel, however it can be partially compensated with increase in temperature of liquid. The strength of the cross wind will adversely affect the ignitibility of a liquid but after a certain speed the wind blowing effect it will render a higher concentration of the fuel near the surface. The mathematically obtained results of this study showed good agreement with experimental values unless for high blowing powers. Further, it was found that for liquid fuels below their flash temperature the heating will induce fluid motion which is the sum of surface tension and buoyancy forces.

Flame spread is a crucial aspect of effective in situ burning; if the fire does not spread to cover a large part of a slick, overall removal efficiency will be low. Flame spreading can be divided into two distinct categories: sub-flash spreading and super-flash spreading with an intervening transition zone characterized by pulsating spread. At all zones, flame spread will increase by increase in fuel temperature, as showcased for ethanol in Figure 1.4.

Degroot and Ybarra [21-24], studied the flame propagation over liquid alcohols (methanol, ethanol, propanol and butanol). The experimental setup consisted of two channels (40×4.0×2.5 and 100×1.5×3.4 cm, respectively) filled with alcohol fuel. Eight thermocouples (Cr–Al, φ=25 μm), regularly spaced along the central line of the fuel surface, record the evolution of the fuel surface temperature (sampling rate N=1 kHz).The initial fuel temperature T_0 was kept uniform along the horizontal with a refrigerant circuit. The alcohol was ignited at one end of the channel and flame spread was observed. The different spreading regimes above liquid fuels have been experimentally described for a wide range of initial surface temperatures. The critical transition temperatures between these regimes have been characterized; they present common characteristics for the four alcohols used in the experiments. The first observed

regime was the uniform regime which happened at temperatures above the critical temperature of the system. Above this temperature the flame spread rate had a constant value (for T= 17.3℃ flame velocity is 65 cm/s). The second regime was the pulsating regime which happened at temperatures below the critical temperature of the system with a velocity of the flame (0-15 cm/s) and the third regime was named pseudo- uniform regime which had a very low constant flame velocity (1 cm/s). The third regime happened for temperatures below the pulsating regime. A preheating zone ahead of the flame (produced by thermo-capillarity vortex) was observed. Thermocapillary motion seems to be responsible for the flame oscillation and flame velocity. The initial surface temperature of the liquid fuel results to be a control parameter of flame spreading regime; therefore, it can be applied to improve fire safety conditions in fuel containers.

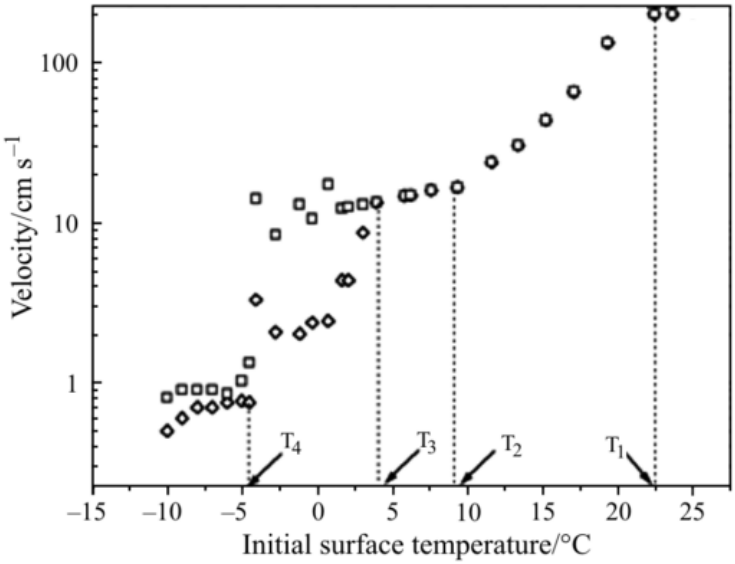

Figure 1.4: Bifurcation diagram for the spreading of flames over liquid ethanol for the 100 cm long channel [24].

In liquid pool fires (at sub-flash temperature) the fuel underneath the leading edge of the flame front is hotter than the unignited fuel. This induces a flow inside the liquid which is driven by surface tension and buoyancy forces. Generally, the hot fuel has a lower interfacial tension than the cold fuel and tends to flow forward over it. These convective mechanisms are found to be the main cause for flame spread [17, 25]. Yumoto *et al.* [26] conducted experiments on a small vessel of Hexane to study the effects of convective motion on burning rate. Hexane was burned

in pyrex glass vessel of 3 cm diameter and 6 cm diameter (both with depth of 6 cm). Most of the experiments were performed in the smaller vessel since more remarkable convective motions were observed in it. The convective motion in the liquid and the cellular convection at the surface were observed by means of a particle tracer and shadow photography, respectively. Aluminum powder of 50 to 74 μm was used as a tracer. A high pressure Mercury lamp of 500 W power was used for observation of two types of convection motion. Temperatures of the liquid were measured with 27 copper- constantan thermocouples of 28 gauge. In order to decrease the flow interference of thermocouples, they were distributed into three vessels and the measurements obtained from the three vessels were combined into one map. Temperatures at the wall of the vessel were measured with four chromel-alumel thermocouples of 28 gauge. The radiative heat flux from the flame to the liquid surface was measured with 18 heat flux meters. Each flux meter was made up of a copper-constantan thermocouple of 28 gauge sealed in a Pyrex tube of 5-mm diameter, and the junction of the thermocouple was blackened with platinum black. These heat flux meters were calibrated against a standard blackbody radiation source. In order to decrease the flow interference of the heat flux meters, they were distributed into eighteen vessels and the measurements were combined in one map. The setup was placed on top of a loadcell record the mass loss of the fuel. The vortices form right after ignition in and on liquid surface. Vortices in the liquid layer are divided into two groups. One group is located in the upper part of the liquid and the other in the lower part. The vortices in the former have large radii and relative by high fluid velocities and those in the latter have small radii and low fluid velocities. A concept introduced in their study is "effective convection thickness" which is the distance from surface of the fuel to the bottom of larger vortices. The effective convection thickness in a 3 cm vessel increased to 2 cm for the first two minutes after ignition and then gradually declined till extinction (the vortices were not observable after 4-5 minutes from ignition). The vertical and horizontal fluid velocities were also obtained with streak photographs. The maximum fluid velocity was recorded to be around 12-13 cm/s (both vertical and horizontal) which happened after 2 minutes from ignition. The temperature recordings show a horizontal gradient of temperature in the liquid in addition to the vertical gradient. The liquid surface temperature increased from 40 $°C$ to 68$°C$ after 3-4 minutes and then declined to 60 $°C$ before extinction. Their study also discussed the forces driving the convective motions in the liquid. Surface tension and buoyancy had been considered as driving forces for fluid

motion. Marangoni and Rayleigh numbers have been used as the relevant dimensionless groups. These dimensionless numbers can be represented as:

$$Ra = \frac{\beta g h_e^3 \Delta T_h}{\vartheta \alpha}$$

$$Ma = \frac{\sigma_T R \Delta T_s}{m\alpha}$$

Where, σ_T is the change of surface tension per degree, R is the radius of the vessel, g is the acceleration due to gravity, and β, μ, ϑ, and α are thermal expansion, viscosity, kinematic viscosity and thermal diffusivity of the liquid, respectively.

It was found that the buoyancy (Rayleigh number) becomes more dominant when the vessel is reduced in diameter. Their study also included deriving a heat balance for estimating the burning rate from dimensionless analysis which is based on the heat transfer thickness, the mean horizontal fluid velocity at the liquid surface, and the Ma/Ra ratio.

Torrance and Mahan [27], studied the fire spread over liquid fuels and influencing parameters on fluid motion. These parameters were grouped as surface tension (expressed as $\frac{T_f - T_0}{\mu} \times \frac{d\sigma}{dT}$), buoyancy (proportional to $g\beta(T_f - T_0)$), molecular properties (through the ratio $\frac{\vartheta}{k}$), fuel layer thickness (L), and flame or thermal disturbance properties. The effect of these parameters was obtained from numerical solutions of the equations governing the liquid phase and was compared with existing fire spread experimental data. The results of this study showed that the reverse surface velocities are dependent only on surface tension and fuel layer thickness. Effects of buoyancy, Prandtl number and flame speed are negligible. By hypothesizing that the flame acts as a stationary or quasi-stationary heat source, a good agreement with reverse velocities and observed flame spread can be obtained in the pulsating regime.

1.2.2 Ullage effect

Normally, the ullage height (vertical distance from fuel surface to the container rim) in a container is increasing due to evaporation of the fuel. Thus, height of the flame is decreased as the fuel is consumed, and the flame goes out at a certain ullage height which is called the self-quenching ullage height. A small circuit of data concerning the ullage height and its effects on

burning rate has been reported in the literature of pool fires [28-31]. The ullage height is especially affective on small size of pool fires. Dlugogorski and Wilson[32], investigated the effect of ullage on properties of small-scale pool fires. An experimental technique was conducted to accurately measure the steady state consumption of ethanol in containers of 45 mm in diameter constructed from various materials (copper and pyrex). The results of their study indicated that the ullage size and vessel material profoundly influence the burning behavior. For the glass containers with different height same fuel consumption rate was observed. For example, the value for burning rate was 0.02 kg/m^2s for ullage of zero and decreased to 0.005 kg/m^2s for ullage size of 10 mm. The same trend for copper was obtained to be totally different. Due to heat conduction loss from the vessels walls to the fuel layer, burning rate stays constant for the first 10 mm of ullage and then decreases. But, the burning rates are higher in copper than in vessels.

1.2.3 Pool fire modeling

A large number of studies on the combustion above the liquid fuel pool have been conducted ranging from the basic observation of burning rate to measurement of flame properties and radiation [33]. All elements of the heat input and output from a fuel layer are studied and documented by previous researchers [30, 34-40]. Numerous empirical values and correlations are obtained from previous studies. However, the two aspects of the pool fire modeling that are more relevant to this study are single-layer conduction models and heat feedback from the flame to fuel. A complete review of the single-layer conduction model for combustion of liquid fuels on water is provided in the next section. Thus, only heat feedback from flame to fuel surface will be reviewed here.

Heat release rate from a pool fire has been documented extensively. An empirical correlation for heat release rate of a pool with respect to its diameter has been developed. The net heat feedback per unit area to the fuel represents a small fraction of the total heat release, this fraction has been found to be independent of the pool diameter and observed to be less than 1% of total heat released for small pool fires [41-43].

Hamins *et al*.[44], investigated the heat feedback from the flame to the surface of burning liquid fuels experimentally. The radial variation of the local radiative and local heat flux incident on the surface of a 0.3 m diameter pool fires were measured. The measurement of the

radiative heat flux was done with a water cooled, nitrogen purged, narrow view-angle gauge. Measurements of the mass burning rate in a burner composed of annular ring was used to estimate the local heat feedback. Fuels used in their study had different range of luminosities and heat release rate. The model for heat balance of the fuel layer used in their study comprised of the total of gained energy due the flame plus energy losses to the surroundings. Energy entering the fuel layer is mainly by convection ($+\dot{Q}_{conv}$) and radiation ($+\dot{Q}_{rad}$) from the flame plus a small fraction due to the conducted heat from the rims of the container ($+\dot{Q}_{cr}$). On the other hand, heat losses terms are defined as conduction to the water sub-layer ($-\dot{Q}_{cond}$) and fuel vaporization heat ($-\dot{Q}_{fuel}$) plus a small fraction of losses due to reflection and re-radiation from the fuel surface ($-\dot{Q}_{ref}$ and $-\dot{Q}_{rerad}$). A pool burner with diameter of 0.3 m was used in the experimental part of the study. The burner was used to measure the radiative heat flux at the surface of the pools burning Heptane, Methyl Alcohol, Methyl Methacrylate, and Toluene. The fuel level was kept 0.5 cm below the rims of burner. Thermocouples were located 5 mm above the fuel surface. The heat flux gauges were installed face up and 7 mm above the fuel surface and also located outside of the pool to capture the total heat flux. The fraction (χ_s) is reported to be 0.010, 0.054, 0.017, and 0.012% for Heptane, Methyl Alcohol, Methyl Methacrylate, and Toluene, respectively. The burning rates are also reported to be 2.6, 0.92, 2.7, and 3.1 g/s for these fuels. The experimental results show that the intensity of energy released by the heptane flame to fuel surface which is received to heat flux gauge decreases from 17,000 (W/m^2-sr) to 7000 (W/m^2-sr) when traveling from center to rim of the container.

1.3 ISB

ISB refers to the controlled burning of oil spilled from a vessel, facility, or a pipeline. For spills on open water, responders usually have to collect and contain the oil using fire-resistant booms, because the oil has to be a minimum thickness to be ignited and sustain burning. The success of an *ISB* is highly dependent on the condition of the oil prior to ignition. Variables such as the degree of weathering, emulsifications and fuel layer depths all impact the efficacy of an in situ burn and can lead to varied success rates[45, 46]. Buist [2, 47], reviewed the current knowledge of limitations imposed by oil slick properties, weather and sea conditions and operational/equipment factors on the use of *ISB*. Some of the limitations and properties relevant to in situ burns are presented below:

Most heat from a burning oil slick is carried away by the rising column of combustion gases, but a small percentage (about 1% to 3%) radiates from the flame back to the surface of the slick. Flame temperatures for crude oil burns on water are about 900 °C to 1200 °C. But the temperature at the oil slick/water interface is never more than the boiling point of the water and is usually around ambient temperatures. There is a steep temperature gradient across the thickness of the slick; the slick surface is very hot (350 °C to 500 °C) but the oil just beneath it is near ambient temperatures. Fuel layer thickness can act as insulator if it is thick enough (more than 10 mm) and can be a heat sink if it is thinner than 1-2 mm. As a rule of thumb for larger size (>3m) of pool fires the burning rate is 3.5-4 mm /min. The residue thickness at burn extinction for 10-20 mm thickness of unemulsified crude oil is about 1mm. When the initial thickness is greater the residue thickness can become 3-5 mm. The residue is a semi-solid, tar like material and in some cases it may sink in fresh and salt water. Ignition and flame spread on the oil slick are functions of oil slick condition (thickness, weathering, emulsification) and ambient (wind speed, temperature, waves). For example, the minimum ignitable thickness for fresh and volatile crude oil is 1 mm. The minimum thickness increases to 2-5 mm for aged crude oil. Also wind speed of more than 12 m/s will create difficulties for the ignition. Emulsion and weathering both have negative effect on removal efficiency. Emulsions of up to 12.5% water content have minimal effects on burning efficiency. Water contents of 12.5% and more will have noticeable decrease on burning efficiency which can be aggravated with weathered oils. Overall, emulsified crude oil will have more difficulties to ignite, display reduced flame spreading and more sensitivity to the wind.

1.3.1 Large and small-scale experiments

The ISB of oil in water is of great interest as a result of off-shore exploration, production and transportation of petroleum. It is also a matter of interest from a safety point of view which is more concerned with hazards associated with burning i.e. boil-over. In addition, the storage of fuels can be a potential hazard and has attracted lots of attention. Thus, there have been numerous studies on the subject [48-51]. Large scale experiments of burning oil slick on water (mostly unconfined scenarios) are not entirely relevant to the problem in hand. Thus, more attention is paid to review the literature on small-scale experiments.

There are a large number of studies devoted to study of burning of crude oil on a water bed in pans with size of less than 1 m in diameter. Ground breaking studies done by Torero *et al*.[41] and Garo *et al*. [52-54] in the last twenty years have covered both the experimental and mathematical aspects of oil burning on water on a small scale. In their work a simple heat conduction models are used to describe the pre-boilover ignition and burning rate of crude oil and heating oil. The results produced by the model are then compared to the experimental data for different fuels to validate the model. The experimental apparatus used in their study was a steel pan with diameters ranging from 15 cm 50 cm and 6 cm deep. The pans were placed on a load cell to measure the fuel consumption rate. The initial fuel layer was kept constant at 13 mm floating on a water bed 1 mm below the pan lip. Fuels used in these experiments had boiling points ranging from 383 K to 560 K and included the heating oil previously used (components with a narrow range of volatility), a crude oil (components with large range of volatility), and five single-component fuels: toluene, n-octane, xylene, n-decane, and hexadecane. The general results of the study show that:

- Regression rates increases for initial fuel layer thickness of less than 5 mm and stays constant for fuel layers greater than 5 mm for all diameters.
- average regression rate decreases as the water content increases
- Weathering has an adverse effect on regression rate (up to 35% reduction)
- Water content drops the regression rate significantly (by more than 60% for water content of 40%)
- Constant combustion fraction (x) found to be 0.18-0.39 % of total heat release rate for all the fuels tested.

The most recent research conducted on the burning of crude oil on water is performed by Brogaard *et al*. [55]. A new experimental apparatus was developed to study ISB of crude and other pure oils (Grane crude oil, n-Octane, and dodecane) with different initial oil layer thicknesses. Their study was conducted in order to obtain burning efficiency, burning rate, regression rate, flame height, and boil-over time. The tests were performed in a pyrex glass cylinder (157 and 260 mm ID) surrounded by water. The burning efficiency ranged between 35% to 65% for crude oil and nearly 100% for pure fuels. Over all the regression rates found to

be increasing in the beginning of the burn and then staying constant till the end of combustion period.

1.3.2 Modeling approaches for ISB

In a pool fire burning on water the heat release from the flame heats the unburned fuel to its boiling point. The heat from the burning surface is transferred through the unburned fuel toward the under-lying waterbed. In this scenario the water bed acts as a heat sink and absorbs the energy of the fuel layer. This forms the basis of a simple one-layer conduction model which was first developed by Twadus and Brzustowski [56]. Later this model was developed to incorporate the radiative feedback from the flame to the fuel surface and provide a tool to assess the time for boil-over [57]. A complete review of heat transfer models for burning of a liquid fuel on water is presented by Hristov [58]. This section represents a number of selected publications on the subject of pool fire modeling.

Garo *et al*.[59], studied the combustion of liquid fuels spilled on water in order to predict the time before boil-over starts. They established a one-dimensional, transient, heat transfer model of a burning liquid fuel floating on water to estimate the temperature profile of fuel and water layers, and the onset of boil-over. Their model included in-depth radiation absorption but neglected the motion in the liquid fuel. The time to boil-over is calculated based on the time that is required for water to reach its saturation temperature. The measured heat flux from previous experiments and average radiation absorption were used as input parameters of the model. These two parameters were obtained from experiments on crude oil, heating oil, and several paraffin's. The estimation of time to boil-over required the knowledge of temperature history. The temperature profile of the liquid was described by the transient, one-dimensional form of energy equation which includes the in-depth energy equation ($\rho C_p \frac{\partial T}{\partial t} = \frac{\partial}{\partial x}\left(k \frac{\partial T}{\partial x}\right) + \frac{\partial q_r''}{\partial x}$). It was assumed that the density, thermal capacity, thermal conductivity, and absorption coefficient are constant and the pans are deep enough for the liquid to be considered as thermally thick. The same equations were written for water layer and were solved with their boundary conditions using an implicit finite different discretization. The calculated temperatures for crude oil and heating oil were in a good agreement with experimental data. The experimental measurements of radiative heat flux absorbed by the fuel were parts of the

input for the model. Measurements indicated an exponential drop in amount of received heat flux as the distance from fuel surface increased. The effort to predict the time to boil-over was done by assuming that boil-over starts at a point in time where the temperature fuel-water interface reaches a constant value (water nucleation temperature). The calculated time for boil-over agreed well with experimental measurements unless for initial fuel layers of less than 8 mm. The model result showed discrepancies of about $\pm$15% with experimental data. For example for a pan of 15 cm diameter the calculated time to boil-over for initial thickness of 11 mm was 490-500 seconds where the experimental value was 510 seconds. Additionally, the time to start of boil-over for different pan sizes was decreasing as larger pans were used. For example, the time to start of boil-over for 25 cm pan of heating oil was 450 s and for a pan size of 1 m it decreased to 250 s and stayed constant for larger diameters.

In another study Garo *et al*.[60], investigated the pre-boilover burning rate of oil on a water bed both mathematically and experimentally. Their study aimed to calculate the combustion efficiency (χ) which is the specific fraction of heat feedback to the flame and represented an important tool in assessing the potential of in-situ burning. Their study utilized a one-dimensional single layer and a one-dimensional two layer heat conduction model which were constructed from existing correlation for pool fires. The results of the model were then compared with experimental results performed in their study. The goal of this comparison was to show that the fraction of the heat feedback was not dependent of pool diameter and solely related to fuel properties. It was assumed that there is no convective motion in the fuel layer and radiation and radiation is fully absorbed at the surface (no reflection or re-radiation). The experiments were performed by burning of a layer of liquid floating on water in stainless steel pans of 0.15, 0.23, 0.30, and 0.50 m in diameter and 0.06 m deep. The thickness of the fuel layer was varied from 2 to 20 mm where the initial fuel level was established 1 mm below the rim for all tests. The fuels used were heating oil (a mixture of hydrocarbons ranging from C_{14} to C_{21}) and crude oil (63% Kittiway, 33% Arabian Light and 4% Oural). The experiments were performed with weathered oil (17%, 20%, and 21.5%) and emulsion levels of 10%, 20%, 30% and 40% water content. The results of their experiment showed that for initial fuel layers of 2 mm to 8 mm the regression rate increased gradually and stayed constant for fuel layers of more than 8 mm for different diameters. Similar trend was observed for different diameters. For example the regression rate of 15 cm diameter was 5 mm/s$\times 10^{-3}$ with initial diameter of 2mm

and increased to 11 mm/s$\times 10^{-3}$ for 20 mm of diameter. The corresponding numbers for 50 cm diameter test were 15 and 22 mm/s$\times 10^{-3}$. The higher degree of weathering resulted in lower regression rate. The decrease in regression rate due to weathering for larger diameters found to be more significant compared to smaller sizes. The regression rate of 50 cm pan dropped from 22 mm/s$\times 10^{-3}$ to 14 mm/s$\times 10^{-3}$ for weathering range of 0 to 21.5 %. Emulsion also had an adverse effect on the regression rate which was more significant for larger pan sizes. The mathematically obtained regression rates were based on the χ value that best fitted the experimental regression rates, thus this fraction is an important tool in assessing the heat feedback from flames. The χ value for fresh crude oil found to be 2.9 $\times 10^{-3}$. For thin fuel layers (< 5 mm) the error increased up to 50%. For heating oil this value had to be adjusted to 3.9 $\times 10^{-3}$ and to 2.4$\times 10^{-3}$ for 24 h weathered oil and to 1.8$\times 10^{-3}$ for 24 h weathered and emulsified crude oil (20% water content). It was found that the effective fraction of the heat of combustion that is used to evaporate the fuel is less than 1 percent.

Evans *et al*. [61], made s stronger connection between the operation of ISB and mathematical modeling of the problem. They studied the combustion of crude oil layers on water to assess the potential of utilizing combustion to remove oil spills. This work has two major sections; first section seeks to quantify the process involved in oil spill combustion on open waters and in broken ice channels. The second part of the document is in regard to chemical analysis of the oil, oil residue, and oil smoke with support from Environment Canada. The objectives of their study include measurements of the fraction of the oil remained after each burn, the characteristics of the residual oil, and characteristics of the combustion products. The experiments involved burning crude oil and few pure hydrocarbons (Decane and Toluene) in a 1.2 diameter pan. The fuel layer thickness for these experiments was chosen to be around 10 mm. Other variables were the initial water temperature and the effect of the wind. Measurements of regression (burning) rate, radiation feedback, and the extent of conduction into the oil and water layers were also recorded for further analysis (The ullage distance was kept constant, 12 mm, with using a sensitive diaphragm-type pressure transducer). The burning efficiency for Alberta Sweet crude, Decane, and Toluene was measured around 89%, 99%, and 93%, respectively. Flame temperatures recorded are in the vicinity of 900 C. Maximum burning rate was obtained when a 2.5 m/s wind was applied to the fire (it also decreased the burning time).

The pattern of HRR was a rapid increase to approximately 1.25 MW followed by a slight decrease to 1 MW and then a rise to the peak value which is 2.5 MW due to boil-over. Pure fuels didn't involve with boil-over and their HRR pattern was a rapid rise to the steady state burning following a decline to extinction. Decane and Toluene did not show the same trend (There was some boiling observed for Decane due to higher boiling point).

Both Decane and Toluene were observed to burn as flame sheets around the perimeter of the pan with very little or no flaming at the central core. This is justified with the greater vapor production rate of the pure hydrocarbons. The radiant energy feedback to the surface in center was recorded twice to that of rim areas which is a consequence of the different quantities smoke generated which affects both the absorption of the radiation by and the emission of radiation from the flames. Also, it was found the energy feedback to the fuel surface did not follow the HRR pattern. Smoke production of the fire has dramatic effects on the amount of energy absorbed by the fuel surface. Decane had very small smoke generation and thus less optical obstruction where Toluene is extremely sooty. Crude oil smoke production increased at first and declined at the end.

The temperature profile of the flame and liquid fuel were also informative in terms of the fuel vapor temperature, liquid surface temperature and the vertical gradient in the fuel layer. The vapor temperature just above the liquid surface was recorded a constant of 174 C and 111 C for Decane and Toluene where crude oil showed a temperature between 270-320 C. The Temperature of the liquid surface was highest for crude oil amongst other pure fuels. For the Alberta Sweet crude oil there was no distinct constant temperature liquid layer discernible. The initial water temperature also ranged from 5 to 28 C. There were no systematic effects on the burning characteristics from water temperature since the conduction for relatively thick layer of the fuel is very small. The water temperature is negligible until burning is nearly complete and the fuel layer is thin enough.

The energy balance proposed in Evans *et al*. study incorporates the radiation feedback to the fuel as the energy source while losses are described in reradiation (and reflection), conduction (and convection), and evaporation terms. The radiation flux incident on the surface was estimated to increase from 45 to 60 kW/m^2 whereas the same value near the rim of the pan

recorded to be constant at 18 kW/m2. The maximum temperature gradient in the oil was recorded to be 29 degrees C/mm corresponding to a heat loss by conduction of 2.5 kW/m^2.

The smoke production study also showed that during boil-over the smoke production is reduced by up to a factor of five when compared to that with no boiling. The total PAH contained in the oil residue and the smoke produced by combustion is less than that contained in the oil prior to the experiment.

1.3.3 Weathering

In oil spill accidents the physical and chemical characteristics of oil interact with the physical and biochemical features of the habitat where the spill occurs. These factors determine how the oil will behave and ultimately what will happen to it. Weathering can happen by a number of processes such as evaporation, emulsification, dispersion, and biodegradation all contribute to the fate of oil when it is spilled. Following are a selected number of reviewed publications focused on the problem of weathering.

Wu *et al*.[62], studied the ignition of weathered oil on a water sub-layer. Their experimental study was designed to provide a tool to assess the ignitibility and flash point of weathered fuels in an oil spill accident. Two experimental apparatus were used in their study: 1- The ASTM D56 Tag Closed Cup tester was used to characterize the thermal properties, i.e. flash point (ignition by a small flame) 2- The Lateral Ignition and Flame Spread Test (LIFT- ASTME-1321) was modified and used to study the fire properties i.e. ignitibility (piloted ignition). These tests were performed with Alaskan North Slope and Cook Inlet crude oils with varying thickness of 6-15 mm. For assessing the flash point some oil was poured into the cup test and was heated at a slow constant rate with ASTM D56. Then a small flame was directed into the cups at regular intervals. The lowest temperature at which application of the flame ignites the vapor above the liquid specifies the flash point. Ignitibity of the crude oils were assessed in a 10 cm square shape pan exposed to external heat flux by means of hot spot using LIFT-ASTM E-1321. It was observed that ANS crude oil in its natural state ignited at ambient temperature so there was no external energy needed. When the oil is weathered the ignition delay time decreased with increase in external heat flux and a linear dependency between heat flux and $t_{ig}^{-1/2}$ (t_{ig} : time to ignition) was attained. Also, the higher levels of weathering required application of greater external heat fluxes. For example 7% (by mass) weathered ANS didn't require

external heat flux to ignite but when the weathering degree increased to 20% 4 kW/m^2 was required to initiate the ignition. For Cook Inlet, it was observed that for fuel layer thickness of 8 mm and above the results was independent of thickness and for thinner layers higher heat flux is required. For instance, the required critical heat flux for igniting the 3mm thick Cook Inlet was recorded to be 2.2 kW/m^2 while for same condition and 8 mm of thickness only 1 kW/m^2 was needed. Also the open cup flash temperature measurements of the two crude oil showed that ANS and Cook Inlet flash points increased to 85℃ and 62 ℃ when weathered by 25% and 20% of mass, respectively.

Walavalkar and Kulkarni[63], studied the combustion of water and oil emulsion when subjected to external heat flux under a cone calorimeter. The purpose of their research was to find ways to widen the window of opportunity for in situ burning. The experiments to study the effects of emulsion on ignitibility and combustion were conducted using diesel and two types of crude oil (Milne Point and Alaska North Slope). The diesel emulsion ranged from 20-80% water content, crude oil emulsions ranged from 0-40% water content. The external heat flux ranged from 0 to 14 kW/m^2. It was observed that emulsion burning is very sensitive to the external heat flux and a threshold value exist for each specific water content that below that sustainable combustion is not possible. Emulsified oil was poured on a 28 by 28 cm container surrounded with a pool of water in an outer container. 20 mm of emulsified oil was added to the inner container and was exposed to an external heat flux of constant flux (ranging from zero to the value that starts the ignition). It was found that more water content requires higher flux of energy to initiate the combustion. For instance, the MPU crude with water content of 35% required 13.4 kW/m^2 while for 25% of water content 11.5 kW/m^2 was enough. With 40% water content in the ANS crude oil, the ignition seemed to be impossible. It was also noted that, as expected, the emulsion of the oil has an adverse effect on the burning rate.

Walavalkar and Kulkarni[63], studied the combustion of water and oil emulsion when subjected to external heat flux under a cone calorimeter. The purpose of their research was to find ways to widen the window of opportunity for in situ burning. The experiments to study the effects of emulsion on ignitibility and combustion were conducted using diesel and two types of crude oil (Milne Point and Alaska North Slope). The diesel emulsion ranged from 20-80% water content, crude oil emulsions ranged from 0-40% water content. The external heat flux

ranged from 0 to 14 kW/m^2. It was observed that emulsion burning is very sensitive to the external heat flux and a threshold value exist for each specific water content that below that sustainable combustion is not possible. Emulsified oil was poured on a 28 by 28 cm container surrounded with a pool of water in an outer container. 20 mm of emulsified oil was added to the inner container and was exposed to an external heat flux of constant flux (ranging from zero to the value that starts the ignition). It was found that more water content requires higher flux of energy to initiate the combustion. For instance, the MPU crude with water content of 35% required 13.4 kW/m^2 while for 25% of water content 11.5 kW/m^2 was enough. With 40% water content in the ANS crude oil, the ignition seemed to be impossible. It was also noted that, as expected, the emulsion of the oil has an adverse effect on the burning rate.

Fan *et al*.[64], discussed processes and factors for estimating time period windows of in-situ burning of spilled oil at sea using available data in the literature. Three crucial steps were identified to assess the time window. Several groups of key factors determine the success of an in-situ burning. The first was to determine the time it takes for evaporative losses to reach an established limitation and compare this time with estimated time of ignition at the ambient sea and wind temperature. The first group is related to ignitibility of floating oils (oil composition, vapor pressure, flash point, boiling point, evaporation rate, sea temperature and wind speed). The second was to determine the water up-take (degree of emulsion) of the spilled oil and compare it to the available data on ignitibility of water-oil. The second group is related to the change in oil properties due to oil weathering during the response time. And the third step was to determine the required heat load from the igniter to increase the temperature of the fuel surface enough so that oil reaches its flash point temperature. This group contains operational and technical considerations, and includes the capability of the resources (vessels and booms) to contain and thicken floating oil and etc. An example is provided to demonstrate the time estimation for a spill scenario. Alaskan North Slope crude oil at sea temperature of 5℃ with wind velocity of 10 and 5 m/s was assumed. It was assumed that the oil is ignitable up to 20.4% evaporation and 25% water content. The trend lines for evaporative loss vs. time and increase in water content vs. time at the specified wind speed was extracted from reported data in literature. It was found that after 9-22 hours from the spill incident the flash point of oil becomes 53℃ (proper temperature to use gelled gasoline igniter) at various wind speeds (5-10 m/s).

Frit-Rasmussen and Brandvik [65], investigated the ignitability of Troll B crude oil (very low wax component) weathered under simulated Arctic conditions (0%, 50% and 90% ice cover). The experiments were performed in different scales at SINTEF's laboratories in Trondheim, field research station on Svalbard in the Barents Sea. The result of the experiment showed that the ignitibility of the Troll B crude oil will increase with more percentage of ice coverage. For a 50% ice covered basin the ignition after 27 h of weathering became impossible where for 90% of ice coverage the weathering time could be increased to 168 h. The burning effectiveness (%) measured with the burning cell was generally high, and varied between 40% and 80% due to different degrees of weathering and heterogeneity in the samples.

1.3.4 Environmental aspect of ISB

In ISB surface oil is removed by transferring most of it into the atmosphere in the form of combustion products and soot. ISB reduces the environmental threat imposed by the oil slick, however, the environmental threat posed by the airborne plume will increase. In both the burned and unburned scenarios, a weathered residue is left on the surface to pollute water-surface resources or shorelines. The amount of residual oil would be much greater without burning and is considerably less weathered. Decision makers need to compare the effects of burning versus not-burning and choose the option that provides the greater net benefit to the environment. Therefore, an analysis on the environmental impact of ISB is essential. The reviewed papers below are presented in order to give a better understanding of the environmental impact of ISB.

Nyden *et al*.[66], conducted a series of laboratory measurements to explore the extent to which benzene and other aromatic components are destroyed when crude oil is burned on open seas. These compounds are considered hazard for human health. The atmosphere above a pan containing Alaskan North Slope crude oil was monitored with a remote sensing FTIR spectrometer during both evaporation and burning. The environmental impact of large sclae in situ burning was examined using different sampling techniques in junction with the FTIR method. A pan 230 m^2 located on Little Island in Mobile, Alabama was used as the test platform. Spectra were measured over a 7 m path about 30 m downwind of the fire. The analyzed data of the large scale test did not show traceable amount of aromatic hydrocarbons (C_6H_6) presumably due to low atmospheric concentration. Significant release of C_6H_6 and

other aromatic compounds are inevitable consequence of an oil spill but it is important to understand whether burning of oil will increase the amount of released aromatics or not. Small-scale test in 10 cm diameter pan containing 540 g of oil (enriched with 20 g of C_6H_6) were conducted. Two conditions with 10 cm pan were studied: 1- Evaporation, 2- Burning. It was found that the concentration of hazardous chemicals (C_6H_6) is lower in burning condition compared to evaporation scenario in a 10 cm pan. Thus, they concluded that the aromatic components are partially destroyed in the burning process. Their conclusions were based on the small scale tests with enriched fuels, thus generalizing the results to large scale, where the burning characteristics is very different, does not seem reasonable.

Mulholland *et al*.[67], investigated the smoke production of crude oil in a 1 m diameter pan and a 2.7 m square pan (equal to 3.1 m diameter). The smoke yield was measured using the carbon balance method by two different procedures: one involved continuous sampling to gas analysis equipment and the second used a portable air-borne smoke sampling package. Three tests were performed at each pan size with a fuel mixture (80% Murbane and 20% Arabian Crude Oil). The average smoke yield by the two methods for larger size agreed well, 0.148 g/g. The value for 1 m diameter pan was 0.1g/g with the first approach and 0.06 g/g with the second approach. The difference in the values of two approaches in the 1 m diameter pan is caused by an issue of sampling in boil-over period. The corresponding burning rate for the two pan sizes were 0.022 and 0.26 kg/s. Over all, he concluded that smoke yield increases as the pan diameter increases up to a value of 2-3 m diameter and stays relatively constant up to a pan diameter of about 15 m.

Evans and Walton [68], investigated the combustion process and smoke generation of crude oil in a 1.2 m diameter pan seating on a water layer. Initial thickness of the oil slicks varied from 2-25 mm. Burning characteristics of three types of crude oil (Alberta Sweet, La Rosa, and Murban) was investigated using a large calorimeter hood. Flame temperature, oil and water temperature, heat release rate, radiation feedback to the fuel surface, and radiation to the surrounding were measured. For thicker oil slicks the heat release rate approached a steady-state, while decreasing slightly, prior to reaching the boil-over phase. The quasi-steady burning phase for Murban and alberta Sweet crude was approximately 0.95 MW (840 kW/m^2) and 1.15 MW (1000kW/m^2). The energy release rate per area was found to be higher for larger pans.

Also, the peak energy release rate value of LaRosa crude was recorded to be 50% greater than Murban crude. Final fuel layer thickness found to be around 0.6-1.2 mm. The analysis on the smoke was done with sampling the smoke at two points of combustion prior to intense burning phase. The Polycyclic Aromatic Hydrocarbons (PAH) content of the smoke was found to be nearly equal to the PAHs content of crude oil, meaning that the combustion process did not destroy these toxics.

Shiu *et al*.[69], reported the water solubility for 42 crude oil and petroleum products in water as a function of temperature, salinity, oil weathering and water-to-oil volume ratio. Their study was concerned over the toxicity viewpoints. The crude oils and petroleum products which were subjected to solubility determinations were weathered by tray evaporation or gas stripping to a defined volume percentage loss. The water used for emulsification process was double distilled. Salt was sodium chloride (ACS grade). All solvents and chemicals used were distilled-in-glass grade. For solubility measurements crude oil solutions were prepared by adding approximately 10 ml of oil to 50-100 ml of water in a 125 ml separatory funnel. The mixture was shaken with wrist action shaker and were gently stirred with a magnetic stirrer for 24 hours and then placed in a temperature bath for 48 hours prior to analysis. The aqueous solubilities of crude oils and petroleum products were determined by three methods: (i)purge-and-trap (vapor) extraction followed by capillary gas chromatograph (GC) analysis, (ii)solid sorbent extraction followed by high pressure liquid chromatography (HPLC), and (iii) fluorescence analysis. Their study showed the change in water soluble fraction concentrations as a function of water-to-oil ratio for three different crude oils. The concentration of the water solubale fraction (WSF) decreased as the water-to-oil ratio increased and, more importantly, the composition of the WSF changed as the ratio changed. At low water-to-oil ratios, for example 5, the WSF was mainly (80% of the total) composed of benzene, toluene, ethylbenzene and xylenes. As the water-to-oil ratio increased, these compounds became less important and accounted for a smaller proportion of the dissolved compounds. The result of their study indicated that the water to oil ratio during oil and water equilibration can significantly influence the concentration of the water soluble fraction that is produced.

Evans[70], investigated means to model smoke yield (mass of smoke particulate produced per unit mass of fuel burned) of pool fires in in-situ burning operations in field tests. In laboratory

tests of liquid hydrocarbon fires, the entire smoke plume can be can be collected and measured with number of techniques. However, quantifying the smoke yield and movement of plumes in real life burning scenarios is hard and assessment of the exposure to population is necessary. Field experiments with effective diameter of 11-14 m were conducted in fire resistant containment booms utilizing the Carbon Balance method to analyze the smoke samples. The analysis was done under three assumptions: 1- The smoke particles are mostly carbon, 2- Samples are collected during a proper time period to average out the natural fluctuations in fire and plume, 3- No preferential separation of smoke particles occur in the smoke plume up to the point where sample is taken. Six measurements were made during two offshore burns of Alberta Sweet Blend Mix crude oil. A mathematical equation for calculating the smoke yield was used and its result showed a reasonable agreement with experimental results (14.8-15.5%). The movement of the smoke plume downwind of the fire was also modeled using the NIST developed Large Eddy Simulation (LES) model in a 6 by 2 km area. The model results were also in agreement with experimental results.

Faksness *et al*.[71], studied the chemical composition and toxicity of a water soluble fraction (WSF) of oil versus the underlying water after in situ burning (ISB) in a laboratory experiment. A system for allowing water sampling after ISB was developed. Seawater samples and oil were collected prior to and immediately after ISB, and chemical analysis was conducted. The chemical characterization of the water showed that the disappearance of water soluble oil components (BTEX, naphthalenes and 2–3 ring PAHs) during ISB was insignificant. The results of toxicity tests were compared with regular WAF systems with unburned weathered oil, and indicated no increase in toxicity in the underlying water after ISB.

Notarianni *et al*.[72], studied the smoke production from large pool fires as a consequence of in situ burning of crude oil spills. Two major NIST facility were used to measure the smoke yield from crude oil pool fires of 0.085 m to 0.6 m. Experiments were conducted under small and large cone calorimeters and the effect of fire diameter on smoke yield was studied. In addition, larger scale experiments (up to 3 m in diameter) were conducted with cooperation of Fire Research Institute in Tokyo. The mesoscale experiments were performed in United States Coast Guard Fire and Safety Test Detachment Facility with sizes of 6.88 m, 12 m, and 17.2 m. Louisiana crude oil and Murban were burned and smoke samples were analyzed with the

carbon balance method. The result of their experiment shows the smoke particulate yield to be around 13%. Also, 2 m diameter had same smoke yield compared to larger sizes (6.88 m to 17.2 m).

1.4 ISB in Ice

Oil spill cleanup in arctic water introduces substantial difficulties because of the total or partial coverage of ice for most of the year. When oil is released underneath the ice surface, the oil would assemble in the ice sheet lower surface. The spring break-up causes the hidden oil to emerge from lower ice sheets forming pools of oil surrounded by ice walls. Typical dimensions can vary from 5 cm to 100 cm depending on the width of the cracks formed during breakup [73-76]. A simulated experiment on subsurface-surface migration of oil in ice is shown below.

Figure 1.5: Rate of oil exposure from beneath sea ice originating from three simulated sub-sea blowouts [9].

Most in situ burning research has focused on open sea burns (warm and cold waters) while varying factors such as oil type, emulsification, degree of weathering (evaporation) and

atmospheric conditions. A relatively small amount of published research has focused on oil spills in ice cavities. This forms the motivation of the current study to explore in situ burning as an application to oil spill response in icy conditions. Experiments are performed using ice cavities of varying diameters to measure mass loss rate when ignited. The expansion of pool fire in the course of combustion is an important parameter to be considered. This particular behavior creates a unique condition which is different from burning of oil slick burns on water and will be discussed thoroughly. A mathematical expression is proposed to estimate burning rates of crude oil in ice cavities of varying size. It is shown that the dynamic environment created by the melting ice creates unique physical behavior unlike an oil slick burning on water [17-20].

Early research and development on *ISB*, which focused on its use for spills on and under solid sea ice, demonstrated its effectiveness in large-scale experimental spills in the Beaufort Sea in 1975 and 1980. More recently, high-level research has addressed using ISB for spills of various concentrations in pack ice and especially in slush and brash ice. The technique has proved very effective for thick oil spills in high ice concentrations and has been used successfully to remove oil spills resulting from pipeline, storage tank and ship accidents in ice-covered waters in Alaska, Canada and Scandinavia [4].

As interest in Arctic oil exploration and production continues to increase, the industry must take steps to ensure that in situ burning is available when needed. This requires that *ISB* is incorporated in contingency planning and that response organizations have the necessary resources and training. Oil spill clean-up operations in the Arctic are to be in-line with regulations of the Arctic Council and in accordance with Annex I of MARPOL (Marine Pollution convention) and IMO (International Maritime Organization).

Figure 1.6: Burn of oil in melt pools at Balaena Bay, NWT 1975.

U.S. research evolved out of the need to develop response techniques after oil production on Alaska's North Slope increased. Norway has also made significant and notable contributions to oil spill research in Arctic waters as they too are an Arctic oil producing nation. [15, 16] As sea ice retreats more each summer the Arctic seaways will inevitably open up to commercial shipping traffic. This increased traffic augments the potential for oil spills to occur as well as the need for more research on how to deal with spills in these conditions. Additionally, with increasing pressures to explore for oil in Alaska's Outer Continental Shelf (OCS), even more potential for oil spills in the presence of ice is possible. Many environmental organizations look at the lack of experience of oil spill response in the presence of ice as a major factor in their opposition to OCS development. The vast majority of offshore operations occur in temperate climates and as a result the oil spill response techniques are tailored to those conditions.

In situ burning research began in the late 1970's at Energetex Engineering. The earliest published research was conducted at the Environmental Protection Agency's Oil and Hazardous Materials Simulated Environmental Test Tank (OHMSETT) facility in Leonardo, New Jersey. A three part research project, conducted between 1984 and 1987, focused on burning of crude

in varying ice concentrations in order to explore the range of conditions in which in situ burning is possible. The major conclusion of this preliminary study was that a 2.5 mm slick can sustain a burn on cold water and that the ice concentration and burn efficiencies are inversely related. [1-3]

Smith and Diaz[77], investigated the small and large scale burning experiment of Prudhoe Bay crude in broken ice in order explore the range of conditions in which the oil can be burned and to determine burning efficiencies of such burns. Laboratory tests were performed in a small aluminum ring around 60 mm in diameter. The slick thickness varied from 2 to 10.5 mm in two different temperature of saline water. In the laboratory tests the minimum slick thickness which resulted in successful ignition was found to be around 2.5 mm for brackish water at temperature of 2-6℃. The same thickness found to be 2 mm for brackish water of temperature around 20 ℃.

The corresponding burning rate for two water temperatures found to be 0.2-0.4 mm/min (30-40% efficiency) for cold and 0.5-0.6 mm/min (60-70% efficiency) for ambient temperature.

The fumed silica wicking agent was used in the experiments found to be effective on enhancing the burning.

Four tests were performed in the OHMSETT tank within a 46.5 m^2 boomed area with varying ice coverage (45-60%), fuel layer thickness (2-4 mm), and wave conditions. Fresh and lightly weathered Prudhoe Bay crude oil burned with burning efficiencies of over 85% for all the tests. The flame spread rates varied from 1.3 to 2.4 m/s, higher ice coverage resulted in less flame spread rate. The thicker oil slick (4mm) and moderate ice coverage (40%) resulted in a higher efficiency (95%). The regular wave generated did not affect the flame spread significantly and caused a reduction of about 5-10% in burning efficiency.

1.4.1 Large-scale experiments

Smith and Diaz [75, 78], reported in-situ burning of two types of crude oil in broken ice. Their experiments were performed in OHMSETT tank in a 5.8 m by 7.3 m test area enclosed by a rigid wood boom. The test area was floating in the middle of a tank. Slick of oil was created with an underwater hose delivering 55 gallons of oil to a point approximately 0.6 m beneath the test area. The data acquisition was done with video recorders (to capture the ice coverage) and

a Climatronic weather station (to make environmental measurement). The water temperature was below 4 ℃ and air temperature was between -6-7 ℃ with wind speed of 2-8 m/s. The result of the burnings indicated that fresh and sparged Prudehoe Bay oil burned in ice coverage of 75-90% removing 60-80% of the oil slick (by mass). Fresh and sparged Amualigak crude oil yielded burn efficiencies of 60-70% in 80-90% ice coverage.

After Smith and Diaz, concluded that in situ burning was a viable means of oil spill cleanup in arctic waters, research to further determine the parameters began in earnest. In 1986, Brown and Goodman [79], conducted a series of burn experiments at the ESSO Research ice basin (30 m by 56 m with varying depth fro, 0.75 to 3 m) in Calgary with Norman Wells crude oil. 25 tests were carried out (by 10-40 L of oil) to evaluate the critical parameters of burning with studying influences of oil weathering, oil thickness, and lead geometry. The water in the basin was frozen naturally to an average thickness of 45 cm. Chain saw were used to cut desired size of basins (1 by 10 m, 5 by 5 m, 5 m diameter, and two triangles each with 1 m base and 4 m perpendicular). Based on the results of the experiments it was found that weathering degrees of up to 20% didn't affect the burning parameters. The efficiency was affected mostly by the fuel thickness and wind speed. For oil thicknesses of around 3 mm with wind speed up to 2.5 m/s the burning efficiencies of most experiment were obtained around 80-90%. The effect of lead geometry on burning rate and burning efficiency found to be important. Where ever oil was confined in a corner by the force of wind (and increased in thickness) relatively higher burning efficiencies were obtained (10%-20% higher). However, no direct relation between ice geometry and burning rate were shown.

Sveum *et al*.[46], as part of spill contingency plan for the Reindalen 1 drilling operation in Norway, researched in situ burning of oil spill in snow. Field experiments with Oseberg crude oil and diesel (1000 L) yielded burn efficiencies of above 90%. The small scale laboratory test yielded 90% to 99% burning efficiency for diesel and 90% to 98% for crude. The crude oil in field tests were ignited with delays up to 13 days after spilling the fuel. But, the burning efficiency didn't change.

Guenette *et al*.[80], also reported field experiments conducted on frozen fjord Spitsbergen, Norway to evaluate the feasibility of conducting in situ burning in a marginal ice zone. Large scale burns (4-10 m^3 oil in volume) were conducted with fresh and emulsified crude oil in a 15

m diameter basin partially field with ice. A series of small basins were also excavated in the ice a short distance downwind of the main basin and contained crude oil at different degrees of evaporation and emulsification to study flame spreading. Measurement instruments (Thermocouples and heat flux gauges) were installed in a steel tower which was placed in the basin to record temperature, heat load and heat fluxes. The ambient temperature ranged from -20 to 5 ℃ and wind speed ranged from 5-15 m/s with some occasional calm periods with no wind. The weathering degree ranged from 0-25 % in volume and water content also ranged from 0-66 %. All experiments with fresh oil in slush ice yielded burning efficiencies of 99% however when 18% weathered oil with 20% water content was used the burning efficiency decreased to 95%. In another experiment a mixture of fresh oil and 50% water to oil emulsion (4000 L fresh oil and 5700 L emulsified) was burned in a contained area with ice coverage of 50% with efficiency of 98%. The measured flame/smoke temperature varied from 400-1370 ℃ with large fluctuations, higher temperatures were measured 3.3 above the surface. Some of the fluctuation were reported to be caused by turbulent eddies of the fire plume which after stabilizing over the entire pool area started a cyclic production of large fire balls.

Buist *et al*.[81], conducted a series of outdoor burn tests at the scale of 30 m^2 with herders and crude oil in a test pool containing pieces of sea ice. These tests were aimed to investigate the concept of using herding agents. The results of these test showed that 1- crude oil slick that were initially un-ignitable were contracted by herder could be ignited and burned in situ both in brash and slush ice condition at sub-zero temperatures (up to -17 ℃), 2- the removal efficiencies measured for the herded slick were comparable to but slightly less than the theoretical maximum achievable for equivalent size, mechanically contained slicks on open waters, 3- The removal rate for the slicks was in the range expected for equivalent sized mechanically contained slick on open water. Table 1.1 below shows a complete review of experiments performed on ice in the last 45 years.

Table 1.1: Chronological review of large-scale ISB experiment on ice.

Authors / year	Ref.	Description	Results: Burning rate/eff.
Glaeser & Vance, 1971, McMinn, 1972	[82] [83]	First series of experiments of ISB on solid ice by USCG in Barrow, Alaska, 1971.	Burning efficiencies of +80% was achieved.

NORCOR, 1975	[84]	54 m^3 of fresh crude oil was released under landfast sea ice in the Arctic. Once the oil came up in the spring, ISB was used on melt pools of oil.	Individual burns up to 90% efficiency. One burn removed 20 m^3. Overall 60% of oil removal.
Energetex, 1977	[85]	Large melt pools of crude oil were burned to study the effect of wind and herding agents on minimum ignitable thickness.	Wind speed up to 7 m/s and herding agents were found to help the process of burning. Efficiency reported 85%.
Dickins & Buist, 1981	[9]	Approximately 19 m^3 of crude oil was discharged under the first-year land fast ice 8 kilometers off shore of McKinley Bay in the Beaufort Sea. Melt pool of varied size (1-100 m^2)were formed before the spring break up.	Fifty percent of the fuel were burnt with ISB. Individual melt pool burn efficiencies were thus on the order of 90%. The average burn rate of small melt pool slicks was 1 mm/min.
Nelson & Allen, 1982	[86]	Oil from an experimental spill under landfast sea ice in Alaska was released to the surface by drilling into the encapsulated lens, and burned after it naturally rose to the surface.	Estimated 95% removal efficiency was reported.
Buist *et al.*, 1983	[87]	Small field experiment with crude oil and emulsions that appeared on the ice surface in spring and a control slick of crude oil were ignited and burned.	73% oil removal efficiency was achieved with the crude oil and a 63% oil removal efficiency was achieved with the emulsion (50% water content).
Bech *et al.*, 1993 and	[46] [88]	Series of small burns of fresh, weathered and emulsified crude was	Fresh, un-emulsified crude oil (8-mm thick) burned

Guenette *et al.*, 1995		carried out on landfast ice at Svalbard in 4m2 basins cut in the ice and filled with water (simulating melt pools).	with removal efficiency of 85+%. And decreased to 75+% with increasing water content. The burn rate decreased for both increasing evaporation and increasing water content.
Dickins *et al.*, 2008	[89]	As part of an experimental spill under landfast ice at Svalbard in 2006, crude oil that surfaced on the ice at the end of the experiment was ignited and burned.	More than 95% of the oil was consumed in the fire (a slick of 27% evaporated Statfjord crude initially 35mm thick and 69 m^2 in area).

1.4.2 Small-scale experiments

The sole study on small-scale ISB of liquid fuel in ice confinements is done by Bellino *et al*.[90]. They studied the mass loss rates of an oil (3:1mixture of motor oil and petroleum ether) burning in ice channels. The ice channel width was varied from 1-4 cm. The mass loss rate of the fuel was captured by placing the setup on top of a load cell. The Temperature profile of the fuel layer was also obtained by use of a thermocouple tree alongside the center of channel. This study exhibited the complexity of performing ISB in melt pools due to changing geometry of channel. This study remains the only study performed to investigate ISB on ice in a laboratory-scale size.

1.4.3 Recent studies and gap in knowledge on ISB in ice

Arctic Standards report prepared by PEW Charitable Trust is a recent document (September, 2013) concerning the oil spills clean-up methods in Arctic. Consistent requirements on how to design, build, install, and operate equipment to safely explore and develop oil and gas resources and respond to accidents in the region using best Arctic science, technology, and practices are developed. Arctic standards discussed in the report account for the area's remote location, lack of infrastructure, and unique operating conditions due to the severe and changing

climate to ensure that oil spills are prevented and the capability exists to respond to a worst-case oil spill [39].

In Situ Burning in Ice-Affected Waters: State of Knowledge Report prepared by Arctic Oil Spill Response Technology Joint Industry Programme (JIP) is the most recent document (October 2013) reviewing the current state of knowledge and technology on the ISB in ice affected waters [4]. The report involves a remarkable chronological review of accidental or experimental ISB that is performed in warm and icy waters. Their review of literature on ISB in ice is presented in three categories of relevant references:

1. Burning oil on solid ice (in melt pools or when spilled directly on ice);

2. Burning oil/snow mixtures; and,

3. Burning oil in slush, brash, drift and pack ice.

The first category is the most applicable part to the current study. Burning of crude oil inside an ice cavity most resembles burning oil in melt pools. The current study will only focus on a scenario for burning of crude oil in small ice cavities. A literature search identified little published data on the burning of oil in an ice confinement. Furthermore, the number of publications on the burning behavior and the dynamic of ice and fuel is found to be even lesser. Due to this reason, current study is performed to fill a gap in knowledge identified through this literature review. Despite the research over the past 45 years, very few studies have publicly addressed the laboratory analysis of oil burning in an ice cavity. Current study presented here aims for systematic measurements of the experimental parameters and better observation of this complicated phenomena. Incorporating the experimental measurements into a basic predictive model is one of the objectives of this study.

1.5 Objective of the current study

There is a need to understand the ISB in ice confinements (dynamic deformation of ice due to unique condition and burning characteristics). To properly address the problem, the following questions must be answered. What is the role of the cavity dynamics on burning of crude oil? What are the burning characteristics in ice cavities of varying sizes? Is it possible to model the burning rate of crude oil in this setting and how it can be generalized for larger scale burnings

in ice? The objective of this research was to study the role of cavity dynamic and determine burn efficiencies of crude oil for different size of ice cavities. Also, to develop a mathematical model to predict burning rate of liquid fuels using the data obtained from experiments. To achieve the goals of this research, several aspects of burning inside a circular ice cavity is investigated. The change in shape of the ice cavity and the oil layer thickness are recorded using a combination of visual images, mass loss, and temperature data along the centerline of the cavity to form a set of data for further analysis.

1.6 Thesis layout

This thesis is organized in five chapters and two appendixes. Chapter 1, being the literature review, is organized to introduce the problem of performing ISB in ice cavities and different aspects associated with it. Chapter 2 reviews the experimental apparatus and parameters involved in this study. Chapter 3 is intended to present the results of the experiments (burning rate and burning efficiency) and provide detailed discussions on geometry change of cavity and temperature profile of the fuel layer. Chapter 4 presents the proposed model for estimating the burning rate and burning efficiency of a fuel in a dynamic geometry. Conclusions and future work of this study are discussed in chapter 5.

A condensed version of the thesis has been accepted for the 35th International Symposium on Combustion, San Francisco, August, 2014. Appendix A contains the original document submitted to 35th International Symposium on Combustion. In Appendix B additional material and photographs are provided to provide the reader with an appreciation of the work.

Chapter 2

2. Methodology

An experimental approach consisting of observations and measurements was used to conduct this research. A detailed description of experimental design and parameters related to this study is provided in this chapter.

2.1 Experimental setup

Figure 2.1, shows the experimental apparatus which was used to study the combustion parameters of crude oil in 5 cm diameter ice cavity. Similar setups were used for diameters of 10, 15, and 25 cm. Three trials at each diameter were conducted to form a data set of twelve trials. Each experiment utilized an ice block with a circular cavity excavated in center. Then, Alaskan North Slope (ANS) Crude Oil was added to the cavity to a certain height. The ice block was placed on a drip pan on top of a load cell (Sartorius "ED 6202S-CW" precision of 0.01 g and 5 data points per second) to record the mass loss. Later, this mass loss was processed to obtain mass loss rates. The loss due to water evaporation assumed to be minimal and ignored. The data for mass loss of ANS crude oil at 5, 10 cm were collected. For the case of D = 15 and 25 cm, the weight of ice block was over the limits of load cell. Because of this, the mass loss rate trend line is not available, but with using 3M oil absorbent pads the remaining oil was collected carefully to approximate the remaining fuel and then calculate burn efficiency. In addition several free burn tests were performed using steel pans with diameters of 10, 15 cm to create a basis to compare the results of burning in ice cavity with free surface pool fires.

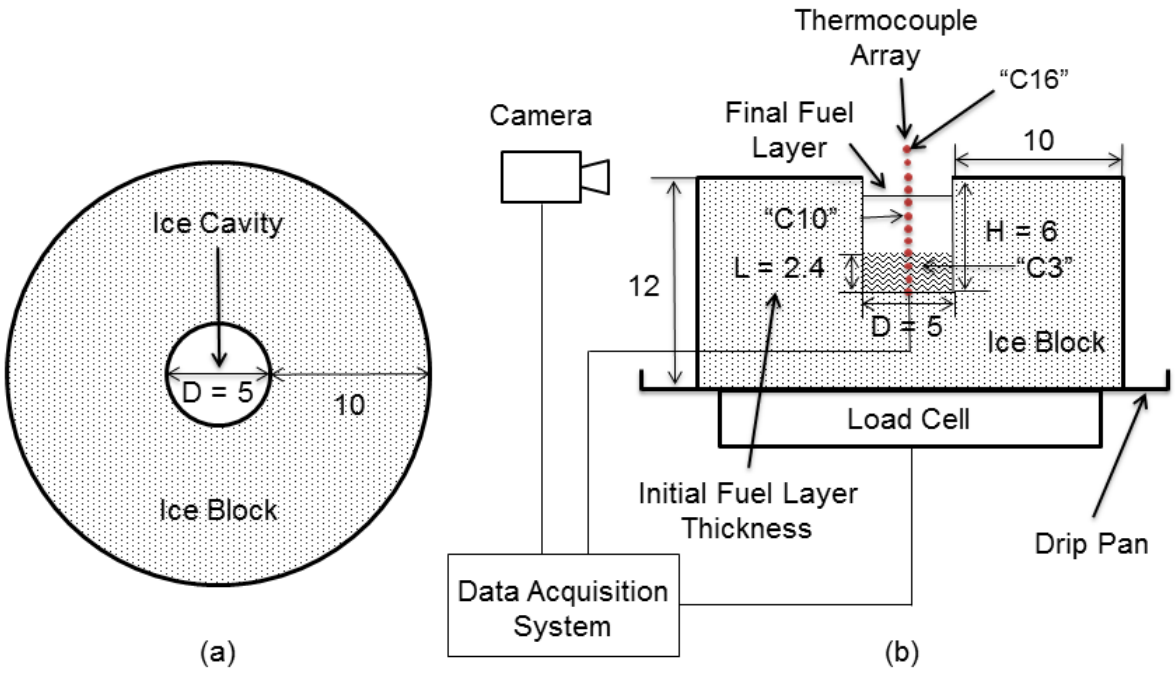

Figure 2.1: Experimental setup. (a) Top view and (b) side view. All the dimensions are reported in cm.

The ice blocks with D = 5 and 10 cm were equipped with Thermocouples (type K, gauge 36, diameter of 0.13 mm) to acquire a temperature profile of the liquid layer to use in mathematical model. A total of sixteen thermocouples, installed on one array, were utilized to record the temperature at different elevation (0.5 cm apart) and obtain temperature of fuel surface and fuel-water interface along centerline of cavity. Thermocouples are shown in Fig. 2.1, along the centerline of the cavity with small solid circles.

ANS crude oil was allowed to burn to extinction in a quiescent environment. Crude oil is a complex mixture of hydrocarbon of various molecular weights and shows a transient set of properties i.e. boiling point of ANS crude oil varies from 38 °C to 570 °C. Table (2.1) lists the relevant properties of crude oil [41].

The experimental procedure comprised of placing the ice block on the load cell then pouring liquid fuel at a certain height (at initial temperature of 20°C) and igniting it immediately. The igniter was held 3 seconds for all trials. All trials represented in this study were allowed to burn to extinction.

Table 2.1: ANS crude oil properties at 25 ℃.

Liquid Density (kg/m^3)	868.6
Viscosity (centi-poise, cP)	11.04
Flashpoint (°C)	-6.7 – 32.3
Boiling Point (°C)	38 – 570
Thermal Conductivity λ (W/m K)	0.132
Specific Heat, C_p(kJ/kg K)	2.3
Latent Heat L_v (kJ/kg)	250

2.2 Experiment parameters

The first step in analyzing a liquid fuel fire is to characterize the physical dimensions of the fuel spill or pool. The area of the initial body of fuel will correlate to the size of the resulting fire. In addition, burning liquid fuels in an unstable substrate (ice cavity) require further arrangements on the quantity of the fuel used in the cavity to prevent overflow of the fuel from the cavity.

Figure 2.2 shows the chief dimensions of a pool fire in an ice cavity. Diameter (D) of the cavity is the most influential factor on the characteristic of burning. The burning regime in classic literature of liquid fires is determined based on the fire area which is a function of diameter. For this study burning in laminar and transient regime (1 < D < 30 cm) was considered.

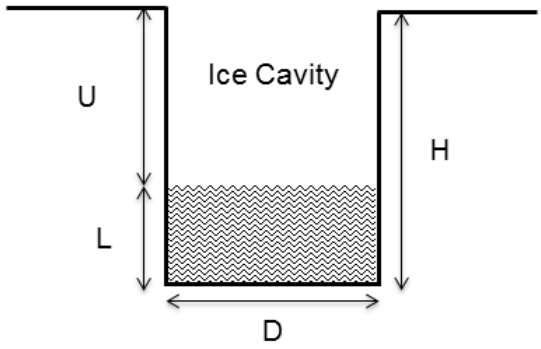

Figure 2.2: Dimensions of cavity.

Four sizes of cavities (D = 5, 10, 15, and 25 cm) were chosen to replicate the burning behavior of transient regime in ice cavities. Total depth (H) of the cavity is also an important factor in relation to the fuel layer thickness (L). Fuel layer thickness is the other factor that is influential on burning behavior. In smaller diameters a large ullage might result in unsuccessful ignition since the flame is deep in the cavity and is air deprived. In typical liquid fires in vessels, because of the regression of fuel surface the ullage is increasing proportional to regression rate. However, burning in ice cavities is different in terms of change in fuel layer thickness. Due to melting of ice and accumulation of water underneath the fuel layer, the fuel layer rises, thus ullage height will be decreasing at all instants during combustion period. There are two possible extinction scenarios for burning of the liquid fuels in an ice cavity: 1) natural extinction where the fuel layer does not reach the ice surface, 2) spillage of the fuel out of the cavity where the fuel surface rises up until it has reached the ice surface. Table 2.2 summarizes the dimensions for some of the preliminary tests. The depth and fuel layer thickness (or depth (D)-initial fuel layer (*L*)) were chosen based on the data obtained from preliminary tests to prevent over flow and spillage during combustion.

Table 2.2: Determining the fuel layer thickness for 5 cm cavity.

ANS crude oil	Initial ullage (cm)	Initial fuel layer thickness (cm)	Depth (cm)	Fuel layer/Depth (cm)	Final ullage (cm)
D = 5 cm	4	2.1	6.1	0.34	1.2
D = 5 cm	3.6	2.4	6	0.4	0.7
D = 5 cm	3.1	3	6.1	0.5	0.3
D = 5 cm	2.8	3.3	6.1	0.54	Over flow

As shown in Table 2.2 for 5 cm trial the ratio of fuel layer thickness to depth should be less than 0.5 in order to have a natural extinction. The initial fuel layer thickness for other diameters was selected to be around 1.5 cm based on previous studies stating the minim required thickness of oil slick needs to be between 1cm and 2 cm to have successful burning [47].

Table 2.3 shows the ice cavity dimensions and crude oil volume for each diameter. These values were chosen on a basis that fuel burns until the extinction is reached by natural means and not by overflow from cavity.

Table 2.3: Experimental matrix.

D (cm)	*H* (cm)	*L* (cm)	Volume of fuel (ml)
5	6	2.4	50
10	8	1.6	125
15	10	1.6	290
25	10	1.5	710

When a liquid fuel is burned in a confinement such as a vessel of diameter (*D*) the ullage (U) increases as the liquid is consumed. However, burning in ice cavities is different because the ice melts because of flame heat flux and similarly causes water accumulation in the ice cavity. Because of melting of ice and accumulation of water underneath the fuel layer, the fuel layer rises, causing the ullage to decrease. This behavior results in two possible extinction scenarios for burning of the liquid fuels in an ice cavity.

First scenario is the natural extinction where the fuel layer does not reach the ice surface and extinguishes because of attainment of a critical layer thickness, where sufficient vaporization is not possible because of heat losses. This behavior is the commonly observed extinction phenomena in oil slick fires in water. This extinction is shown in Fig. 2.3 a.

The second extinction is because of the rapid change in geometry of the cavity because of melting of ice and corresponding water formation. The accumulation of water underneath the fuel layer can result in spillage of the fuel out of the cavity because of rapid melting of water. This makes the confined spill bounded by the cavity walls into an unconfined spill scenario. The fuel pouring out of the cavity forms a thin fuel layer on the ice surface which extinguishes quickly. This behavior is relatively unexplored in fire science literature. This type of extinction is shown in Fig. 2.3 b

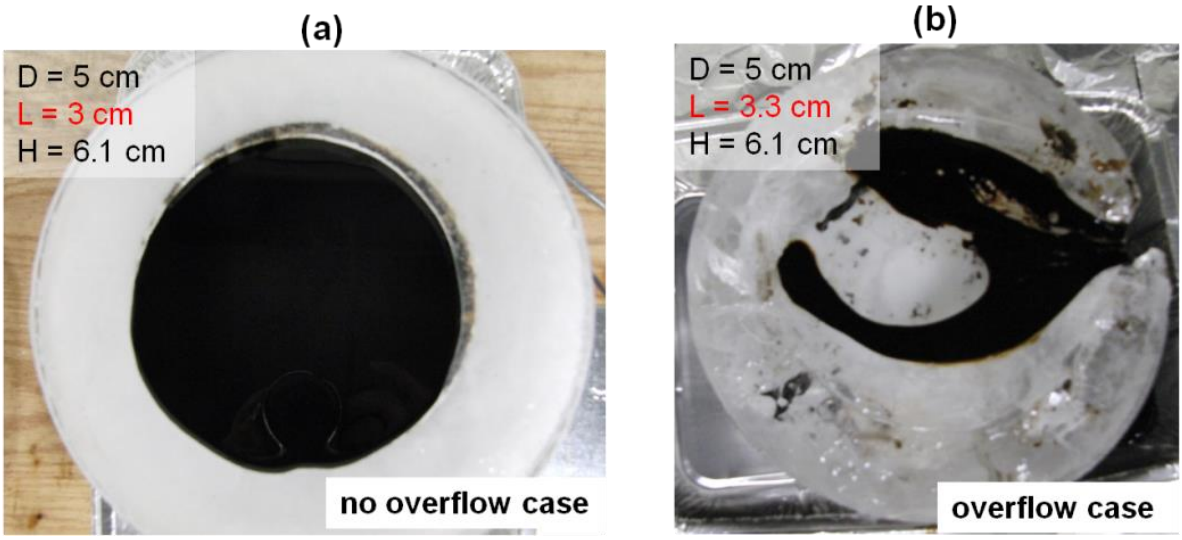

Figure 2.3: Extinction scenarios: (a) Case where oil is confined in the cavity and extinguished because of attainment of a critical thickness (~3mm), and (b) extinction observed due to overflow. ANS crude oil, D = 5 cm.

In this study, it was decided to explore conditions necessary for natural extinction alone and extinction scenarios due to overflow were not included in the analysis. A critical ratio defined as height of cavity/fuel layer thickness was established using ANS crude to denote the threshold where spillage of fuel out of the cavity is experimentally observed. A series of preliminary tests with different cavity heights and fuel layer thicknesses were performed to establish the critical ratio. Tests were then performed such that the burning never resulted in fuel spillage out of the cavity.

Chapter 3

3. Results and analysis

As discussed, four sizes (5 – 25 cm) of ice cavities were considered for this study. This was to ensure a broad range of combustion behavior in transient regime is observed. Unlike burning in solid vessels, combustion in an ice cavity is a new phenomenon. Heat loss mechanisms are magnified by substantial low temperature of ice. In addition, icy walls of the cavity are unsteady and will melt when exposed to heat causing water to flow down and raise the fuel layer. The fuel layer gets thinner by increase in pool surface area and loosing mass due to evaporation of fuel from combustion. A lip (small lateral cavity described in a previous study [90]) in the icy wall during the final stages of combustion is also observed. Similar behavior is also observed during lava flow creating erosion channels [91]. The novelty of this phenomenon that makes the problem distinguished from a typical pool fire is the significant heat losses caused by icy walls and also, the change in geometry of cavity during combustion time.

The mechanisms in which the heat losses function in and out of fuel layer are depicted in Fig. 3.1. The heat flux received by the fuel layer in a pool fire is a summary of the heat feedback from the flame to fuel surface which occurs in forms of convective ($\dot{Q}_{cv,g-l}$), and radiative ($\dot{Q}_{rad,f-l}$) heat transfer. The terms $\dot{Q}_{rr,l-g}$ and $\dot{Q}_{ref,l-g}$ take into account surface re-radiation and reflection from fuel surface, respectively. In-depth conduction, $\dot{Q}_{cd,l-w}$, to underlying cold water encompasses a great portion of heat loss. The conductive term, $\dot{Q}_{cd,l-i}$, represents the heat loss to the surrounding icy walls. Dissimilar to pan fires where conducted heat through rims of pan contributes to temperature rise of fuel layer, icy walls act in an opposite fashion. Convective transport ($\dot{Q}_{cv,l-i}$) induced by significant temperature difference in this setting enhances the heat loss as well. $\dot{m}L_v$ Denotes the energy required to vaporize the fuel [11, 30, 40].

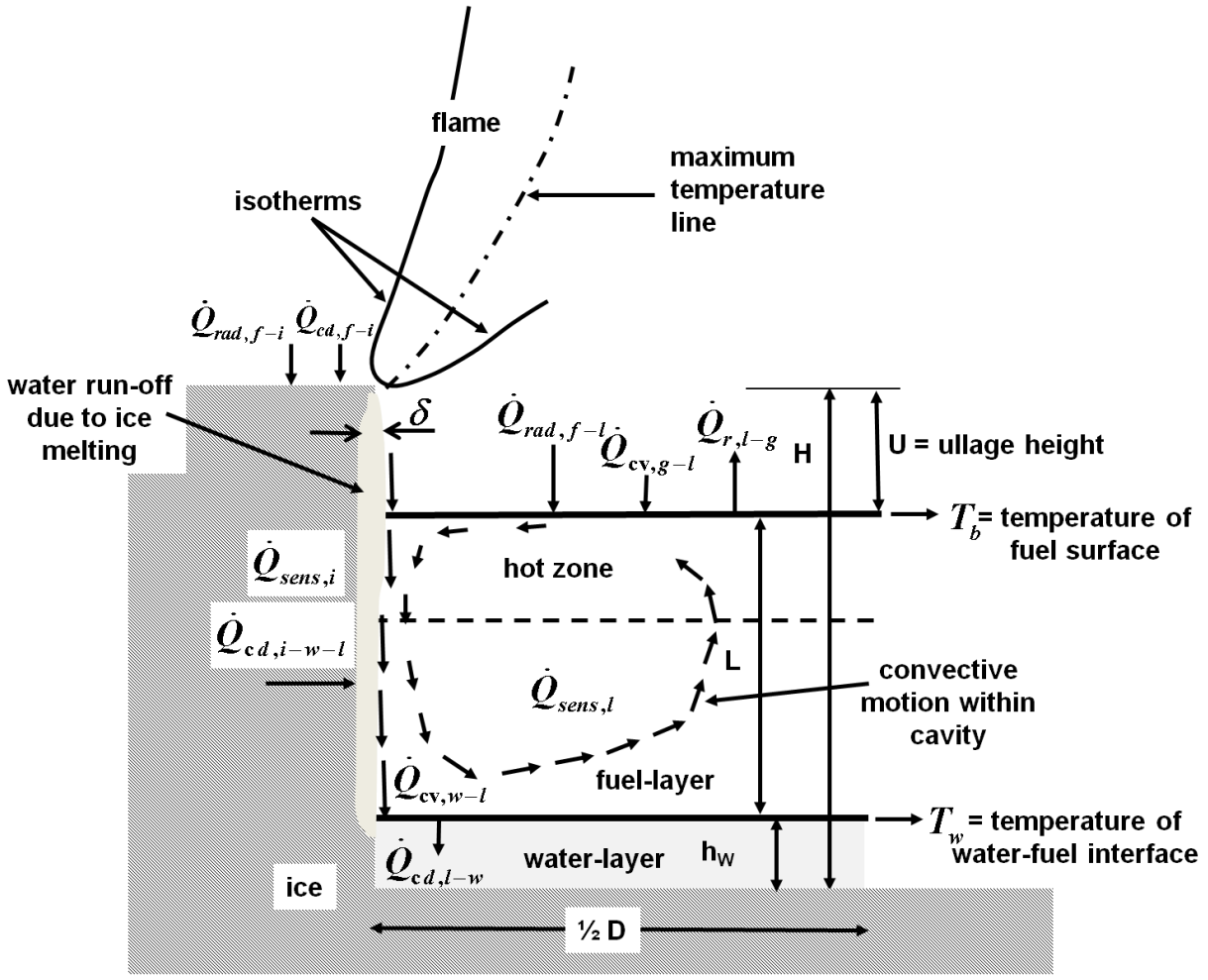

Figure 3.1: Heat transfer mechanism involved in burning inside ice cavity.

The magnitude of $\dot{m}\,L_v$ defines the mass-burning rate, which is the main focus for calculating the burning rate with mathematical model.

3.1- Effects of cavity expansion and fuel layer thickness on burning rate

Figure 3.2, illustrates the mass loss rate of ANS crude oil for 5 and 10 cm diameter cavities. Each plot represents three repeated trials. There are two phases observed for the burning behavior, first being the continuous increase to reach a peak and then a rapid decline to extinction (separated by a vertical line in Fig. 3.2). The two phases are demarcated using the maximum mass loss rate. The first phase where the burning rate is found to grow steadily is caused by expansion of pool fire due to melting of ice. The dependence on pool dimension can be explained further in terms of changes in the relative importance of the mechanisms by which heat is transferred to the fuel surface from the flame. The heat flux from the flame melts the ice

thereby widen the cavity. The widening process of cavity provides more burning surface for the liquid and increases the mass loss rate [90].

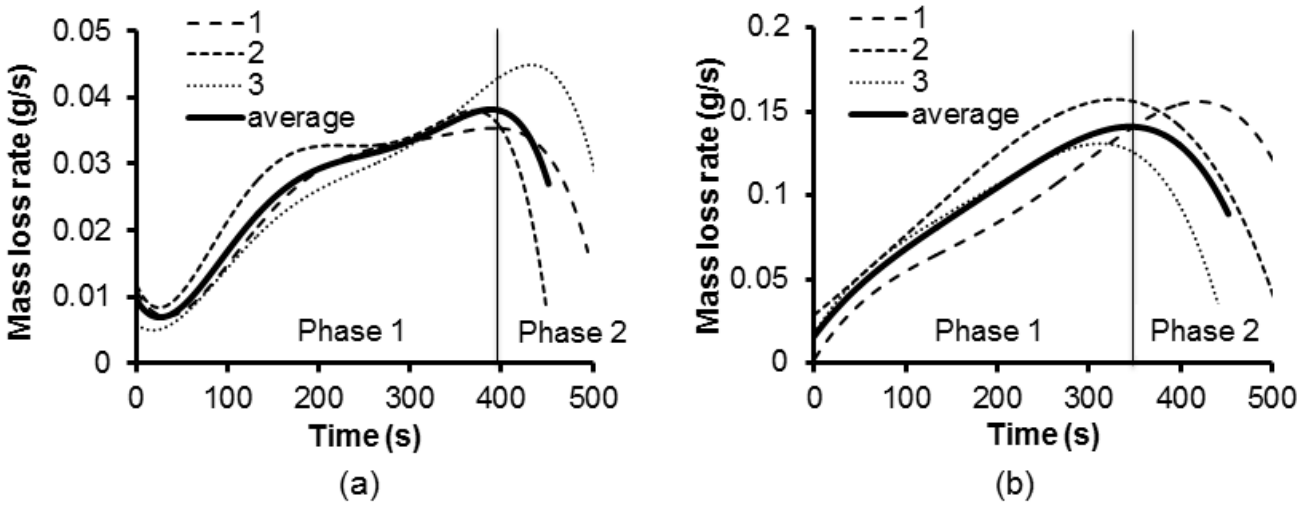

Figure 3.2: Mass loss rate for 5cm (a) and 10 cm (b) diameter cavity. Average mass loss rate is shown in solid line.

Table 3.1 shows data on burning behavior of crude oil for various initial diameters. Due to limited capacity of the load cell used for these experiments the mass loss for 15 and 25 cm trials were not recorded and the average mass loss rate is calculated by dividing the burned mass over time of combustion. As presented in Table 3.1, average burning rates increase significantly at larger diameters. Average burning rate per unit area also improves as the initial diameter of cavity is increased. This increase may be due to the decrease in the wall effects as diameter increases whereby, the net heat losses denoted by $\dot{Q}_{cd,l-i}$ in Fig. 3.1 are reduced. Average burning efficiency for 5 cm cavity is 32% and it grows to 73% for a 25 cm cavity.

Table 3.1: Burning properties of ANS crude oil at different sizes of cavities. [a] Boil-over

	Average MLR (g/s)	Average MLR per unit area (g/s cm^2) × 10^{-3}	Maximum MLR (g/s)	Burn Efficiency (%)
5cm	0.026	0. 43	0.037	32
10 cm	0.09	0.6	0.14	47
15 cm	0.28	0.83	-	56

25 cm [a]	1.44	2.1	-	73

As shown in Fig. 3.2, Phase 2 is relatively shorter in duration (10-30% of total burn time). The steep decline through extinction is indicative of presence of a significant heat loss from the fuel layer. The insulating effect of fuel layer keeps the burning slick surface at a high temperature by reducing heat loss to the water underneath. As the fuel layer thins, gradually more heat is conducted through it. This conduction heat loss (represented by $\dot{Q}_{cd,l-w}$ in Fig. 3.1) continues until enough heat is transferred through the fuel layer to allow the temperature of the surface oil to drop below its fire point, which translates into extinction of the flame. As represented in Table 3.2, the final fuel layer thickness for 5 and 10 cm diameters cavity is recorded around 2-3 mm (Fig. 3.3b) for ANS crude oil which is in agreement with reported literature [92, 93]. More specifically, for fresh ANS crude oil burn in 40 cm diameter pans in brash and frazil ice condition the terminal fuel layer thickness is reported around 2 mm [1]. The slight difference between reported terminal thickness in literature (2 mm) and experimentally obtained (2-3 mm) data can be explained by the use of smaller diameter in solid ice medium (D = 25 cm or less). Table 3.2 provides the relevant data for the cavity expansion and fuel layer thickness shrinkage. The pool diameter increase is significant for smaller cavities (expansion of about 280%) but it lessens as initial diameter is increased.

Table 3.2: Data for ANS crude oil burns in different sizes of cavity. [a]Boil over increased the burning rate and flame height dramatically and resulted in a thinner fuel layer at extinction.

Initial diameter of cavity (cm)	Diameter of Cavity at Extinction (cm)	Fuel layer thickness at extinction (cm)	Time to extinction (s)
5	13.5	0.26	490
10	17.5	0.29	460
15	25	0.26	450
25[a]	35	0.06	340

The dynamic change of cavity and thickness of fuel layer are shown in Fig. 3.3. Figure 3.3a, illustrates the growth of cavity for 5 cm and 10 cm trials. The final diameters of 5 cm and 10

cm trials are 13.5 cm and 17.5 cm, respectively. Trend-line represented in Fig. 3.3b, is picturing the thinning process of fuel layer. It has shown that regardless of the initial thickness the thinning process continues till the final thickness is reached (2-3 mm). The two identified phases of burning rate are separated using a grey bar in Fig. 3.3. As discussed, although the diameter is increasing but the insulating impact of fuel layer becomes less effective as it thins (Fig. 3.3). The resultant effect is a rapid deceleration of the mass loss rate as the fuel layer thickness surpasses its critical thickness for sustained combustion.

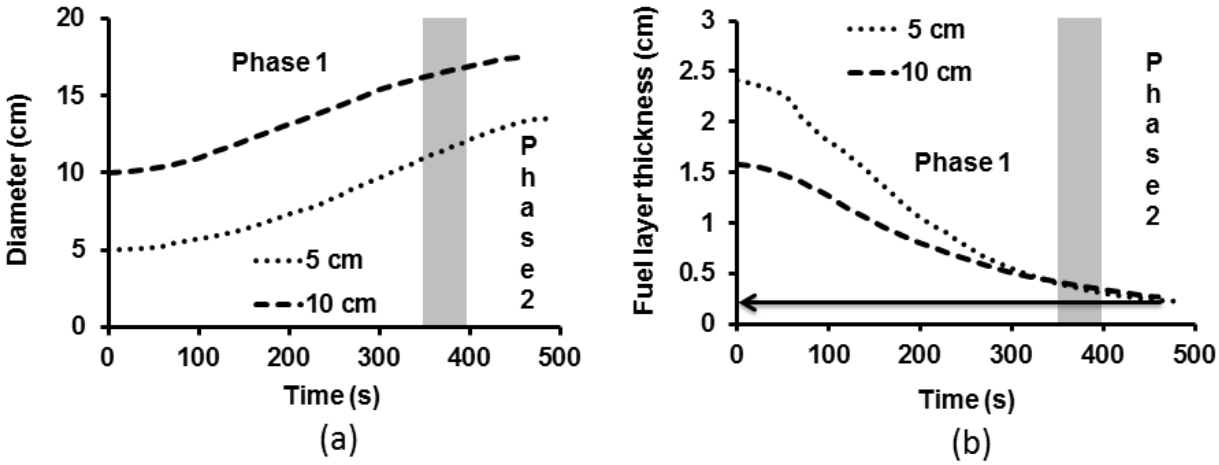

Figure 3.3: a) Expansion of ice cavity in course of combustion. b) Fuel layer thickness decline. The arrow is indicating the terminal fuel layer thickness.

Figure 3.4 depicts the expansion of cavity for 5 cm (a) and 10 cm (b) trials in sequential time steps. Phase 1 and 2 are recognizable from these images as well. The first four images of each set illustrate the increasing period of burning rate (phase 1) where the fire is growing in size and the last image with a characterized weak flame is representing the decay period (phase 2).

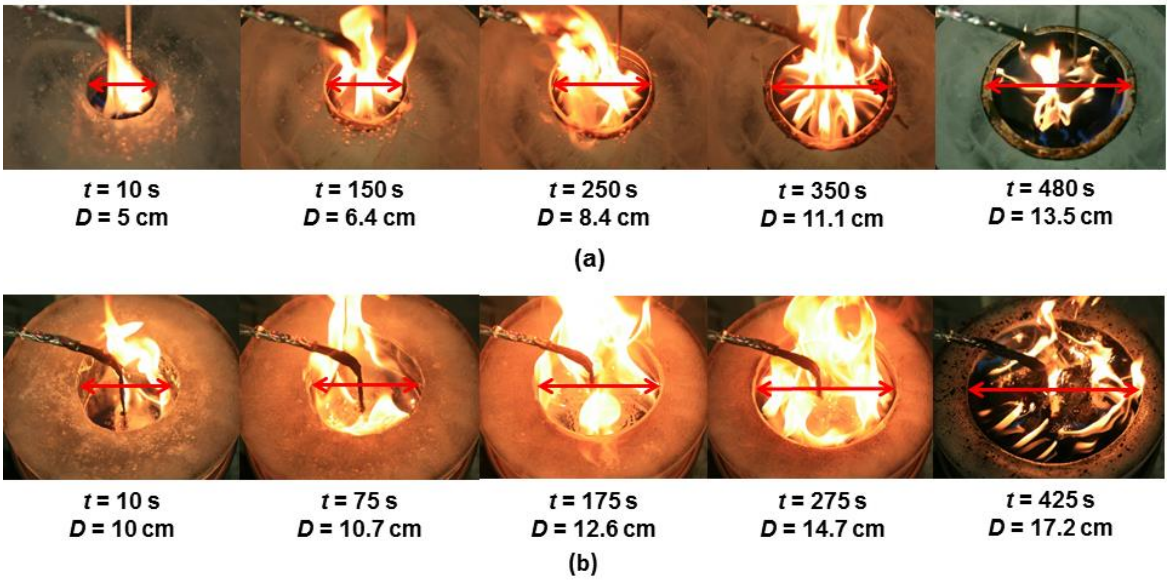

Figure 3.4: a) and b) Showcasing cavity expansion for 5 and 10 cm trial.

Figure 3.4 also shows the rising of the fuel layer as the cavity grows in size. As discussed earlier, the ice melting causes water accumulation inside the cavity causing the fuel layer to rise up. There exists a strong coupling between the geometry change (rate of ice melting) and the burning dynamics (rate of fuel vaporization, flame shape) which can be analyzed if the heat transfer processes are further explored. This is achieved by analyzing the temperature data.

3.2 Temperature profile

The surface temperature of a freely burning liquid is close to, but slightly below, its boiling point. As discussed previously, crude oil does not have a fixed boiling point and the lighter components have a tendency to burn off first. Therefore, the surface temperature will increase with time as the remaining crude becomes less volatile [11]. The ice blocks with initial diameter of 5 and 10 cm were equipped with 16 thermocouples (TC) with the arrangement discussed in section 2. The thermocouple arrangement is shown in Figure 3.5. Solid lines show the initial form of cavity and dashed lines are representing the final shape of cavity. Temperature recordings show three different trend lines. TCs located below initial fuel layer have recorded the temperature of liquid phase (first crude oil and then water). TCs between initial and final fuel layer location recorded the temperature of gas phase and after the elevation of liquid phase they sunk. Elevation of the liquid layer causes a sudden drop in temperature. The third group of TCs has been out of liquid phase for the entire length of experiment and

they have only recorded the gas phase temperature which is used as an average flame temperature (T_f).

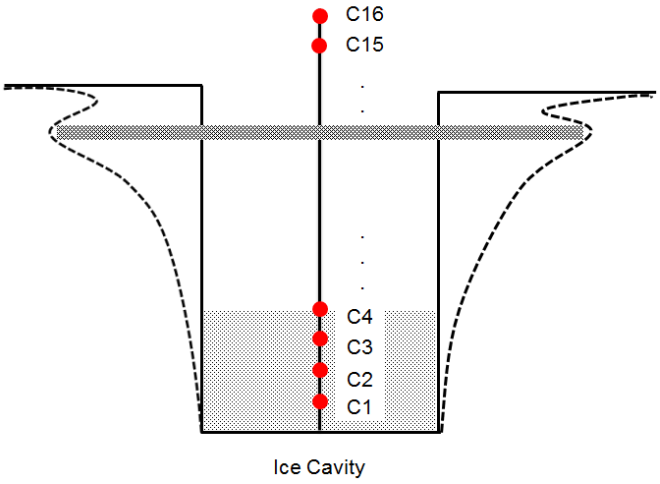

Figure 3.5: TC arrangement used in 5 cm and 10 cm ice cavities.

The measurements from the second group of TCs were analyzed to find the surface temperature of liquid. A sudden drop of temperatures (~200 °C) for second group of TCs is identified in a time period shorter than 5 seconds. This moment was defined to be the point where the TC immerses into liquid phase. The measured temperatures of the TC for a period of 10 seconds after this moment was averaged and assumed to be the instant surface temperature of crude oil. Then, a line was fitted to these surface temperatures to acquire the upper surface temperature trend line of the crude oil (Fig. 3.6). As shown in Figure 3.6, it is possible to identify the two burning phases with regards to temperature of fuel surface.

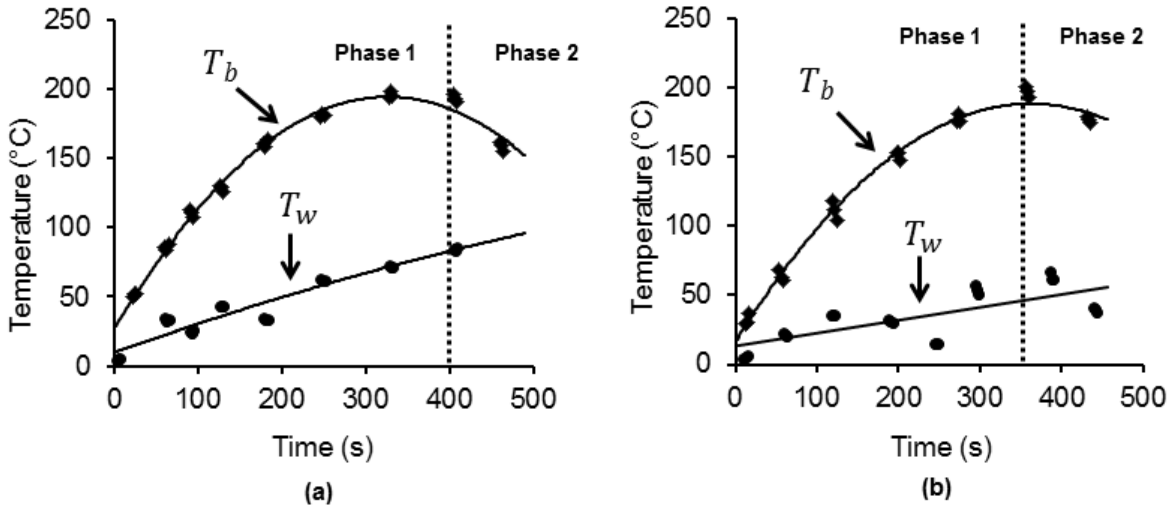

Figure 3.6: a) 5 cm b) 10 cm temperatures corresponding to top and bottom of fuel layer. Fitted lines are representing the fuel surface temperature and fuel-water interface.

The surface temperature is generally increasing in the first phase up until the burning enters the second phase. Declining temperature in Phase 2 also verifies the presence of a significant heat loss that halts the combustion process. Knowing the fuel layer thickness also enabled to interpolate the temperature reading of adjacent TCs to obtain the temperature of fuel and water interface. These fitted lines (Fig. 3.6) were used to develop a temperature profile for the fuel which later was used in the mathematical model.

Chapter 4

4.1 Mathematical model

The burning of a pool fire can be modeled if the relevant heat transfer conditions and corresponding vaporization/mass burning rate are known. In the case of a liquid pool in an ice channel/cavity, the melting of channel walls causes additional heat transfer processes to interact with the burning behavior as shown in Fig. 3.1. These processes coupled with the change in geometry of the vaporizing boundary of the liquid (because of melting ice) will cause changes to the burning behavior normally observed in pool fires. The mass loss rate may never reach a steady state before the extinction because of the geometry change. The small-scale tests in this study systematically characterized the heat transfer mechanisms because of the interaction of an oil layer with a water, cold rigid boundary, and cold non-rigid boundary (ice).

The experimental results from the current study as well as prior theoretical work on the subject of pool fires [34-38, 94-96] is used to derive and evaluate an overall energy balance to obtain an expression for the burning rate.

The heat flux received by the fuel layer comprises of convective ($\dot{Q}_{cv,g-l}$), and radiative ($\dot{Q}_{rad,f-l}$) heating supplied by the flame. As shown in Fig. 3.1, the flame also supplies heat ($\dot{Q}_{cd,f-i}$ and $\dot{Q}_{rad,f-i}$) to the ice causing it to melt and the consequent water enters the cavity and accumulates at the bottom forming a water sub layer of height h_w. $\dot{Q}_{sens,i}$ denotes the sensible and latent heat of ice necessary for the phase change of ice to water. As burning continues, the water layer increases thereby causing the fuel layer to rise up in the cavity and decrease the ullage height *U*. The ice melting will also cause the shape of the cavity to change with time. The cavity size will increase mainly near the fame anchoring point (flame leading edge). This will cause the fuel layer to stretch laterally thereby reducing its thickness (*L*). The melted water layer falling down the ice wall has a thickness denoted by δ in Fig. 3.1. The term $\dot{Q}_{r,l-g}$ denotes the heat loss via surface re-radiation and reflection from the fuel surface.

A sketch of the simplified energy balance at the fuel layer is shown in Fig. 4.1. In-depth conduction ($\dot{Q}_{cd,l-w}$) to underlying cold water encompasses a significant portion of the heat loss. Compared with fires in a confined vessel, this heat loss is enhanced because of the changing shape of the cavity (increase in diameter) as discussed previously. $\dot{Q}_{cd,l-w}$ is a function of the fuel layer thickness (L), and temperatures of fuel surface and fuel-water interface represented as T_b and T_w in Fig. 4.1. Both thickness (L) and T_w are influenced by the melting ice and corresponding change in the fuel layer geometry. The conductive term, $\dot{Q}_{cd,l-i}$, represents the heat losses to the surrounding icy walls.

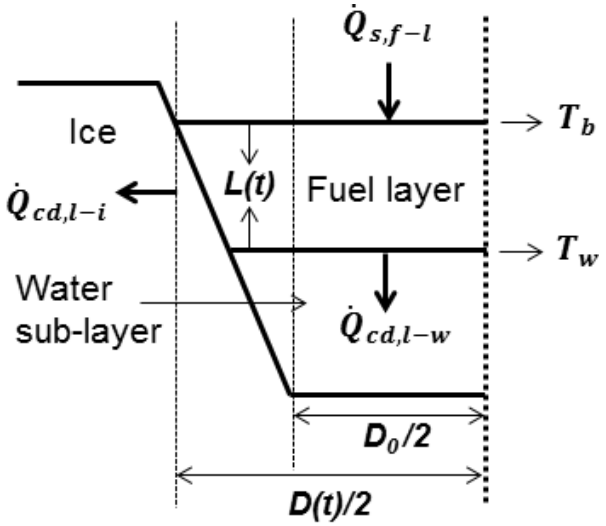

Figure 4.1: Schematic diagram for modeling heat transfer mechanisms involved in the fuel layer.

Compared with fires in confined metal vessels where heat conduction through vessel-rims contributes to temperature rise of fuel layer, icy walls act in an opposite fashion and significantly cool the fuel layer via lateral conduction of heat. If the heat transfer is high enough, which is possible if the fuel boiling points are high, further melting of ice occurs thereby increasing δ and h_w and decreasing U. Convective transport ($\dot{Q}_{cv,l-i}$) can comprise of natural convection (driven by buoyancy forces) and Marangoni convection (driven by surface tension difference). The latter is especially important in this environment because there exist significant temperature differences (ANS crude oil surface temperatures are ~ 120 – 350ºC and ice temperature can be ~-30ºC or lower!).

Finally, $\dot{Q}_{sens,l}$ denotes the sensible and latent heat energy that is used up by the fuel layer to vaporize. This term expressed as $\dot{m}L_v$ is used to obtain an expression of the mass burning rate and discussed next.

4.2 Model formulation

There have been numerous attempts to model heat losses from fuel layer to underlying water in pan fires [41, 53, 59]. Similar to these studies, an expression for the energy balance of the fuel layer is used to estimate burning rate of crude oil in an ice cavity. The results from the model are then compared with experimental results for different cavity sizes (5 - 25 cm) to validate the efficiency of the model. The following simplifying assumptions are made:

1. Convective motion within the liquid ($\dot{Q}_{cv,l-i}$) is ignored. This is because this term is most difficult to quantify or measure experimentally. Note that it will weakly affect the fuel layer when burning high viscosity fuels, and perhaps it may be reasonable for the ANS crude oil which is highly viscous.
2. Reflection and re-radiation from the surface is ignored ($\dot{Q}_{r,l-g}$ and $\dot{Q}_{rr,l-g}$)
3. The ullage effect is ignored. In other words, we do not take into account the increase in the burning rate that may be caused because of the rise of the fuel layer because of melting of water in the cavity.
4. Constant properties are used in the model (ρ, ρ_∞, C_p, L_v) as shown in Table 2.1. Thermal conductivity of crude is a function of temperature and composition. These effects are ignored and a constant thermal conductivity calculated at 200 ºC is assumed [97].
5. The geometry of the ice cavity changes with time. It is assumed that this change is linear.
6. The formation of the ice lip or lateral ice cavity is not accounted.
7. The in-depth fuel layer temperature profile is assumed to be linear. In other words, knowing temperature of the fuel surface, fuel-water interface, and the thickness of the fuel layer is sufficient to quantify the in-depth losses via conduction.
8. The influence of the film of water on the wall of the ice on the heat and mass transfer process is ignored.

Given assumptions 1 – 8, the energy balance of the fuel surface can be written as:

$$\dot{Q}_{s,f-l}(t) - \dot{Q}_{cd,l-w}(t) - \dot{Q}_{cd,l-i}(t) - \dot{m}(t)L_v = 0 \qquad (1)$$

Where $\dot{Q}_{s,f-l}$ is the net heat flux per unit area reaching the surface, $\dot{Q}_{cd,l-w}$ is the net heat conducted to water sub-layer, $\dot{Q}_{cd,l-i}$ is the net heat loss by conduction to icy walls and $\dot{m}L_v$ denotes the mass burning rate multiplied by the heat of gasification. Note that the heat feedback from the flame to the fuel surface ($\dot{Q}_{cv,f-l}$ and $\dot{Q}_{rad,f-l}$) is combined and denoted by $\dot{Q}_{s,f-l}$.

The heat balance is similar to that used in classic pool fire literature [40] except for two main differences:

1. The term, $\dot{Q}_{cd,l-i}$, which denotes the heat loss by conduction from the side of the fuel layer is typically positive as heat is usually conducted from the vessel rims to the fuel.
2. All the heat transfer terms depend on the changes in the cavity and fuel layer geometries. Thus, modeling the distribution of heat transfer from the flame to the liquid surface has to account for the change in cavity geometry.

Given the two differences, each term in Eq. 1 is further explained below:

I. The flame heat flux ($\dot{Q}_{s,f-l}(t)$):

The flame provides the required energy for the liquid fuel to vaporize and sustain the combustion. This energy feedback has been studied extensively [30, 34-40] and it has been found that the heat flux reaching the surface can be expressed as

$$\dot{Q}_{s,f-l}(t) = \chi\, \rho_\infty C_p \left[T_\infty g\left(T_f - T_\infty\right)\right]^{\frac{1}{2}} D(t)^{5/2} \qquad (2)$$

where ρ_∞, C_p, and T_∞ are properties of air at ambient temperature; T_f is the temperature of hot gases above the liquid and is assumed to be constant (1100 K) [41]. χ is a specific fraction of the heat released fed back to the fuel surface and is independent of pool diameter and fuel layer thickness for large pool fires. The value corresponding to χ is documented well [41-43, 98]. However, for pool size smaller than 1 m in diameter χ can be very small [41]. Similar to Torero *et al.* [41], χ had to be adjusted to 5×10^{-3} to best fit the experimental trend lines. The changes in the diameter of cavity, $D(t)$, and the thickness of the fuel layer, $L(t)$, are obtained

experimentally from the small-scale test data performed using 5 and 10 cm initial diameter cavities.

Experimental data show that the change in diameter *D(t)* and fuel layer thickness *L(t)* (Fig. 3.3 "a" and "b" shown below once again for convenience) follow an approximately linear trend with respect to time (at + b) where "a" equals to $\frac{Final-Initial}{time}$ and "b" is the initial value.

If a linear increase in diameter and decrease in thickness is assumed, three input parameters of an initial value, final value and the time duration of the burn are required to formulate an expression for *D(t)* and *L(t).* Since the change in diameter is not significant as size increases, or in other words, the expansion of the ice cavity decreases with increasing scale, it is expected that this assumption should improve from small to large-scale.

II. In-depth conduction ($\dot{Q}_{cd,l-w}(t)$)

As the fuel layer burns it thins thereby increasing the heat loss to the water sublayer below. This heat loss is mostly because of conduction from the fuel surface which is close to the boiling point (~120 to 400 ºC) and the water-fuel interface which can be anywhere from 0 to 100 ºC depending on the temperature of the water. The loss term represented by $\dot{Q}_{cd,l-w}(t)$ is given by:

$$\dot{Q}_{cd,l-w}(t) = \pi \left(\frac{D(t)^2}{4}\right) \left(\frac{\lambda_l}{L(t)}\right) (T_b(t) - T_w(t)), \qquad (3)$$

where, λ_l is the thermal conductivity of the fuel and is assumed to be constant. For the small-scale tests, $T_b(t)$ and $T_w(t)$ are obtained experimentally as shown in Fig. 3.6. $T_b(t)$ and $T_w(t)$ for the 10 cm trial were time averaged and used as constant values in modeling the larger sizes (assumption 7).

III. Conduction to icy walls ($\dot{Q}_{cd,l-i}(t)$)

The conduction to icy walls is also a source of heat loss, especially during the early stage of combustion when the fuel layer is relatively thick and surface in contact with ice is larger. This term is calculated by assuming that the fuel layer comprises of a cylinder of diameter *D*(t) and

height L(t). The curved surface area of the cylinder is then estimated from simple geometry and the heat loss to icy walls is calculated as:

$$\dot{Q}_{cd,l-i}(t) = \frac{\lambda_l}{\frac{D(t)}{2}} (2\,\pi(\frac{D(t)}{2})\, L(t))\,(\frac{T_b+T_w}{2}(t) - T_{ice}). \qquad (4)$$

The temperature at the center of the fuel layer is assumed to be the average between $T_b(t)$ and $T_w(t)$ while the temperature of icy walls, T_{ice}, is assumed to equal to 0 ºC.

IV. Mass loss rate

The mass loss rate can be obtained by combining Eq. (1-4) as:

$$\dot{m}(t) = \frac{\dot{Q}_{s,f-l}(t) - \dot{Q}_{cd,l-w}(t) - \dot{Q}_{cd,l-i}(t)}{L_v}. \qquad (5)$$

Equation 5 is used to obtain the mass loss rate of a liquid fuel in an ice-cavity.

4.3 Model results

Figure 4.2 shows the experimental and calculated mass burning rate for the 5 cm and 10 cm diameter ice cavities with ANS crude oil. As shown in Fig. 4.2 the model does a reasonable job at predicting the mass loss rate vs. time.

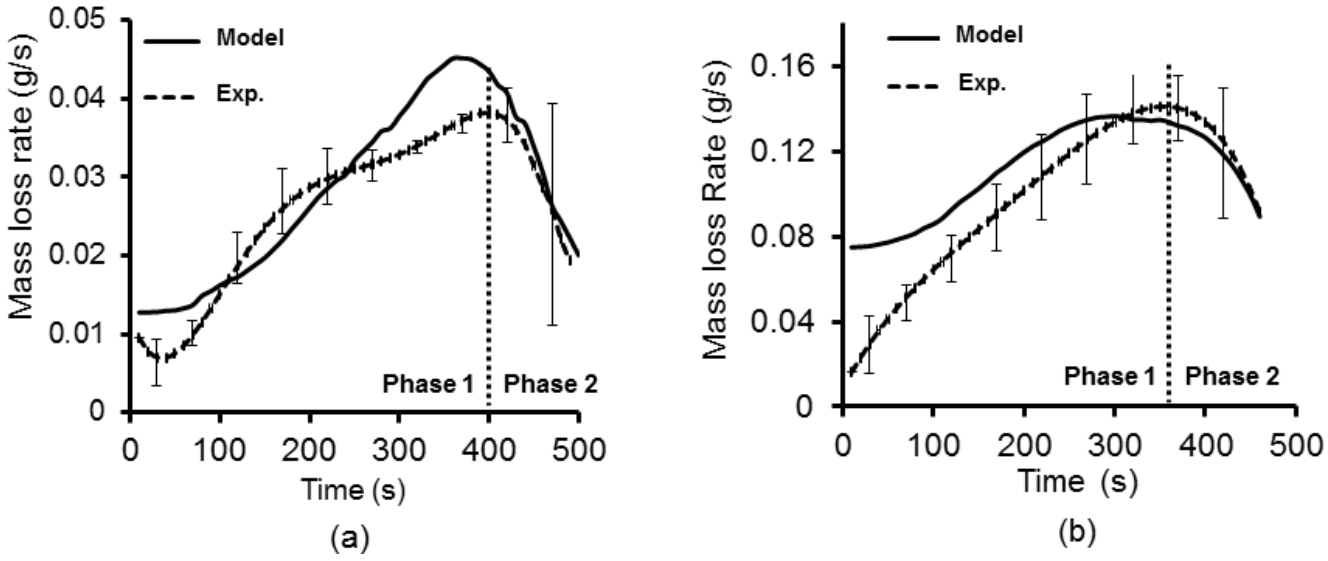

Figure 4.2: Comparison between experimental and calculated mass loss rate for 5 cm (a) and 10 cm (b) trials (the error bars represent the experimental burning rate due to variation between repetitions).

Both phase 1 and phase 2 are captured by the model. The over-prediction during initial stages, as shown in Fig. 4.2, is mainly because of ignored effect of ullage (assumption 3). After the elevation of the fuel layer by ice melting, the ullage decreases resulting in a more effective burning of the fuel. During phase 2, the fuel layer penetrates into the ice, creating an ice lip (small lateral cavity). This effect has not been modeled and may be the cause of the lack of agreement by the model and experiments in this stage. The ice lip conceals a certain quantity of the liquid fuel from the heat flux from the flame, causing a reduction in combustion efficiency.

Figure 4.3 compares the experimentally obtained burning efficiencies with the mathematical model. The burning efficiencies calculated by the model are in agreement with the experimental. This model does not address boil-over scenarios, thus the predicted $\dot{m}$ for 25 cm is much lower (by 40%) than the experimental value.

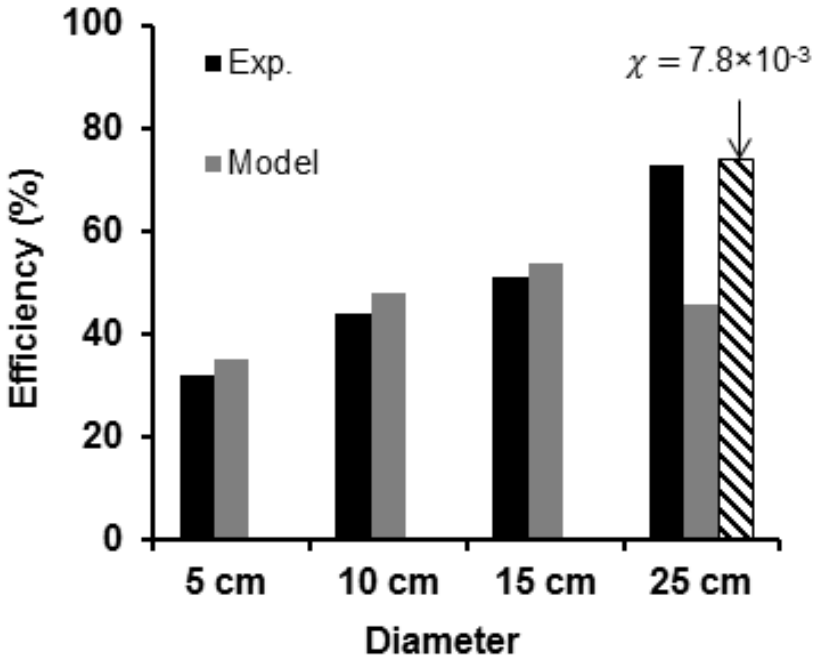

Figure 4.3: Comparison between experimental and calculated burning efficiencies. χ is equal to 5×10^{-3} for all cases except for 25 cm.

The influence of the fraction of heat fed back to the fuel (χ) is shown in Fig. 4.3 by making χ equal 7.8×10^{-3} (~ 50% increase). On doing so, the efficiency matches the experimental value. This exercise demonstrates the need to improve our understanding of input parameters and develop a *guide* that can be applied towards estimation of parameters required for mathematically modeling burning behavior under such situations.

4.4 Model limitations and cautionary note

The model formulated in this study is a first step towards predicting the burning rate of an oil spill in an ice cavity. Significant modification to existing pool fire models in the form of geometry changes and lateral conduction losses have been incorporated. However, several assumptions that were used in deriving the energy balance need further study. Chief among them is the value assigned to χ, which was assumed to be a constant. Another assumption that may influence the model results is having the flame temperature as a constant. Flame temperature which was used in Eq. (2) utilizes the gas temperature in the centerline above the surface and computes the $\dot{Q}_{s,f-l}$ solely by that specific temperature [99]. The assumption of

constant properties may also result in discrepancies between the model predictions and the experimental values because of the multicomponent nature of the crude oil.

Chapter 5

5.1 Conclusions & Future work

A series of experiments were conducted to develop an understanding of the burning of crude oil in circular ice cavities. The burning rate of a fuel layer within ice cavities of varying diameters was studied to understand how the cavity expansion affects it. The mass loss rate is primarily enhanced by the cavity diameter and is limited by the fuel layer thickness. Ice melting over the course of the trial created a highly dynamic burning environment. It decreased ullage and increased the fuel surface area, enhancing the thinning of the fuel layer. Due to strong heat losses any benefits created by the high burning rates were quickly overcome. However, the rapid decrease in fuel layer thickness is the more prominent factor in reducing mass loss rates. The temperature profiles along the centerline of the oil layer were used to estimate heat losses of the fuel layer to the water sub-layer and icy walls. An energy balance for the fuel layer was used to estimate the mass loss rate. The model was relatively successful but further developments are necessary. Modeling and understanding such complex burning conditions requires describing other phenomena, such as the ullage and lip creation. There are just a few studies regarding the movements inside a liquid fuel. The penetration in to the ice is enhanced by convective motions, thus, it is proposed for the future work to include a thorough study on convective motions of the fuel layer for various fuels. Flow visualization methods shall be used to identify the movement pattern and their regimes. The model also could be improved by incorporating other physical phenomena i.e. the effect of ullaget. In addition it is a necessary task to perform tests that are more similar to a realistic oil spill incident. Thus it is proposed the following parameters could be added to the problem parameters:

- Degree of weathering
- Cold environment
- Various fuels

The question of quantifying these parameters and other physical processes involved with burning of liquid fuels in ice in the fragile arctic ecosystem is a future concern and consequent direction that needs work.

References

1. S. L. Ross, *Tests to Determine the Limits to In Situ Burning of Thin Oil Slicks in Broken Ice*. 2003, Report to Minerals Management Service and ExxonMobil Upstream Research. Herndon, VA, U.S.
2. Buist, I., et al., *In situ Burning.* Pure Appl. Chem., 1999. **71**(1): p. 43-65.
3. E. DeCola, T.R., S. Fletcher, S. Harvey,, *Offshore Oil Spill Response in Dynamic Ice Conditions*. 2006, Nuka Research and Planning Group, LLC; Harvey Consulting, LLC.
4. I.A. Buist, S.G.P., B.K. Trudel, S.R. Shelnutt, A. H. Walker, D.K. Scholz, P.J. Brandvik, J. Fritt-Rasmussen, A.A. Allen, P. Smith,, *In Situ Burning in Ice-Affected Waters: State of Knowledge Report*. 2013, JIP.
5. *Advancing Oil Spill Response in Ice-Covered Waters*. 2004, United States Arctic Research Commission & Prince William Sound Oil Spill Recovery Institute.
6. I. Singsaas, K.R.S., R. Lundmark Daae, B. Johanseb, L. Solsberg, , *Testing of Oil Skimmers Via Field Experiments in the Barents Sea*. 2010, SINTEF & Counterspill Research Inc.
7. Per Johan Brandvik, J.f.-R., Roger Daniloff, Janne Lise Resby, Frode leirvik, , *Establishing, Testing and Verification of a Laboratory Burning Cell to Measure Ignitibility for In-Situ Burning of Oil Spills*, in *Oil in Ice*. 2010, SINTEF Materials and Chemistry.
8. A. A. Allen. *Controlled Burning of Crude Oil on Water Following the Grounding of the Exxon Valdez.* in *Proceedings of the 1991 Oil Spill Conference* 1991. San Diego, CA: American Petroleum Institute, Washington, D.C.
9. D.F. Dickins, I.B., *Oil and Gas Under Sea Ice*. 1981, Prepared by Dome Petroleum Ltd.
10. Bellino, P.W., *A Study of Spreading and In Situ Burning of Oil in an Ice Channel*. 2012, Worcester Polytechnic Institute.
11. Drysdale, D., *An Introduction to Fire Dynamics*. 3rd ed. 2011: John Wiley & Sons Ltd.
12. J.P. Garo, P.G., J.P. Vantelon & A.C. Fernandez-Pello. *Experimental study of the burning of a liquid fuel spilled on water* in *Twnety sixth Symposium on Combustion*. 1994.
13. Hottel, H.C., *Review: Certain Laws Governing the Diffusive Burning of Liquids.* Fire Research Abstracts and Reviews, 1959. **1**: p. 41-43.
14. Hall, A.R., *Pool Burning: a review.* Oxidation and Combustion Reviews, 1973. **6**: p. 169-225.
15. Murad, R.J., *Experimental Investigation of Ignition of Pools of Liquid Hydrocarbon Fuels*. 1970, Princeton university.
16. R. Murad, J.L., H. Isoda and M. Summerfield,, *A Study of Some Factors Influencing the Ignition of a Liquid Fuel Pool* Combustion and Flame, 1970. **1**(15): p. 289-298.
17. I. Glassman, J.G.H., Fire Research Abstracts and Reviews, 1968. **10**: p. 217-234.
18. K.A. Murty, *Ignition of Liquid Fuels*. 1988: The SFPE Handbook of Fire Protection Engineering; National Fire Protection Association, Quincy, MA, U.S.,. p. 1315-1325.
19. Ross, H.D., *Ignition of and Flame Spread Over Laboratory-Scale Pools of Pure Liquid Fuels.* Prog. Energy Combuat. , 1994. **20**: p. 17-63.
20. Murad, R.J., et al., *A Study of Some Factors Influencing the Ignition of a Liquid Fuel Pool.* Combustion and Flame, 1970. **1**(15): p. 289-298.
21. Degroote, E., *Control Parameters of Flame Spreading in a Fuel Container.* Journal of Thermal Analysis and Calorimetry, 2007. **87** (1): p. 149–151.
22. Ybarra, E.D.a.P.L.G., *Flame Propagation Over Liquid Alcohols, Part II. Steady propagation regimes.* Journal of Thermal Analysis and Calorimetry, 2005. **80**: p. 549–553.

23. Ybarra, E.D.a.P.L.G., *Flame Propagation Over Liquid Alcohols Part III. Pulsating regime.* Journal of Thermal Analysis and Calorimetry, 2005. **80**: p. 555–558.
24. E. Degroote, P.L.G.Y., *Flame Propagation Over Liquid Alcohols, Part I. Experimental results.* Journal of Thermal Analysis and Calorimetry, 2005. **Vol. 80** (1): p. 541–548.
25. Torrance, K.E. and R.L. Torrance, *Fire spread over liquid fuels: Liquid phase parameters.* Symposium, International, on Combustion, 1975. **15**(1): p. 281-287.
26. T. Yumoto, A.T., T. Handa,, *Combustion Behavior of Liquid Fuel in a Small Vessel: Effect of Convective Motion in the Liquid on Burning Rate of Hexanein the Early Stage of Combustion.* Combustion and Flame, 1977. **30**: p. 33-43.
27. K.E. Torrance and R.L. Mahajan, *Fire spread over liquid fuels: Liquid phase parameters.* Symposium (International) on Combustion, 1975. **15**(1).
28. Artemenko, E.S.B., V. I.,, *Burning of liquid in vessels with change of level.* Combustion, Explosion, and Shock Waves,, 1968. **4**: p. 39.
29. Khudiakov, V.I.B.a.G.N., *Diffusion Burning of Liquids*. 1961, U.S. Army translation NIST No. AD296762.
30. Nakakuki, A., *Heat Transfer Mechanisms in Liquid Pool Fires.* Fire Safety Journal, 1994. **13**: p. 339-363.
31. Ndubizu, C.C., Ramaker, D. E., Tatem, P. A. & Williams, F. W., *A model of freely burning pool fires.* Combustion Science and Technology, 1983. **31**: p. 233.
32. Dlugogorski, B.Z. and M. Wilson. *Effect of Ullage on Properties of Small-scale Pool Fires*. in *Asia-Oceania Association for Fire science and Technology*. 1995. Khabarovsk.
33. Babrauskas, V., *Estimating Large Pool Fires Burning Rates.* Fire Technology, 1983. **19**: p. 251.
34. D.J. Rasbah, Z.W.R., G.W. Stark, *Properties of Fires of Liquids.* Fuel, 1956. **35**: p. 94.
35. Wang, Z.X., *A three layer model for oil tank fires.* Int. Symp. on Fire Safety Science,, 1988. **2**: p. 209.
36. Souil, J.M., Vantelon, J. P., Joulain, P. & Grosshandler, W. L., *Experimental and theoretical study of thermal radiation from freely burning kerosene pool fires.* Prog. Astron. Aeron.,, 1985. **105**: p. 388.
37. Nakakuki, A., *Heat Transfer in Pool Fires at a Certain Small Lip Height.* Combustion and Flame 2002. **131**: p. 259-272.
38. Nakakuki, A., *Heat Transfer in Small Scale Pool Fires.* Combustion and Flame 1994. **96**: p. 311-324.
39. Nakakuki, A., *Heat Transfer in Hot-Zone-Forming Pool Fires.* Combustion and Flame 1997. **109**: p. 353-369.
40. A. Hamins, J.Y., T. Kashiwagi . *A global model for predicting the burning rates of liquid pool fires*. 1999.
41. Torero, J.L., et al., *Determination of the Burning Characteristics of a Slick of Oil on Water.* Spill Science & Technology Bulletin, 2003. **8**(4): p. 379-390.
42. Mudan, K.S., Croce, P.A.,, *Fire hazard calculations for large open hydrocarbon fires* in *The SFPE Handbook of Fire Protection Engineering*. 1995. p. 3197-3240.
43. Gritzo, L.A., Nicolette, V.F., Tieszen, S.R., Moya, J.L., Holen, J.,, *Heat transfer to the fuel surface in large pool fires*. Transport Phenomena in Combustion, ed. S.H. Chan. Vol. 2. 1996: Taylor and Francis Publishers.
44. A. Hamins, S.J.F., T. Kashiwagi, *Heat Feedback to the Fuel Surface in Pool Fires.* Combustion Science and Technology, 1994. **97**(1-3): p. 37-62.

45. Per Johan Brandvik, K.R.S., Ivar Singaas, Mark Reed, *Short state-of-the-art Report on Oil Spills in Ice-Infested Waters.*, in *Oil in Ice*. 2006, SINTEF Materials and Chemistry.
46. Sveum Per, C.B. *Burning of oil in snow*. in *Arctic and Marine Oil Spill Program* 1991. Ottawa, Ontario.
47. Buist, I. *Window of Opportunity for In Situ Burning*. in *In Situ Burning of Oil Spills Workshop Proceedings*. 1998. New Orleans, Louisiana.
48. Koseki, H., Kokkala, M.A. and Mulholland, G.W.,, *Experimental Study of Boilover in Crude Oil Fires.* Fire Safety Science, Proceedings of the third International Symposium 1991: p. 865-874.
49. Garo, J.-P., Koseki, Hiroshi, Vantelon, Jean-Pierre, Fernandez-Pello, Carlos, *Combustion of liquid fuels floating on water.* Thermal Science, 2007. **11**(2): p. 119-140.
50. W. C. Fan, J.S.H.a.G.X.L., *Experimental study on the premonitory phenomena of boilover in liquid pool fires supported on water.* J. LOSS Prev. Process Ind., 1995. **8**(4): p. 221-227.
51. Evans, D.D.W., W. D. . *Burning of oil spills*. in *U.S./Japan Government Cooperative Program on Natural Resources (UJNR). Fire Research and Safety. 11th Joint Panel Meeting.* 1990.
52. J. P Garo, S.G., .J. L. Torero, J. P. Vantelon, , *Determination of the Thermal Efficiency of Pre-boilover Burning of a Slick of Oil on Water.* Spill Science & Technology Bulletin 1999. **5**(2): p. 141-151
53. VANTELON, J.P.G.a.J.P., *Effect of the Fuel Boiling Point on the Boilover Burning of Liquid Fuels Spilled on Water.* Symposium (International) on Combustion, 1996. **26**: p. 1461–1467.
54. J. P. Garo, J.P.V., J.M. Souil, C. Breillat,, *Burning of weathering and emulsified oil spills.* Experimental Thermal and Fluid Science, 2004. **28**(7): p. 753-761.
55. N. L. Brogaard, M.X.S., J. Fritt-Rasmussen, A. S. Rangwala, G. Jomaas *A new Experimental Rig for Oil Burning on Water - Results for Crude and Pure Oils*. in *International Symposium on Fire Safety Science,* . 2014. Canterbury, New Zealand.
56. Hristov, J., et al., *Accidental burning of a fuel layer on a waterbed: a scale analysis of the models predicting the pre-boilover time and tests to published data.* International Journal of Thermal Sciences, 2004. **43**(3): p. 221-239.
57. E.M. Twardus, T.A.B., *The burning of crude oil spilled on water.* Adchivum Combustionis, Polish Acad. Sci, 1981. **20**(1-2): p. 49-60.
58. Hristov, J. *Burning of a Slick of Fuel on Water, Qualitative Analysis of the Heat Transfer Model and the Pre-boilover Time on the Basis of Data Available*. in *Transport Phenomena in Two Phase Flow*. 2001. Bourgas.
59. Garo, J.P., et al., *Combustion of Liquid Fuels Spilled on Water. Prediction of Time to Start of Boilover.* Combustion Science and Technology, 1999. **147**(1-6): p. 39-59.
60. J. P. Garo, J.P.V., S. Gandhi, J. L. Torero, *Determination of the Thermal Efficiency of Pre-boilover Burning of a Slick of Oil on Water.* Spill Science & Technology Bulletin, 1999. **5**(2): p. 141-151.
61. Evans, D.D., et al. *Burning, Smoke Production and Smoke Dispersion From Oil Spill Combustion*. in *Arctic and Marine Oilspill Program (AMOP) Technical Seminar 11th*. 1988. Ontario, Canada.
62. Wu, N., et al. *Effect of Weathering on Piloted Ignition and Flash Point of a Slick of Oil.* in *Arctic and Marine Oilspill Program (AMOP) Technical Seminar*. 1998. Ottawa.

63. Walavalkar, A.Y. and A.K. Kulkarni. *Combustion of Floating, Water-In-Oil Emulsion Layers Subjected to External Heat Flux.* in *Arctic and Marine Oilspill Program (AMOP) Technical Seminar, 23rd*. 2000. Alberta, Canada.
64. Nodvik, A.B., M.A. Champ, and K.R. Bitting, *Estimating Time Window for Burning Oil at Sea: Processes and Factors.* Spill Science & Technology Bulletin, 2003. **8**(4): p. 347-359.
65. Fritt-Rasmussen, J. and P.J. Brandvik, *Measuring ignitability for in situ burning of oil spills weathered under Arctic.* Marine Pollution Bulletin, 2011(62): p. 1780-1785.
66. Marc R. Nyden, W.C., Darren lowe, Richard Harris. *Application of FTIR Remote Sensing in Environmental Impact Assessment of Oil Fires*. in *International Specialty Conference Proceedings*. 1993. Pittsburgh, PA.
67. Mulholland, G.W., W. Liggett, and H. Koseki. *Effect of Pool Diameter on the Properties of Smoke Produced by Crude Oil Fires*. in *Symposium (International) on Combustion, 26th*. 1996. Pittsburgh.
68. David D. Evans, W.D.W. *Burning of Oil Spills*. in *Fire Research and Safety. 11th Joint Panel Meeting.* 1989. Berkeley, CA.
69. Wan Ying Shiu, M.B., Alice M. Bobraf, Aila Maijanenf, *The Water Solubility of Crude Oils and Petroleum.* Oil & Chemical Pollution 1990. **7**: p. 57-84.
70. Evans, D.D. *Large Fire Experiments for Fire Model Evaluations*. in *7th International Interflam Conference*. 1996. Cambrdige, England.
71. Faksness, L.-G., et al., *Chemical composition and acute toxicity in the water after.* Marine Pollution Bulletin, 2012(64): p. 49-55.
72. Notarianni, K.A., D.D. Evans, and W.D. Walton. *Smoke Production from Large Oil Pool Fires*. in *International Fire conference*. 1993. London.
73. N. K. Smith and A. Diaz. *In-place Burning of Crude Oil in Broken Ice- 1985 Testing at OHMSETT*. in *in Arctic and Marine Oilspill Program*. 1985. Ottawa, Canada.
74. Diaz, N.K.D.a.A. *In-place Burning of Prudhoe Bay Oil in Broken Ice*. in *Proceedings of the 1985 Oil Spill Conference,*. 1985. Washington D.C.
75. Diaz., N.K.S.a.A. *In-place Burning of Crude Oil in Broken Ice* in *Proceeding of 1987 Oil Spill Conference*. 1987. Washington D.C.: American Petroleum Institute.
76. H. M. Brown, R.H.G., *In situ Burning of Oil in Ice Leads,* in *Arctic and Marine Oil Spill Program Technical Seminar*. 1986.
77. Diaz, N.K. and A. Diaz. *In-place Burning of Prudhoe Bay Oil in Broken Ice*. in *Proceedings of the 1985 Oil Spill Conference*. 1985. Washington D.C.
78. Smith, N.K. and A. Diaz. *In-place Burning of Crude Oil in Broken Ice- 1985 Testing at OHMSETT*. in *Arctic and Marine Oilspill Program*. 1985. Ottawa, Canada.
79. Brown, H.M. and R.H. Goodman. *In-situ Burning of Oil in Ice Leads*. in *Arctic and Marine Oil Spill Program Technical Seminar, 9th Proceedings*. 1986. Edmonton, Alberta.
80. Guennete, C.C. and R. Wighus. *In-situ Burning of Crude Oil and Emulsions in Broken Ice*. in *Arctic and Marine Oilspill Program Technical Seminar, 15th*. 1996. Ottawa, Ontario.
81. Buist, I., et al., *Field Research on Using Oil Herding Surfactants to Thicken Oil Slick in Pack Ice for In-situ Burning* 2006.
82. Glaeser, J.L.a.G.P.V., *A Study of the Behavior of Oil Spills in the Arctic.* , in *Fina Report to the USCG Office of Research & Development, Applied Technology Division, Groton, CT, U.S. Project Number 714708/A/001,002.* 197. p. 60p.
83. McMinn, T.J., *Crude Oil Behaviour on Arctic Winter Ice. U.S. Coast Guard*. 1972, Office of Research and Development, Groton, CT, U.S. NTIS-AD-754261. 56 pp.

84. NORCOR, *The Interaction of Crude Oil with Arctic Sea Ice. Beaufort Sea Project.* , in *NORCOR Engineering and Research Ltd. (NORCOR).* 1975: Technical Report No. 27, Canada Department of the Environment, Victoria, BC, Canada.
85. Energetex, *Ignition and Burning of Crude Oil on Water Pools and Under Arctic Spring Time Conditions.* . 1977, Energetex Engineering (Energetex): Arctic Petroleum Operators Association (APOA) Project 141. APOA, Calgary, AB, Canada, 70 p.
86. Nelson, W.G.a.A.A.A. *The Physical Interaction and Cleanup of Crude Oil with Slush and Solid First Year Sea Ice*. in *Proceedings of the Fifth Arctic and Marine Oilspill Program (AMOP) Technical Seminar,*. 1982. Edmonton, Canada.
87. Buist, I.A., S.G. Potter, and D.F. Dickins. *Fate and behaviour of water-in-oil emulsions in ice.* . in *Proceedings of the Sixth Arctic and Marine Oilspill Program (AMOP) Technical Seminar, June 14-16,* . 1983. Edmonton, AB. Environment Canada, Ottawa, ON, Canada,.
88. C. C. Guennete and R. Wighus. *In-situ Burning of Crude Oil and Emulsions in Broken Ice* in *Arctic and Marine Oilspill Program Technical Seminar*. 1996. Ottawa, Ontario.
89. Dickins, D.F., P.J. Brandvik, J. Bradford, L-G. Faksness, L. Liberty, and R. Daniloff. . *Svalbard 2006 Experimental Oil Spill Under Ice: Remote Sensing, Oil Weathering Under Arctic Conditions and Assessment of Oil Removal by In-situ Burning.* . in *Proceedings of the 2008 International Oil Spill Conference (IOSC)*. 2008. Savannah, GA.: American Petroleum Institute, Washington, DC, U.S.
90. P. W. Bellino, A.S.R., M.R. Flynn, , *A study of in situ burning of crude oil in an ice channel.* Proceedings of the Combustion Institute, 2013. **34**(2): p. 2539-2546.
91. H.E. Huppert, R.S.J.S., J.S. Turner, N.T. Arndt Nature 309 1984. **309**: p. 19-22.
92. Ian, B., *In Situ Burning of Oil Spills in Ice and Snow.*
93. Buist, I., *Window-of-Opportunity for In Situ Burning.* Spill Science & Technology Bulletin, 2003. **8**(4): p. 341-346.
94. Zhang, X.L., et al., *Influence of an external radiant flux on a 15-cm-diameter kerosene pool fire.* Combustion and flame, 1991. **86**(3): p. 237-248.
95. Artemenko, E.S. and V.I. Blinov, *Burning of liquids in vessels with change of level.* Combustion, Explosion, and Shock Waves, 1968. **4**(1): p. 39-42.
96. Orloff, L. and J. de Ris, *Froude modelling of pool fires.* Proc. Combust. Instit., 1982. **19**: p. 885.
97. R.C.Reid, J.M.P., B.E. Poling, , *The Properties of Gasses & Liquids,*. 4th ed. 1987: McGraw-Hill, Inc.
98. G. Cox, *Combustion Fundamentals of Fire*. 1995: Academic Press, London.
99. Keshavarz, G., F. Khan, and K. Hawboldt, *Modeling of pool fires in cold regions.* Fire Safety Journal, 2012. **48**: p. 1-10.

Appendix A

A study on burning of crude oil in ice cavities

Hamed Farmahini Farahani[a], Xiachuan Shi[a], Albert Simeoni[b], Ali S. Rangwala[a],

[a] Department of Fire Protection Engineering, Worcester Polytechnic Institute, Worcester, MA 01609, USA

[b] BRE Center for Fire Safety Engineering, Institute of Infrastructure and Environment, School of Engineering, University of Edinburgh, Edinburgh, EH9 3JL, UK

Abstract

In-situ burning (ISB) is a practical means of oil spill cleanup in icy conditions. This study considers one example of oil spill scenario: burning oil in an ice cavity. A new set of parameters to the classical problem of confined pool fires in vessels arises under these unique conditions. The icy walls of the cavity create a significant heat sink causing considerable lateral heat losses, especially for the small cavity sizes (5-10 cm). The melting of ice due to the heat from the flame causes the cavity geometry to change. Specifically, the diameter of the pool fire increases as the burning proceeds. This widening causes the fuel to stretch laterally thereby reducing its thickness at a faster rate. The melted ice water causes the oil layer to rise up, which causes the ullage-height ratio to decrease. The reduction in ullage and increase in diameter counter-act the reduction in thickness due to the widening. This results in a strong coupling between the mass loss rate ($\dot{m}$) and the geometry change of the pool and cavity. To systematically explore this process, experiments were performed in circular ice cavities of varying diameters. It was found that due to the cavity expansion the average $\dot{m}$ of crude oil in the ice cavity is greater than the $\dot{m}$ in a pan. For example, while efficiency of 10 cm pan is close to 100%, its $\dot{m}$ found to be 50%

less than the $\dot{m}$ in an ice cavity with similar initial diameter. A mathematical model was developed to predict mass loss rates and efficiencies which are in reasonable agreement with the experimental results. Extension of the model to larger sizes, comparable to realistic situation in the Arctic is discussed.
Keywords: Crude oil, ice, cavity, mass loss rate, efficiency.

1. Introduction

Oil spill cleanup in Arctic waters induces substantial difficulties because of the total or partial ice coverage for most of the year. When oil is released underneath the ice surface, it collects below the ice sheet. The spring break-up causes the hidden oil to emerge from lower ice sheets, forming pools of oil surrounded by ice walls. Typical dimensions can vary from 5 cm to 100 cm depending on the width of the cracks formed during breakup [1-4].

In-situ burning is a practical countermeasure to oil spill incidents. This method gasifies the contaminant by burning the released oil in the spill site. Oil removal from the spill surface can be remarkably efficient and at high rates under favorable condition. Removal efficiencies for thick slicks can easily exceed 90%. The method is ideally suited for remote places because of the small number of equipment and personnel needed to reach potentially high clean up efficiencies [5-7]. After burning, collection and transport of the residue reduce significantly because the liquid fuel is mostly converted to gas. In Arctic broken-ice, where oil spill cleanups are hindered and mechanical means of cleanup are not applicable, *in-situ* burning may be the most proper solution. There have been extensive efforts to investigate *in-situ* burning of oil in cold-climates since the late 1960's. These studies are mainly focused on burning of oil on open waters in presence of ice where oil is not confined by icy walls [2, 8-11].

To achieve a better understanding on the burning of crude oil, a series of experiments were conducted in different sizes of ice cavities to mimic burns of liquid fuels in icy conditions. Bellino et al. [12] reported mass loss rates of oil (3:1 mixture of motor oil and petroleum ether) burning in ice channels. The focus of this study is to further explore the burning behavior of crude oil using a circular ice cavity where corner effects are eliminated. Unlike burning an oil slick on open waters, burning of liquid fuel in an ice cavity shows unique characteristics. Melting of ice due to the heat from the flame causes the geometry of cavity to change. The icy walls of

the cavity and cold water beneath the fuel layer create a significant heat sink causing considerable heat losses especially for smaller cavity sizes.

What is the role of the cavity dynamics on the burning of crude oil? What are the burning characteristics in ice cavities of varying sizes? Is it possible to model the mass loss rate of crude oil in this setting and how can it be generalized to larger scale? To answer these questions, the change in shape of the ice cavity and the oil layer thickness are measured experimentally using a combination of visual images, mass loss, and temperature data along the centerline of the cavity. In addition, a mathematical model is developed to predict mass loss rate and burning efficiency of crude oil. Results from the model are then compared with experimental results.

1. Experimental setup and procedure

Figure 1 shows the experimental apparatus with crude oil in a 5 cm diameter ice cavity. Similar setups were used for diameters of 10, 15, and 25 cm. Three trials at each diameter were conducted to form a data set of twelve trials. Each experiment utilized an ice block with a circular cavity excavated in its center.

Table 1 shows the initial ice cavity dimensions and crude oil volumes for each diameter. There are two possible extinction scenarios for burning of the liquid fuels in an ice cavity: natural extinction and spillage of the fuel out of the cavity. The depth (H) and initial fuel layer (L) were chosen based on the data obtained from preliminary tests to prevent over flow and spillage during combustion. The ice block was placed on a drip pan on top of a load cell (precision of 0.01 g) to record the mass loss. Later, this mass loss was processed to obtain mass loss rates ($\dot{m}$). The mass loss data of crude oil at 5, 10 cm were collected. For 15 and 25 cm cavities, the weight of ice blocks were over the limit of load cell and 3M oil absorbent pads were used to collect the remaining oil to estimate average $\dot{m}$.

The ice blocks with D = 5 and 10 cm were equipped with Thermocouples (type K, gauge 36, and 0.13 mm diameter) to acquire a temperature profile of the liquid layer to use in the mathematical model. A total of sixteen thermocouples, installed on one array, were utilized to record the temperature at different elevations (0.5 cm apart) and obtain temperature of fuel surface and fuel-water interface along cavity centerline. Thermocouples are shown in Fig. 1 with small solid circles.

The experimental procedure comprised of placing the ice block on the load cell then pouring Alaskan North Slope (ANS) crude oil in the cavity (at the initial temperature of 20°C) and igniting it immediately. All trials represented in this study were allowed to burn to extinction in a quiescent environment.

2. Results and Analysis

3.1- Effects of cavity expansion and fuel layer thickness on mass loss rate

Figure 2, illustrates the mass loss rate of ANS crude oil for the 5 and 10 cm diameter cavities. Experimental data from three trials is presented with an average trend shown by the dark solid curve. There are two phases observed for the burning behavior: first a continuous increase to reach a peak and then a rapid decline to extinction. The two phases are demarcated using the maximum mass loss rate in Fig.2. The first phase where the $\dot{m}$ is found to grow steadily is mainly caused by diameter expansion due to ice melting. The dependence on *D* can be explained by the relative importance of the mechanisms by which heat is transferred to the fuel surface from the flame. The heat flux from the flame melts the ice thereby widening the cavity. The cavity widening process provides more burning surface for the liquid and increases the mass loss rate [12].

The distance between the top of a vessel and the fuel surface is defined as the ullage height. In pool fires confined in vessels, the ullage height increases as the fuel burns. This results in an exponential decay in $\dot{m}$ leading to flame instabilities and ultimately flame extinction. When the pool fire is bounded by ice walls, an opposite trend is observed. This is because the heat flux from the flame melts the ice walls, resulting in a water sub-layer that is formed below the fuel layer. As the fuel continues to burn, more water accumulates resulting in the ullage decrease and a corresponding increase in $\dot{m}$. Further enhancement in $\dot{m}$ is achieved by the cavity expansion. This behavior was observed for all cavity sizes.

Table 2 shows data on burning behavior of crude oil for various initial diameters. The average $\dot{m}$ is calculated by dividing the burned mass over the duration of combustion. Table 2 shows that the average $\dot{m}$ along with $\dot{m}''$ increases at larger diameters. This increase may be due to the decrease in the wall effects as diameter increases. The burning efficiency for 5 cm cavity is 32%

and it increases to 73% for a 25 cm cavity. For 25 cm trials the onset of boil-over increased the $\dot{m}$ and efficiency dramatically.

As shown in Fig. 2, Phase 2 is relatively short in duration (10-30% of total burn time). The steep decline to extinction is indicative of the presence of a significant heat loss from the fuel layer. The insulating effect of the fuel layer keeps the burning slick surface at a high temperature by reducing heat loss to the water underneath. As the fuel layer thins, more heat is gradually conducted through it. This conduction heat loss continues until enough heat is transferred through the fuel layer to make the temperature of the oil surface to drop below its fire point, which translates into the extinction of the flame. It is possible that the convective losses also play a role during this phase. Especially, for thin fuel layers a significant axial gradient exists, which can lead to thermocapillary or Marangoni effects [13]. Table 3 shows that the final fuel layer thickness is around 2-3 mm. For an *in-situ* burn of fresh ANS crude oil slicks (40 cm diameter) in brash and frazil ice conditions the final fuel layer thickness is reported around 2 mm [5]. In large scale pool fires on ice and snow with an initial fuel layer thickness of 1-2 cm, the final fuel layer thickness is reported to be 1 mm [8, 14]. The difference between the final thicknesses reported in literature (1-2 mm) and those obtained here (2-3 mm) may be due to the smaller cavity diameters that induce higher heat losses to the walls. Table 3 also shows the cavity expansion. The pool diameter increase is significant for smaller cavities (expansion of about 280%) but it lessens as the initial diameter is increased.

Figure 3 illustrates the cavity expansion for 5 cm (a) and 10 cm (b) trials in sequential time steps. The fuel layer lying at the bottom of the cavity gradually rises to level with the ice surface by the end of the burning period. Phase 1 and 2 are recognizable from these images as well. The first four images of each set illustrate the increasing period of $\dot{m}$ (phase 1), where the fire is growing in size. The last image, with a characterized weak flame, is representing the decay period (phase 2).

3.2 Temperature profiles

The surface temperature of a freely burning liquid is slightly below its boiling point. Crude oil does not have a fixed boiling point and the lighter components have a tendency to burn off first. Therefore, the surface temperature will increase with time as the remaining crude becomes less volatile [15]. The ice cavities with initial diameter of 5 and 10 cm were instrumented with 16

thermocouples (TCs). The temperature recordings show three distinct trends. TCs located below the initial fuel layer recorded the temperature of the crude oil first and finally that of water. TCs between the initial and final fuel layer locations recorded the temperature of gas phase and because melting of ice caused the fuel layer to rise, eventually recorded the temperature of crude oil surface and that of water. Elevation of the liquid layer causes a sudden drop in the temperature recorded by these TCs. The third group of TCs remained in the gas phase for the entire length of experiment and only recorded the gas phase temperature.

The measurements from the second group of TCs were analyzed to find the fuel surface temperature (T_b) and consequently that of the water sub-layer underneath (T_w). The progression of T_b and T_w during the burning is shown in Fig. 4 for 5 and 10 cm trials. The temperature drop previously described for the second TCs group was taken as ~200 °C in a time period shorter than 5 seconds. This moment was defined being the TC immersion into the liquid. The measured temperature of the TC for a period of 10 seconds after this moment was averaged and assumed to be the instant surface temperature of crude oil. Then, a line was fitted to these surface temperatures to acquire the upper surface temperature trend line of the crude oil (Fig. 4). As shown in Fig. 4, once again, it is possible to identify the two burning phases with regards to the fuel surface temperature, T_b. The declining temperature in Phase 2 also confirms the presence of a significant heat loss that halts the combustion process. Knowing the fuel layer thickness also enabled to interpolate the temperature reading of adjacent TCs to obtain the temperature of the fuel-water interface. These fitted lines (Fig. 4) were used to develop a temperature profile for the fuel, which later was used in the mathematical model.

3.3 Mathematical model

Figure 5 shows the energy balance on the fuel layer control volume. The fuel surface receives heat from the flame by convection, $\dot{Q}_{cv,g-l}$, and radiation $\dot{Q}_{rad,f-l}$. Heat is lost via conduction through the sides, $\dot{Q}_{cd,l-i}$, and the bottom, $\dot{Q}_{cd,l-w}$. L_v denotes the heat of vaporization of the liquid. The mass loss rate of the liquid can be expressed as:

$$\dot{m}L_v = \dot{Q}_{cv,f-l} + \dot{Q}_{rad,f-l} - \dot{Q}_{cd,l-w} - \dot{Q}_{cd,l-i}. \qquad (1)$$

While deriving Eq. (1), the convective motion in the liquid is ignored. Reflection and re-radiation from the liquid surface are ignored. The heat feedback from the flame to the fuel surface ($\dot{Q}_{cv,f-l}$ and $\dot{Q}_{rad,f-l}$) is denoted by $\dot{Q}_{s,f-l}$ (Fig. 5). The ullage effect is assumed to be minimal and is ignored. The density, ρ_l, thermal conductivity, λ_l, and heat of vaporization, L_v, of crude oil are assumed to be constant [16,17].

Note that the heat balance is similar to that used in classical pool fire literature [18-20] except for two main differences: 1) The term, $\dot{Q}_{cd,l-i}$, which denotes the heat loss by conduction from the side of the fuel layer is typically positive as heat is usually conducted from the vessel rims to the fuel and 2) all of the heat transfer terms depend on the changes in the cavity and fuel layer geometries. Thus, modeling the distribution of heat transfer from the flame to the liquid surface has to account for the change in cavity geometry. Using the data represented in Table 3, it is assumed that $D(t)$ and $L(t)$ follow a linear trend with respect to time (at + b) where "a" equals to $\frac{Final-Initial}{time}$ and "b" is the initial value.

Similar to an earlier study by Torero et al. [11], the heat flux reaching the surface can be expressed as:

$$\dot{Q}_{s,f-l}(t) = \chi\, \rho_\infty C_p \left[T_\infty g\left(T_f - T_\infty\right)\right]^{\frac{1}{2}} D(t)^{5/2} \qquad (2)$$

where ρ_∞, C_p, and T_∞ are the air properties at ambient temperature; T_f is the temperature of hot gasses above the liquid and it is assumed to be constant (1100 K) [11]; χ is a specific fraction of the heat released fed back to the fuel surface and it is assumed to be a constant value equal to 5×10^{-3}. The changes in the diameter of cavity, $D(t)$, and the thickness of the fuel layer, $L(t)$, are obtained experimentally. $\dot{Q}_{cd,l-w}(t)$ is representing the in-depth conduction to the water sub-layer is given by:

$$\dot{Q}_{cd,l-w}(t) = \pi \left(\frac{D(t)^2}{4}\right) \left(\frac{\lambda_l}{L(t)}\right) \left(T_b(t) - T_w(t)\right) \qquad (3)$$

where, λ_l is the thermal conductivity of the fuel and is assumed to be constant (0.9 W/m K) at elevated temperatures [21]; $T_b(t)$ and $T_w(t)$ are obtained experimentally as shown in Fig. 4. $T_b(t)$ and $T_w(t)$ for the 10 cm trial were averaged and used as constant values in modeling 15 cm and 25 cm trials. The conduction to icy walls is also a source of heat loss, especially during the

early stage of combustion when the fuel layer is relatively thick and surface contact with ice is larger. This term is given by:

$$\dot{Q}_{cd,l-i}(t) = \frac{\lambda_l}{\frac{D(t)}{2}} (2\,\pi(\frac{D(t)}{2})\,L(t))\,(\frac{T_b+T_w}{2}(t) - T_{ice}) \qquad (4)$$

The temperature at the center of the fuel layer is assumed to be the average between $T_b(t)$ and $T_w(t)$ while the temperature of icy walls, T_{ice}, is defined as a constant (273 K). Furthermore, the heat loss due to evaporation of liquid can be characterized as $\dot{m}(t)L_v$ where L_v is the latent heat of evaporation of the fuel (250 kJ/kg) [11]. Combining Equations (1-4) the $\dot{m}(t)$ can be expressed as:

$$\dot{m}(t) = \frac{\dot{Q}_{s,f-l}(t) - \dot{Q}_{cd,l-w}(t) - \dot{Q}_{cd,l-i}(t)}{L_v}. \qquad (5)$$

Equation (5) is used to calculate the mass loss rate ($\dot{m}(t)$) for ANS crude oil. Figure 6 shows the calculated trend lines of $\dot{m}$ for the 5 cm and 10 cm cases. The experimental curves are also included to provide comparison with the model. The average estimated $\dot{m}$ (g/s) for D = 5, 10, 15, and 25 cm are 0.028, 0.11, 0.3, and 0.84 (g/s), which translates to burning efficiencies of 35, 48, 54, and 46%, respectively.

Figure 7 compares the experimental obtained burning efficiencies and those of the model. The burning efficiencies calculated by the model are in agreement with the experimental values except for the 25 cm trial. The 25 cm trial involved boil-over and burned vigorously. This model does not address boil-over scenarios, thus the predicted $\dot{m}$ for 25 cm is much lower (by 40%) than the experimental value. However, by adjusting the χ to 7.8×10^{-3} the average $\dot{m}$ becomes equal to 1.45 (g/s). The impact of adjusting the value of χ for the 25 cm trial is illustrated in Fig. 7.

The overprediction during initial stage, as shown in Fig. 6, is mainly due to ignored effect of ullage. After the elevation of the fuel layer by ice melting, the ullage decreases resulting in a more effective burning of the fuel. During Phase 2, the fuel layer penetrates into the ice, creating an ice lip (small lateral cavity described in Bellino et al. [12]. This effect has not been modeled and may be the cause of the slight overprediction by the model. The ice lip conceals a certain

quantity of the liquid fuel from the heat flux from the flame, causing a reduction in combustion efficiency.

Significant assumptions were used in developing the model. Chief among them is the value assigned to χ, which was assumed to be a constant. It is important to investigate and perhaps to model this effect in future. The assumption of constant properties may also result in discrepancies between the model predictions and the experimental values, due to the multi-component nature of the crude oil. It will therefore be necessary to develop bench-scale testing platforms to provide material properties (λ_l, ρ_l) of crude oil as a function of temperature.

4. Conclusions

A series of experiments were conducted to develop an understanding of the burning of crude oil in circular ice cavities. The burning rate of a fuel layer within ice cavities of varying diameters was studied to understand how the cavity expansion affects it. The mass loss rate is primarily enhanced by the cavity diameter and is limited by the fuel layer thickness. Ice melting over the course of the trial created a highly dynamic burning environment. It decreased ullage and increased the fuel surface area, enhancing the thinning of the fuel layer. Due to strong heat losses any benefits created by the high burning rates were quickly overcome. However, the rapid decrease in fuel layer thickness is the more prominent factor in reducing mass loss rates. The temperature profiles along the centerline of the oil layer were used to estimate heat losses of the fuel layer to the water sub-layer and icy walls. An energy balance for the fuel layer was used to estimate the mass loss rate. The model was relatively successful but further developments are necessary. Modeling and understanding such complex burning conditions requires describing other phenomena, such as the ullage and lip creation.

Acknowledgments

This study was funded by the Bureau of Safety and Environmental Enforcement, US Department of the Interior, Washington, D.C., under Contract Number E12PC00056. The contents do not necessarily reflect the views and policies of the BSEE, nor does mention of the trade names or commercial products constitute endorsement or recommendation for use.

[1] H.M. Brown, R.H. Goodman, In situ burning of oil in ice leads. in: Arctic and Marine Oil Spill Program (AMOP) Technical Seminar, 9th Proceedings, 1986, p. 176–191.

[2] N.K. Smith, A. Diaz, In-place burning of crude oil in broken ice: 1985 testing at OHMSETT, in: Arctic and Marine Oil Spill Program (AMOP) Technical Seminar, 8th Proceedings, 1986, p. 176–191.

[3] N.K. Smith, A. Diaz, In-place burning of Prudhoe Bay oil in broken ice: 1985 testing at OHMSETT, in: Proceedings of the 1985 Oil Spill Conference, API Publication No. 4385, American Petroleum Institute, Washington, DC, 1985, p. 405–409.

[4] N.K. Smith, A. Diaz, In-place burning of crude oils in broken ice, in: Proceedings of the 1987 Oil Spill Conference, API Publication No. 4352, American Petroleum Institute, Washington, DC, 1987, p. 483–387.

[5] S.L. Ross Environmental Research Ltd., D.F. Dickins Associates Ltd., Alaska Clean Seas, Tests to Determine the Limits of *in situ* Burning of Thin Oil Slicks in Broken Ice. SL Ross Environmental Research Ltd. and DF Dickins Associates Ltd. And Alaska Clean Seas, 2003.

[6] P. Sveum, C. Bech, M. Thommasen, Burning oil in snow. Experiments and implementation in a Norsk hydro drilling contingency plan, in: Arctic and Marine Oil spill Program (AMOP) Technical Seminar, 14th Proceedings, 1991, p. 339–410.

[7] D. Dickins, P.J. Brandvik, J. Bradford, L.V. Faksness, L. Liberty, R. Daniloff. 2006 Experimental Oil Spill Under Ice: Remote Sensing, Oil Weathering Under Arctic Conditions and Assessment of Oil Removal by In-situ Burning, in: International Oil Spill Conference Proceedings No. 1, 2008: Vol. 2008, p. 681-688.

[8] I.A. Buist, In situ Burning of Oil Spills in Ice and Snow, Alaska Clean Seas, 2000.

[9] E. DeCola, T. Robertson, S. Fletcher, S. Harvey, Offshore Oil Spill Response in Dynamic Ice Conditions: A Report to WWF on Considerations for the Sakhalin II Project. Alaska, Nuka Research, XXp, 2006.

[10] D. Evans, W. Walton, H. Baurn, R. Lawson, R. Rehm, R Harris. Measurement of large scale oil spill burns, Proceedings of the Thirteenth Arctic and Marine Oil Spill Program Technical Seminar, Edmonton, Canada, 1990, p. 1-24.

[11] J.L. Torero, S.M. Olenick, J.P. Garo, J.P. Vantelon, Spill Science and Technology Bulletin, 8 (1999) 379–390.

[12] P.W. Bellino, A.S. Rangwala, M.R. Flynn, Proc. Combust. Inst. 34 (2012), p. 2539–2546

[13] T. Yumoto, A. Takahashi, T. Handa, Combustion Behavior of Liquid Fuel in a Small Vessel, Combust. Flame 30, (1977), p. 33-43.

[14] I. Buist, Spill Science and Technology Bulletin 8. No. 4, 2003, pp. 341–346.

[15] D. Drysdale, An Introduction to Fire Dynamics, 3rd ed., John Wiley & Sons Ltd, p 191, 2011.

[16] A. Hamins, J.C. Yang, T. Kashiwagi, A Global Model for Predicting the Burning Rates of Liquid Pool Fires, NISTIR 6381, National Institute of Standards and Technology, 1999.

[17] A. Nakakuki, Fire Safety Journal 23, (1994) 339-363.

[18] V. T. Blinov, G. N. Kyudyakov , "Diffusion Burning of Liquids", Akademii Nauk SSSR, Moscow, 1961, English Translation by US Army, 1961.

[19] J. P. Garo, S. Vantelon, Gandhi, J. L. Torero, Spill Science and Technology Bulletin, Vol. 5, No. 2, (1999) 141-151.

[20] H.D. Ross, Progress in Energy and Combustion Science 20, (1994) 17-63.

[21] R.C.Reid, J.M. Praustinz, B.E. Poling, The Properties of Gasses & Liquids, 4th ed., McGraw-Hill, Inc, 1987, p 556.

Table 1. Experimental matrix.

D (cm)	*H* (cm)	*L* (cm)	*V* (ml)
5	6	2.4	50
10	8	1.6	125
15	10	1.6	290
25	10	1.5	710

Table 2. Average burning properties of crude oil.

Size	$\dot{m}$ (g/s)	$\dot{m}''$ (g/s m^2)	Efficiency (%)
5 cm	0.026	4.3	32
10 cm	0.1	6	44
15 cm	0.28	8.3	51

25 cm	1.44	21	73 [a]

[a] Boil over

Table 3. Change in cavity size and fuel layer thickness

Initial D (cm)	Final D (cm)	Final L(cm)	Time (s)
5	13.5	0.26	490
10	17.5	0.29	460
15	25	0.26	450
25	35	0.06 [a]	340

[a] Boil-over increased the $\dot{m}$ and flame height dramatically and resulted in a thinner fuel layer at extinction.

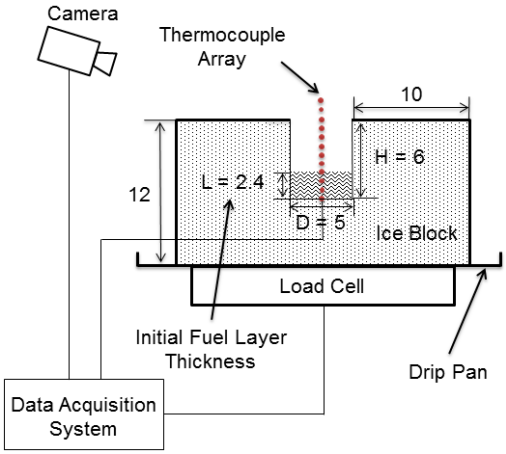

Figure 1. Experimental setup. The dimensions are reported in cm.

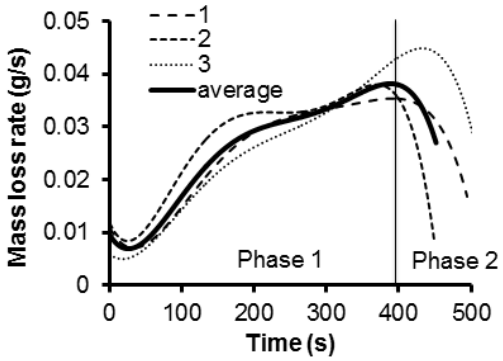

(a)

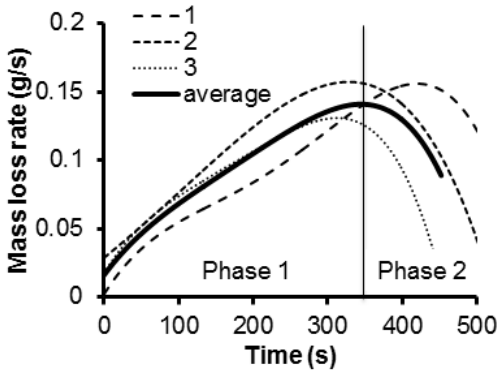

(b)

Figure 2. Mass loss rate ($\dot{m}$) for 5 cm (a) and 10 cm (b) trials.

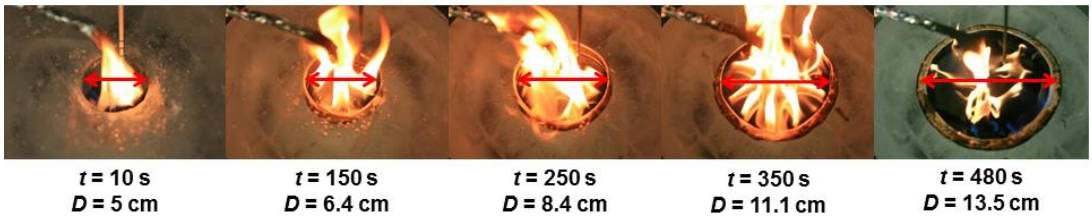

(a)

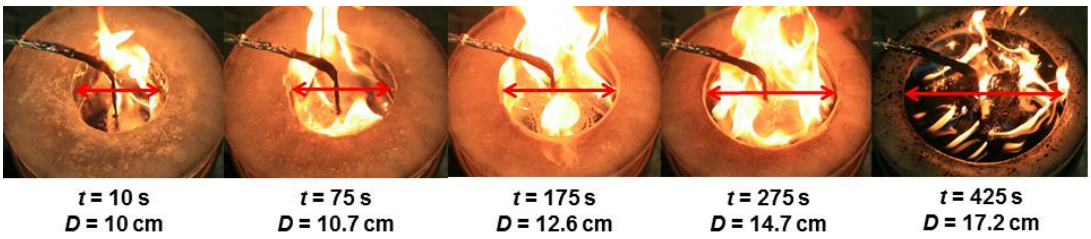

(b)

Figure 3. Showcasing cavity expansion for a) 5 cm and b) 10 cm trials.

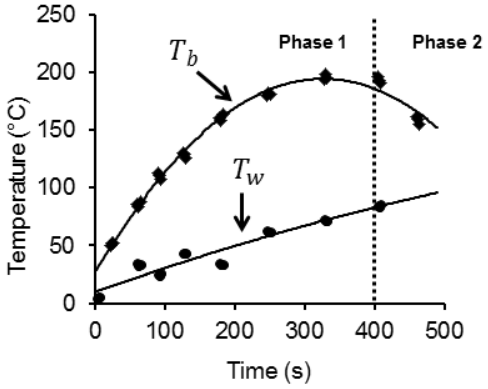

(a)

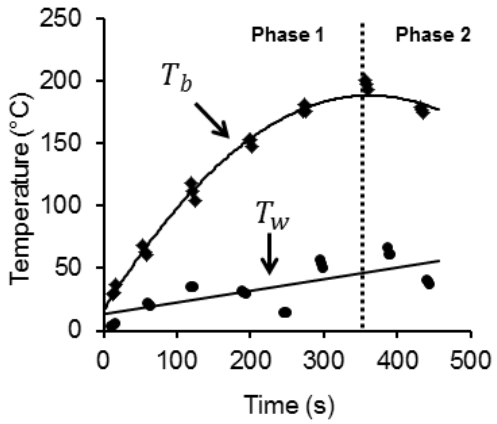

(b)

Figure 4. a) 5 cm and b) 10 cm temperature distributions corresponding to the top and bottom of the fuel layer.

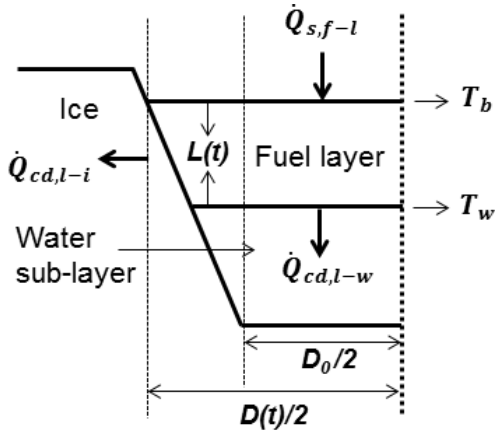

Figure 5. Schematic diagram used to model the heat transfer mechanisms of the fuel layer.

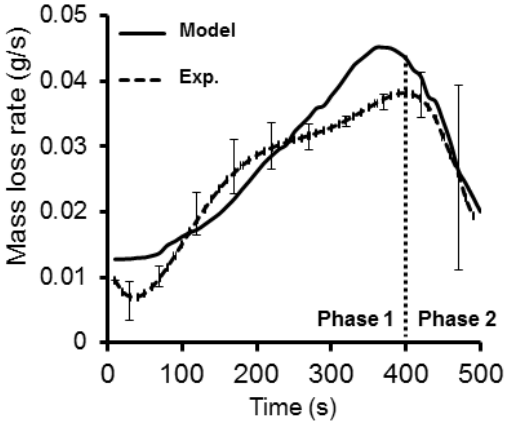

(a)

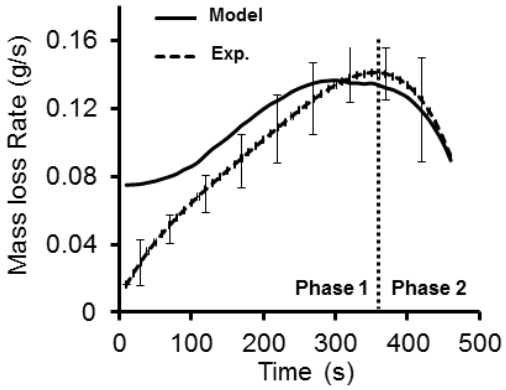

(b)

Figure 6. Comparison between experimental and calculated mass loss rate for 5 cm (a) and 10 cm (b) trials (the error bars represent the experimental burning rate due to variation between repetitions).

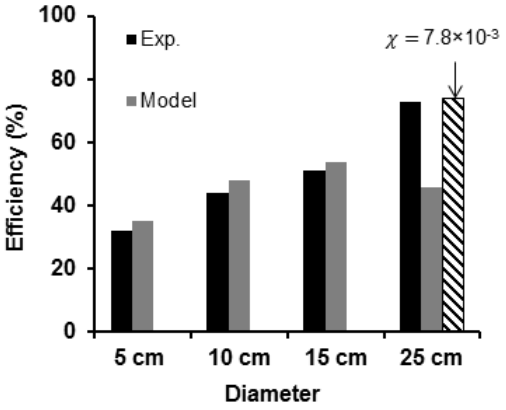

Figure 7. Comparison between experimental and calculated burning efficiencies. χ is equal to 5×10^{-3} for all cases except noted.

Appendix B

Figure B.1 and B.2 provide the raw mass loss data for the 5 cm and 10 cm trials.

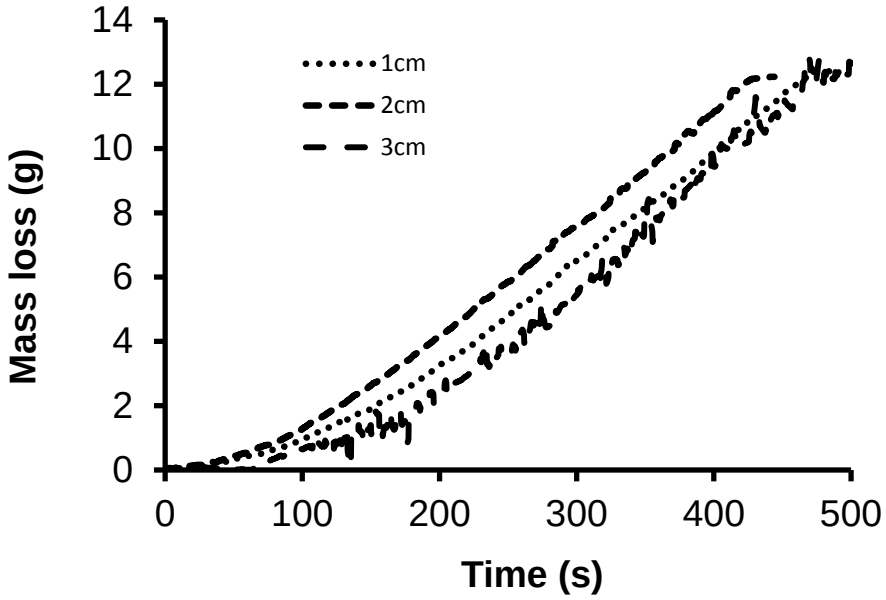

Figure B. 1: Mass loss of 5 cm trials.

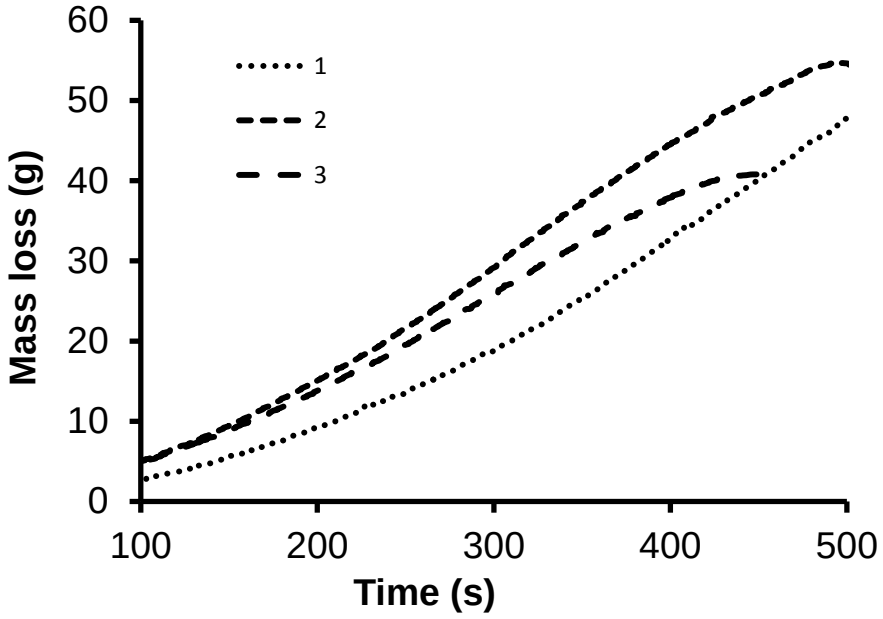

Figure B. 2: mass loss of 10 cm trials

Figure B.3 and B.4 provide the temperature data with respect to location of TCs at t = 50 s time steps for the 5 cm and 10 cm trials.

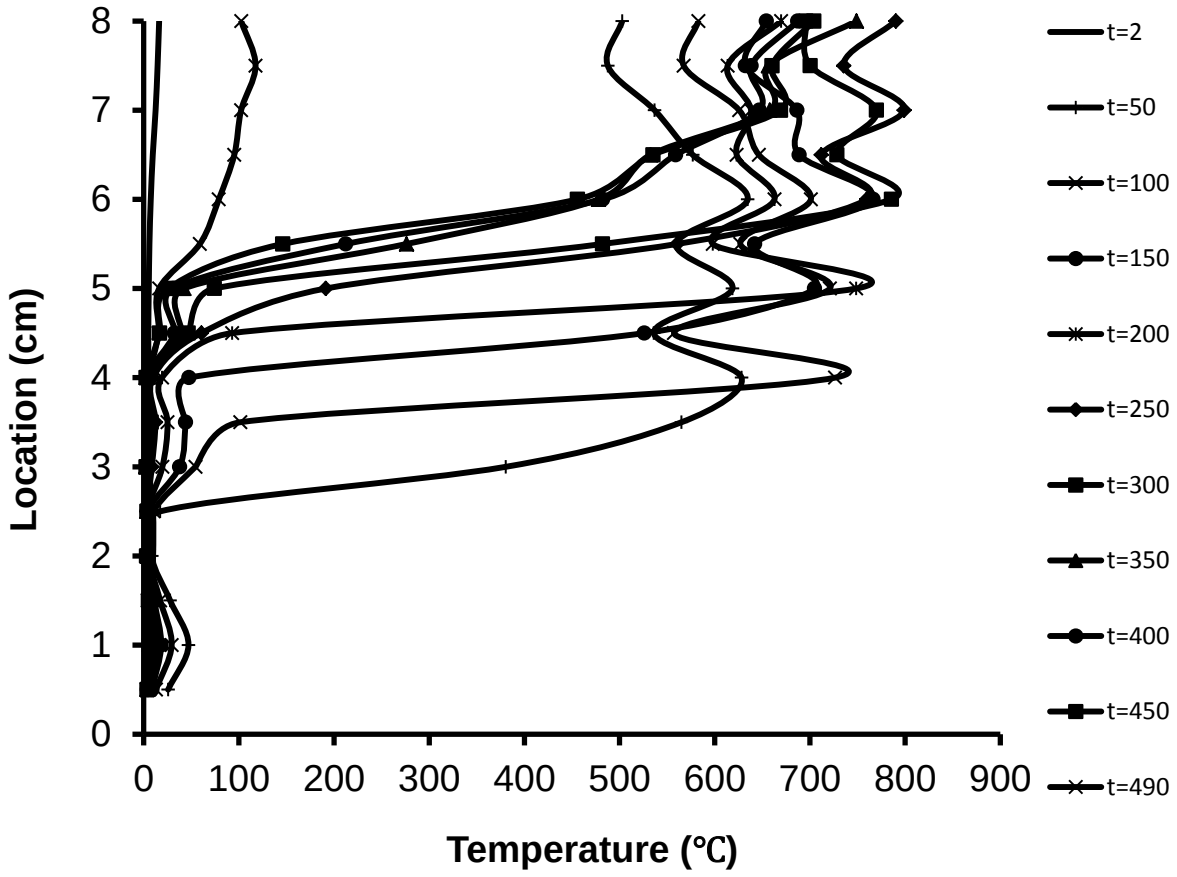

Figure B. 3: Temperature recording of 5 cm trial based on different location in cavity.℃

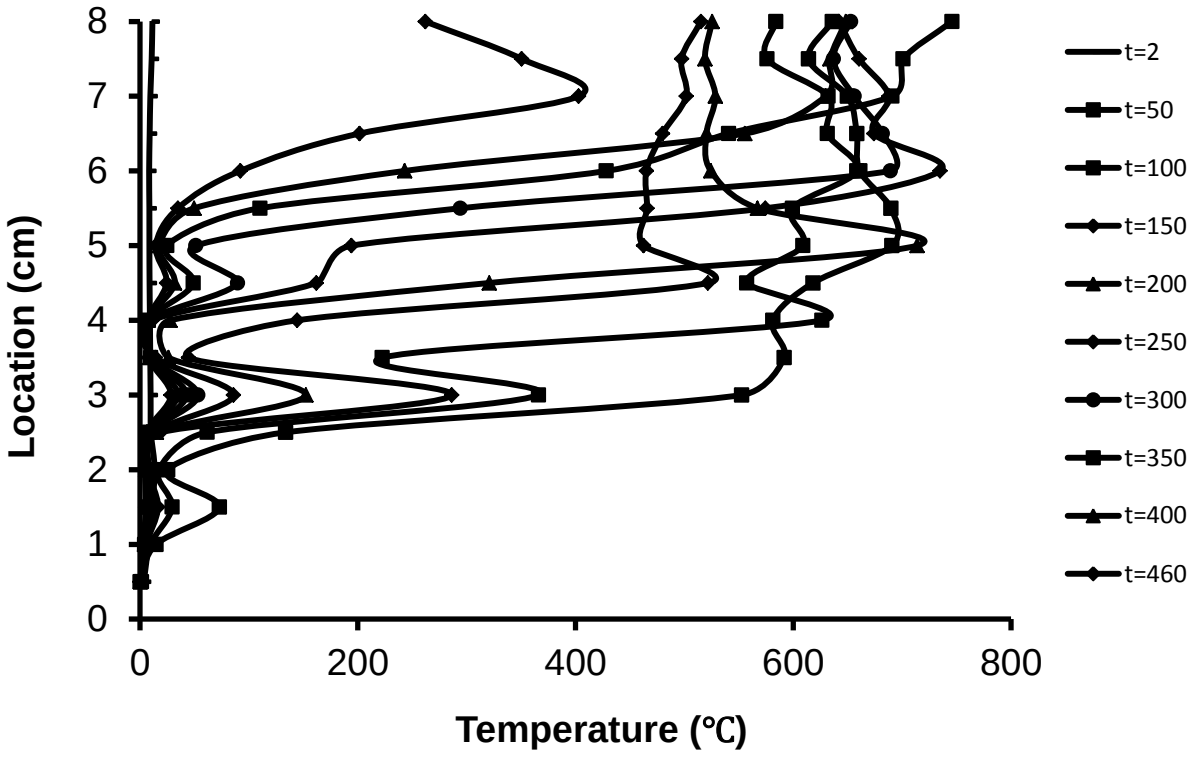

Figure B. 4: Temperature recording of 5 cm trial based on different location in cavity

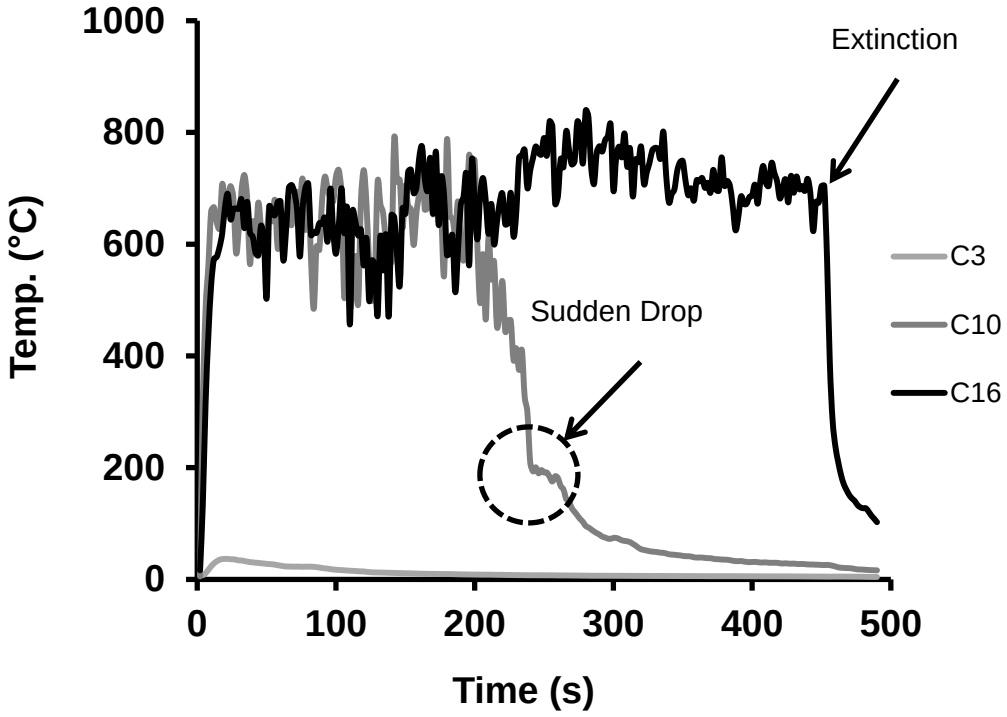

Figure B. 5: Temperature recording of three TCs each representing a group described in section 3.2.

The following photographs are a presented to provide the reader with an appreciation of the work and perhaps assist in future research endeavors.

Figure B. 6: Free burn of crude oil in 10 cm pan

Figure B. 7: Free burn of crude oil in 15 cm pan

Xylene and Octane were used in preliminary test to identify the optimum fuel layer thickness to prevent overflow.

Figure B. 8: Burn test of Xylene in 5 cm ice cavity- top view

Figure B. 9: Burn test of Xylene in 5 cm ice cavity- front view

Figure B. 10: Burn test of Octane in 5 cm ice cavity- top view

Figure B. 11: Burn test of Octane in 5 cm ice cavity- front view

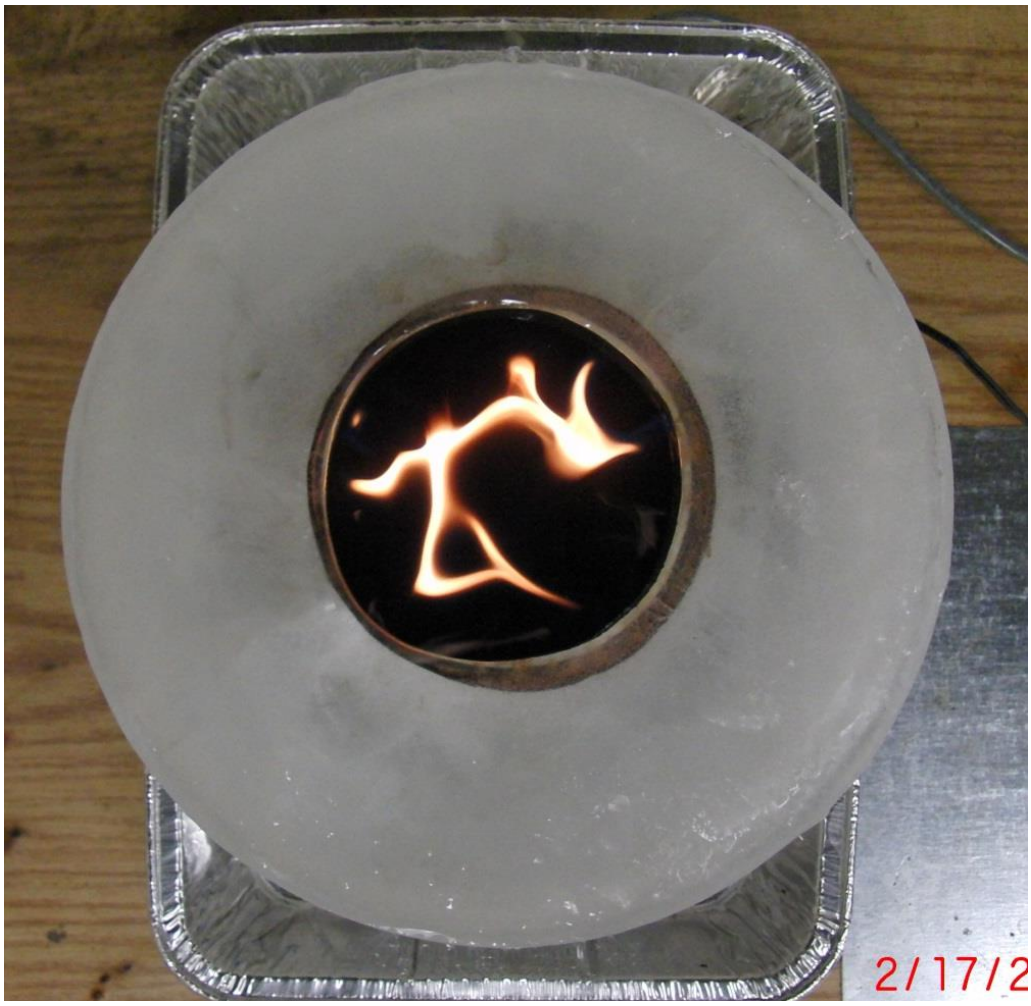

Figure B. 12: Burn test of Crude oil in 5 cm ice cavity- top view

Figure B. 13: Burn test of Crude oil in 5 cm ice cavity- front view

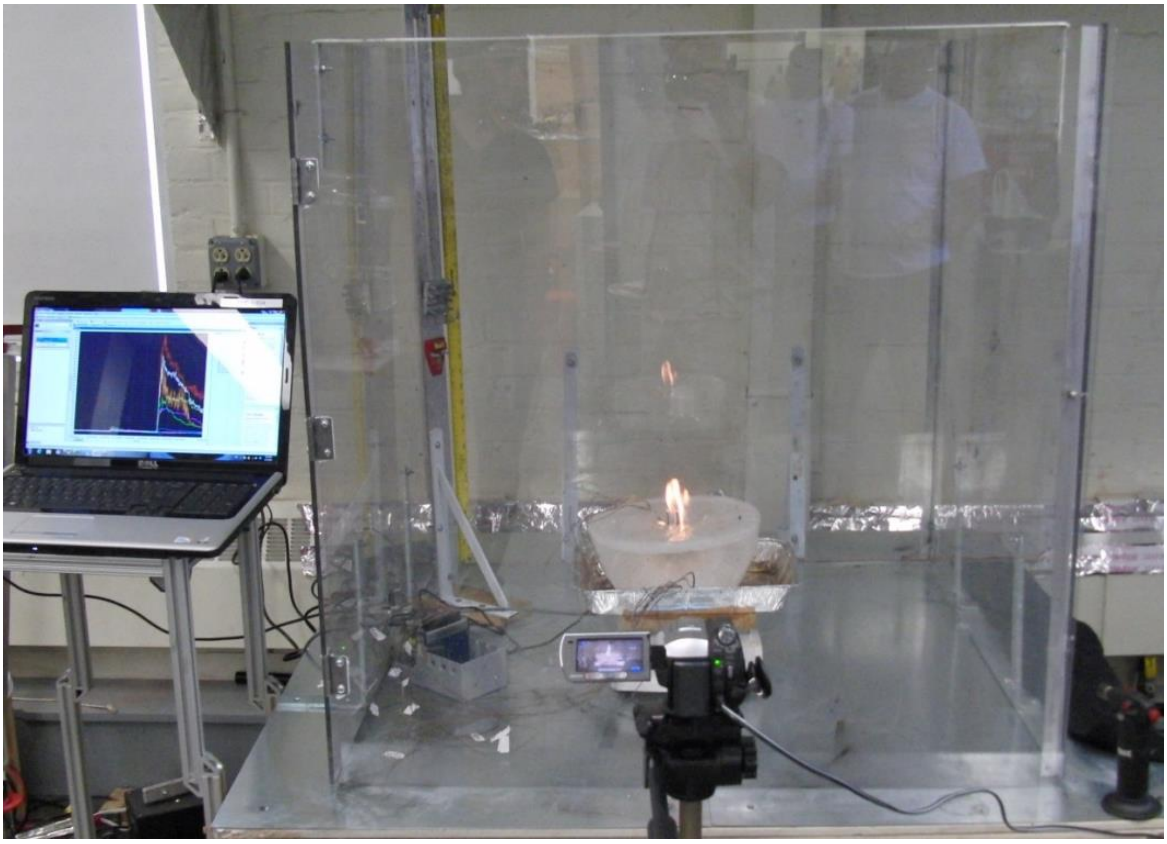

Figure B. 14: Experimental apparatus used for the tests.

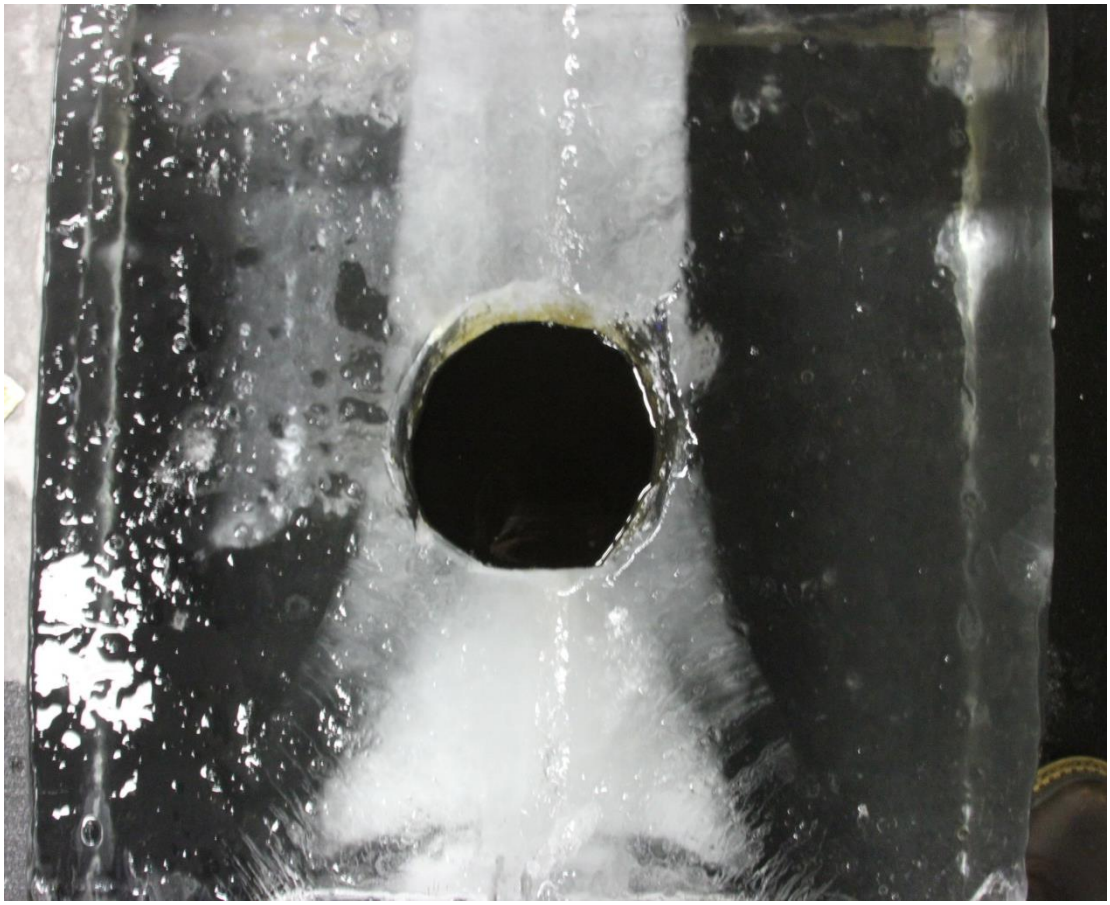

Figure B. 15: Burn test of Crude oil in 15 cm ice cavity- top view before ignition

Figure B. 16: Igniting the crude oil

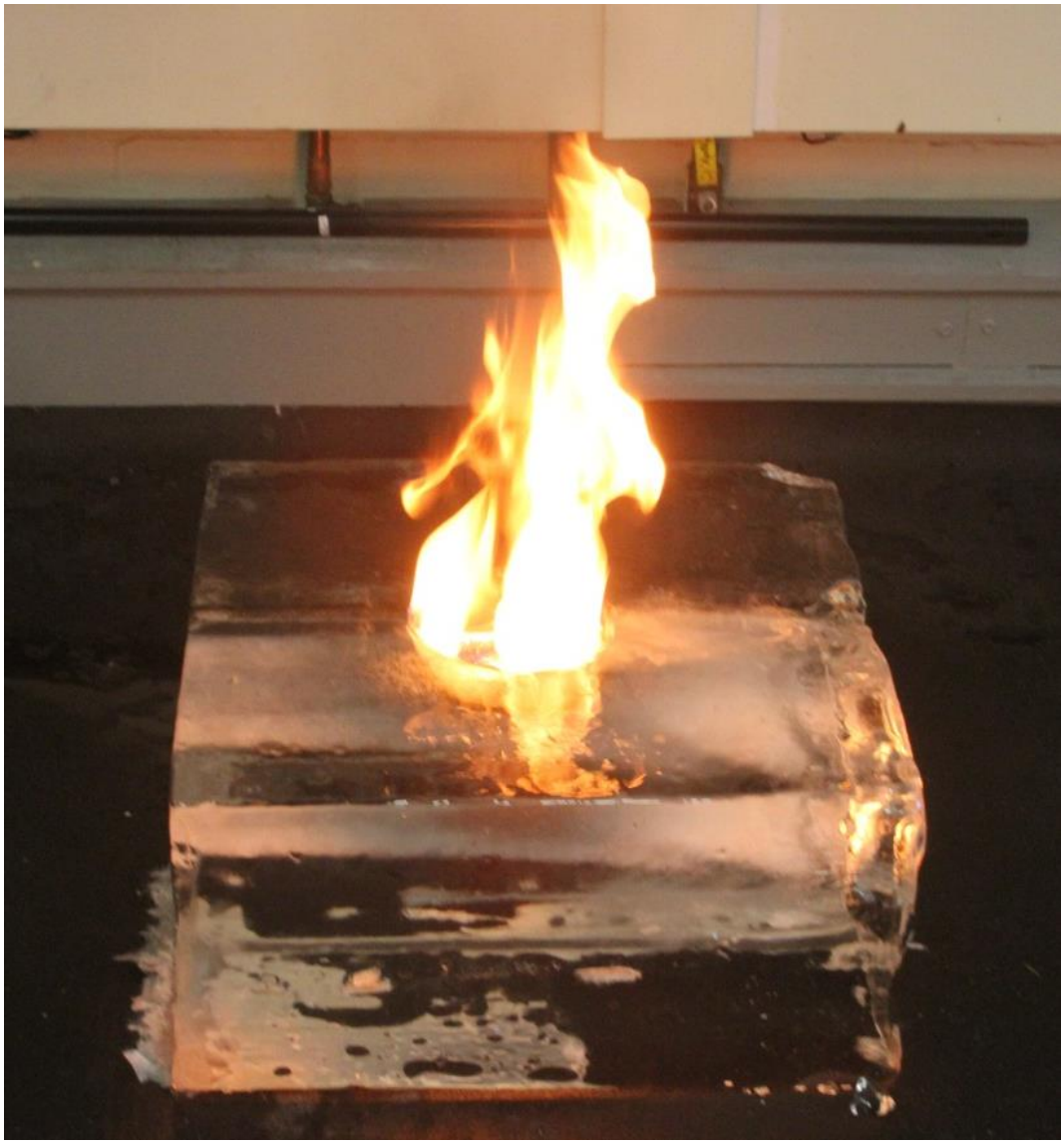

Figure B. 17: Burn test of Crude oil in 15 cm ice cavity- front view

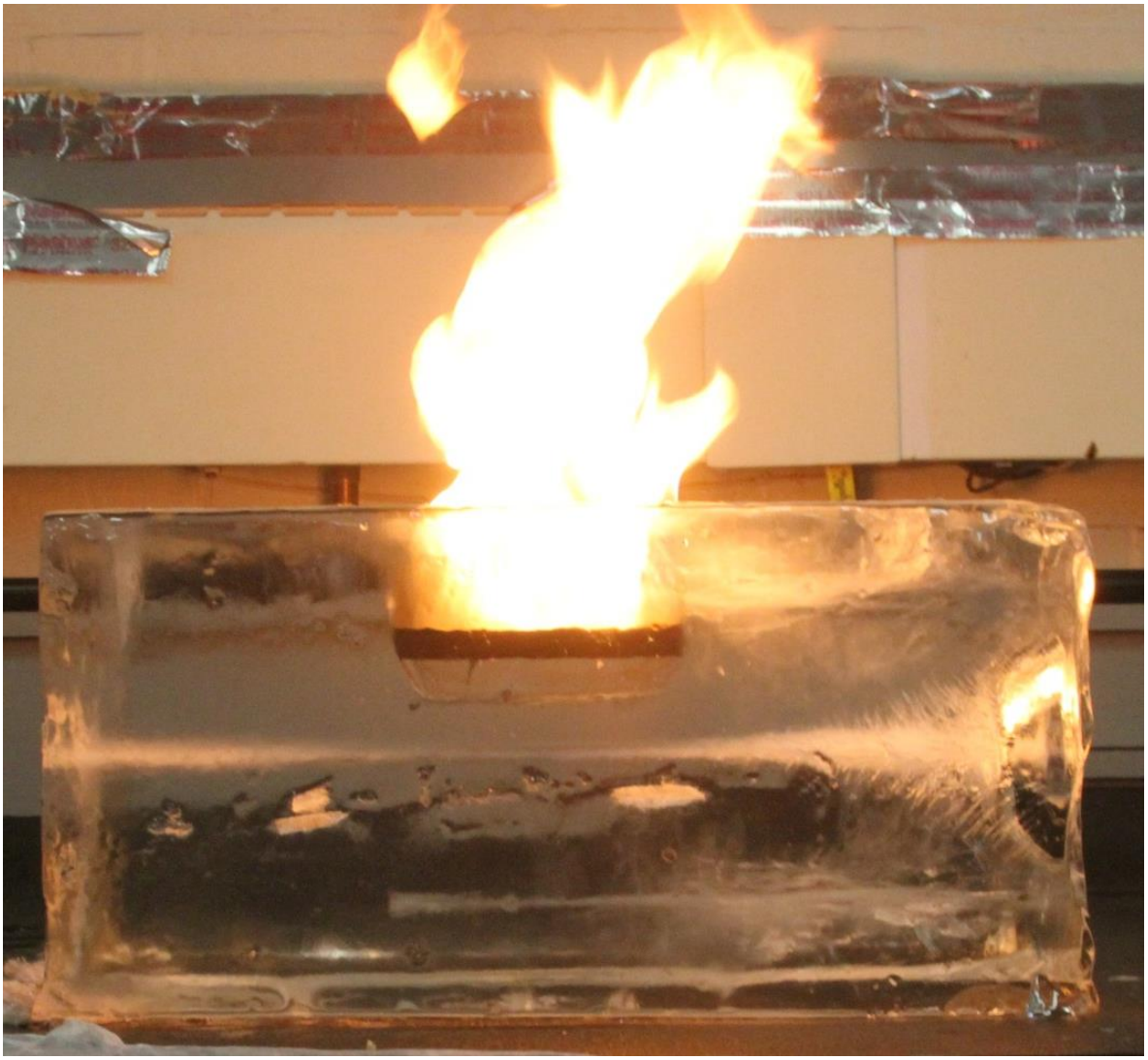

Figure B. 18: Burn test of Crude oil in 15 cm ice cavity- side view- Water is being collected under the crude oil and pushing up the fuel layer slowly

Figure B. 19: Cross section of the cavity after the extinction initial diameter of 15 cm

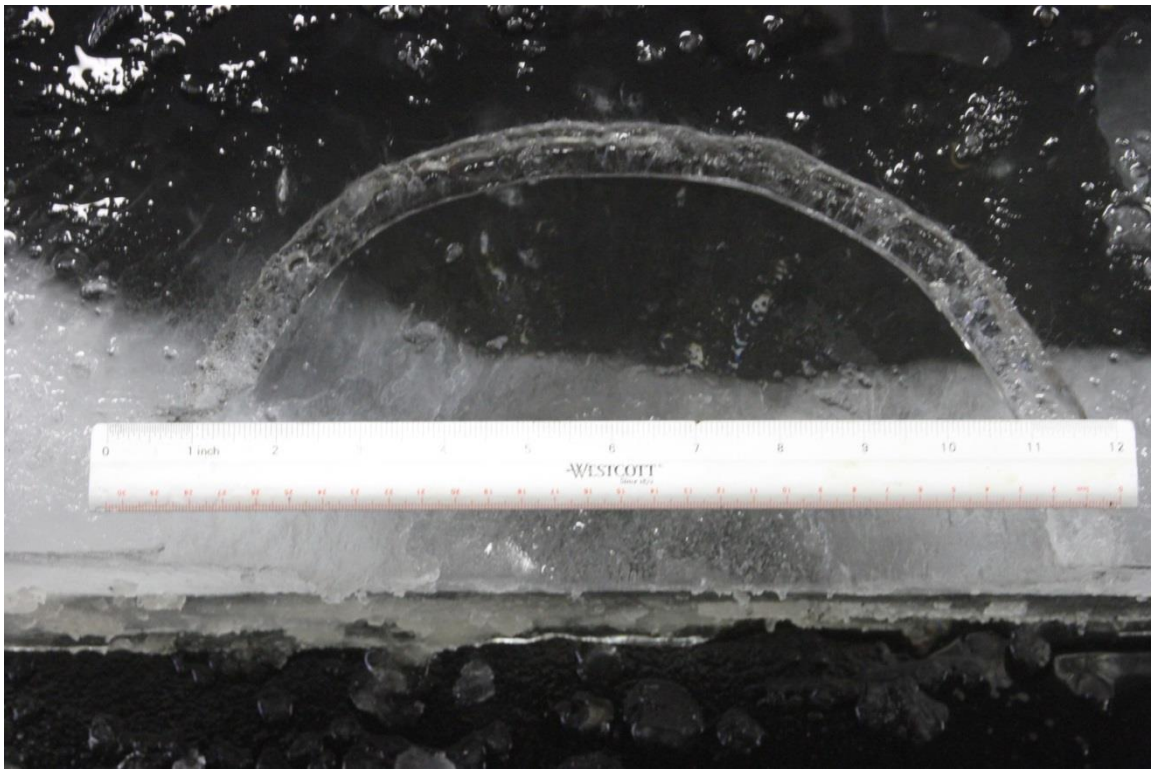

Figure B. 20: Top view of 15 cm diameter ice cavity after extinction.

Figure B. 21: Onset of boil-over for 25cm diameter ice cavity.

Figure B. 22: Side view of 25 cm diameter ice cavity after extinction.

Figure B. 23: Side view of 25 cm diameter ice cavity after extinction.